universität wien

MASTERARBEIT | MASTER'S THESIS

Titel | Title

Towards a robust and efficient protocol optimizing the generation of stable transgenic *HvTol* single knock-out barley plants using CRISPR/Cas9

verfasst von | submitted by
Moritz Schmid

angestrebter akademischer Grad | in partial fulfilment of the requirements for the degree of
Master of Science (MSc)

Wien, | Vienna, 2026

Studienkennzahl lt. Studienblatt | degree programme code as it appears on the student record sheet:	UA 066 832
Studienrichtung lt. Studienblatt | degree programme as it appears on the student record sheet:	Masterstudium Botany
Betreut von | Supervisor:	Dipl.-Ing. Dr. Verena Ibl Privatdoz.

Inhaltsverzeichnis

Danksagung

First and foremost, I would like to thank Dipl.-Ing. Dr. Verena Ibl for giving me the opportunity to join CELBICS and work on such an interessting project. Thank you for supporting me and giving me helpful and constructive advices when needed. Secondly—however, most importantly—I would like to thank Stefan Plott for guiding me threw my research, teaching me so many great techniques, reaching me a hand when needed and letting me try all of my ideas so I could figure out a way of my own. Thank you for cheering me up, watching my plants and just being around! You have been a great supervisor! Thank you Madeleine, for introducing me into the wonderful world of plant tissue cultures and for always helping me when Stefan wasn't around. Thank you to Martin and Patrick for showing me where to find stuff—even if I asked repeatedly. Last but not least, I'd like to thank Luigi for making any challenging lab day quite a bit more fun.

Development of cloning strategy and primer design (sgRNA) was done by Mag. Dr. Alois Schweighofer (May Perutz Labs) and Madeleine Schnurer (CELBICS). Confocal microscopy was performed at the Core Facility Cell Imaging and Ultrastructure Research, University of Vienna - member of the Vienna Life-Science Instruments (VLSI). pHUE411 was a gift from Qi-Jun Chen (Addgene plasmid #62203 ; `http://n2t.net/addgene:62203`; RRID:Addgene_62203). I would like to express my special thanks to Martin Dockner for introducing me to LaTeX and providing the document template for this master's thesis.

Zusammenfassung

Die vorliegende Arbeit zielte darauf ab, eine vollständige *Agrobacterium*-vermittelte Transformationspipeline für Gerste (cv. Golden Promise) zu optimieren, um dabei stabile CRISPR/Cas9-Knockout-Linien für einzelne *HvTol*-Gene zu erzeugen. Die TOL-Proteinfamilie fungiert als funktionelles Äquivalent von ESCRT-0 in der endosomalen Sortierung und spielt eine wichtige Rolle während der Kornentwicklung, wobei die spezifischen Funktionen der einzelnen Familienmitglieder in Gerste weitgehend unbekannt sind.

Insgesamt wurden vier CRISPR/Cas9-Konstrukte (pHUE411-*HvTol1*, -*HvTol2*, -*HvTol3*, -*HvTol8*) mittels Golden Gate-Klonierung erfolgreich generiert und durch Restriktionsanalyse sowie Sangersequenzierung validiert. Bei der Validierung dieser Konstrukte in transienten Transformationsexperimenten in *Nicotiana tabacum* konnte diesen dabei keine Aktivität anhand einer signifikanten Reduktion der GFP-Fluoreszenz zugesprochen werden. Dies ist vermutlich in einer unzureichenden Aktivität der expressionssteuernden monokotyledonen Promotoren in einem dikotyledonen Wirt begründet und konnte nicht auf eine unzureichende Funktion des CRISPR-Systems zurückgeführt werden.

Die stabile Transformation wurde über mehrere experimentelle Durchläufe etabliert, von denen die zwei erfolgreichsten hier dargestellt werden und erzielten mehrere methodische Fortschritte: die eingeführte Timentin-Behandlung eliminierte *Agrobacterium*-Überwuchs effektiv, und modifiziertes Transitionsmedium (TM2) verbesserte die Sprossregeneration deutlich gegenüber dem ursprünglichen TM-Medium. Zum ersten Mal wurden in diesem Labor Gerstenpflanzen erfolgreich aus Gewebekultur bis zur Bodenkultur regeneriert.

PCR-Screening aller Regeneranten ergab jedoch keine Nachweise für stabile Transgen-Integration. Mehrere Faktoren wurden dabei als Ursachen identifiziert: zum einen die Verwendung des nicht-hypervirulenten *Agrobacterium*-Stammes GV3101 anstelle von AGL1, zum anderen überdimensionierte Embryonen (3.0–3.5 mm statt 1.5–2.0 mm), zusätzlich wurde die Hygromycin-Aktivität durch wiederholte Gefrier-Tau-Zyklen kompromittiert, wodurch die Selektion in späteren Regenerationsstadien ausblieb.

Trotz alledem liefert diese Arbeit eine funktionale Transformationspipeline mit klar identifizierten Optimierungspunkten für zukünftige Experimente, einschließlich der Verwendung von

AGL1, strenger Embryogrößenselektion, frisch aliquotiertem Hygromycin und kontinuierlicher Selektion während aller Kulturstadien, sowie den erarbeiteten methodischen Fortschritten.

Abstract

This study aimed to optimize a complete *Agrobacterium*-mediated transformation pipeline for barley (cv. Golden Promise) to generate stable CRISPR/Cas9 knockout lines targeting individual *HvTol* genes. The TOL protein family functions as the plant equivalent of ESCRT-0 in endosomal sorting and plays an important role during grain development, yet the specific contributions of individual family members remain largely unknown.

A total of four CRISPR/Cas9 constructs (pHUE411-*HvTol1*, -*HvTol2*, -*HvTol3*, -*HvTol8*) were successfully generated via Golden Gate cloning and validated by restriction analysis and Sanger sequencing. When validated in transient transformation experiments in *Nicotiana tabacum*, no activity could be attributed to these constructs based on GFP fluorescence reduction, likely due to insufficient activity of monocot-derived promoters in the dicot host, rather than insufficient function of the CRISPR system itself.

Stable transformation was established over several experimental runs, the two most successful of which are presented here, achieving several methodological advances: timentin treatment effectively eliminated *Agrobacterium* overgrowth, and modified transition medium (TM2) substantially improved shoot regeneration compared to the original TM formulation. For the first time in this laboratory, barley plants were successfully regenerated from tissue culture to soil.

However, PCR screening of all regenerants revealed no evidence of stable transgene integration. Several contributing factors were identified: (i) use of the non-hypervirulent *Agrobacterium* strain GV3101 instead of AGL1, (ii) oversized embryos (3.0–3.5 mm instead of 1.5–2.0 mm), (iii) compromised hygromycin activity due to repeated freeze-thaw cycles, and (iv) removal of selection during later regeneration stages. This work provides a functional transformation pipeline with clearly identified optimization points for future experiments, including the adoption of AGL1, strict embryo size selection, freshly aliquoted hygromycin, and continuous selection throughout all culture stages, as well as the methodological advances established herein.

1 Introduction

Barley (*Hordeum vulgare*, L.) is considered to be among the earliest crops to have been cultivated, with domestication dating back approximately 10,000 years to the Fertile Crescent (Pourkheirandish & Komatsuda, 2007). Its cultivated form, *H. vulgare* ssp. *vulgare*, descended from the wild relative *H. vulgare* ssp. *spontaneum* C. Koch. Both are annual diploids classified in the tribe Triticeae of the grass family Poaceae (Devos, 2005; Pourkheirandish & Komatsuda, 2007).

Today, barley is the fourth most widely grown cereal globally, after wheat, maize, and rice (Zeng et al., 2020). It is cultivated in around 100 countries and is used as livestock feed, for malting and brewing, and as a food source in many traditional diets (Zeng et al., 2020; Zhang et al., 2023). As a group, cereals supply roughly half of all calories consumed worldwide, delivering substantial amounts of protein, dietary fibre, and micronutrients (Bouchard et al., 2022; Prasadi & Joye, 2020). Among them, barley is notable for its capacity to thrive under a wide range of environmental conditions, from cool maritime climates to drought-prone semi-arid zones (Kosová et al., 2023). Its diploid genome of approximately 5.1 gigabases, organised across seven chromosomes, is considerably less complex than the hexaploid genome of wheat, making barley a particularly accessible model for genetic and genomic studies (Mascher et al., 2017), which becomes increasingly important in light of the growing pressures that climate change exerts on cereal agriculture. Heat waves, water scarcity, salinisation and irregular rainfall are expected to reduce yields across major production areas (Kosová et al., 2023; Teng et al., 2023). Such stresses can be particularly disruptive during grain filling, the phase in which the endosperm accumulates starch and storage proteins that largely define final grain mass and nutritional value (Sreenivasulu et al., 2010; Teng et al., 2023). As global food demand rises with population growth alongside it, developing high-productivity cultivars that maintain stable yields under increasingly adverse conditions has become one of the central challenges in crop science (Shahinnia, Carrillo & Hajirezaei, 2021).

Targeted genome editing, most notably the CRISPR/Cas9 system (Jinek et al., 2012), provides a powerful tool to tackle this challenge. By enabling precise alterations at defined genomic loci, it allows researchers to analyse and enhance traits such as drought tolerance, pathogen

resistance, and grain quality (Ahmar, Hensel & Gruszka, 2023; Erdoğan, Cevher-Keskin, Bilir, Hong & Tör, 2023). However, applying genome editing effectively requires a thorough understanding of the biological processes one aims to modify. In the context of barley grain development, the endosomal sorting machinery is of particular interest, as its role in protein trafficking during grain filling remains largely uncharacterised (Roustan et al., 2020).

1.1 Endosomal sorting and the role of TOL proteins in plants

In eukaryotic cells, plasma membrane proteins that are no longer needed, or must be down-regulated, are removed from the cell surface by endocytosis and directed to the lysosome, or in plants to the lytic vacuole, for degradation. The principal sorting signal that marks a membrane protein for this degradative route is the covalent attachment of ubiquitin (Paez Valencia, Goodman & Otegui, 2016). Along the endosomal pathway, ubiquitinated cargo is recognised by a series of protein complexes collectively known as the Endosomal Sorting Complex Required for Transport (ESCRT) machinery, which sorts the cargo into intraluminal vesicles (ILVs) of multivesicular bodies (MVBs). Upon MVBs fusing with the vacuole, the ILVs and their contents are released into the lumen and degraded by resident hydrolases (Henne, Buchkovich & Emr, 2011; Vietri, Radulovic & Stenmark, 2020).

The canonical ESCRT machinery comprises four hetero-oligomeric complexes: ESCRT-0, -I, -II and -III – together with the AAA-ATPase Vps4/SKD1, which recycles ESCRT components back into the cytosol after each round of vesicle formation (Hurley, 2010). In yeast and metazoans, ESCRT-0 initiates the pathway by clustering ubiquitinated cargo on the endosomal membrane via its VHS and ubiquitin-interaction (UIM) domains. ESCRT-I and ESCRT-II then cooperate to deform the membrane into a bud, while ESCRT-III polymerises into filaments that drive the constriction and scission of the vesicle (Henne et al., 2011; Vietri et al., 2020). While ESCRT-I, -II and -III are well conserved in plants, the same is not true for ESCRT-0. The complex is built around the Vps27/Hse1 and Hrs/STAM heterodimers in yeast and mammals, respectively—proteins whose VHS and ubiquitin-binding domains enable them to act as the initial receptors for ubiquitinated cargo (Hurley, 2010; Paez Valencia et al., 2016). Despite extensive homology searches, no proteins with a comparable domain architecture have been identified in any sequenced plant genome (Gao, Zhuang, Shen & Jiang, 2017; Paez Valencia et al., 2016). Instead, plants encode a family of TOM1-like (TOL) proteins that carry similar VHS and GAT domains. Interaction studies in *Arabidopsis thaliana* have shown that these proteins bind ubiquitin directly and function as receptors in the early steps of the ESCRT pathway, strongly suggesting that they fulfil the cargo-recognition role of ESCRT-0 (Korbei et al., 2013; Moulinier-Anzola et al., 2020). In

Arabidopsis, nine TOL genes (*TOL1–TOL9*) have been identified, all of which encode proteins carrying these VHS and, in most cases, GAT domains (Korbei et al., 2013; Moulinier-Anzola et al., 2020). These properties allow TOL proteins to localise to both the plasma membrane and endosomal compartments, where they mediate the ubiquitin-dependent internalisation and vacuolar degradation of cargo proteins such as the auxin efflux carrier PIN2 (Korbei et al., 2013). While the TOL family as a whole mediates this process, individual members differ in their subcellular distribution and in the types of ubiquitin linkage they preferentially recognise, suggesting a degree of functional specialisation within the family despite substantial overlap (Moulinier-Anzola et al., 2020). As they are broadly expressed across *Arabidopsis* organs including roots, stems, leaves, flowers and siliques (Moulinier-Anzola, De-Araujo & Korbei, 2014), the TOL family thus appears to serve a constitutive role in membrane protein turnover—yet how this role is partitioned among individual members remains an open question.

While the TOL–ESCRT axis has been studied primarily in *Arabidopsis*, recent work has begun to reveal its relevance for cereal grain development. In a proteomics study that set out to characterise the endomembrane-associated protein landscape during grain filling, Roustan et al. (2020) identified homologues of the *Arabidopsis* TOL1, TOL2, TOL3 and TOL8 proteins, alongside several ESCRT-III subunits and the disassembly ATPase VPS4, amongst a broader set of proteins whose abundance changed significantly during this process. The TOL homologues were most abundant during early development (6–10 days after pollination) except TOL3, which peaked at the mid-storage stage (10–12 DAP) together with the ESCRT-III subunits SNF7.1 and SNF7.2, while VPS4 accumulated progressively until late development (Roustan et al., 2020). Additionally, transmission electron microscopy and live-cell imaging of transgenic reporter lines confirmed that MVBs are present in the vicinity of protein bodies in the starchy endosperm (Roustan et al., 2020). These protein bodies undergo extensive fusion during endosperm maturation (Ibl, Kapusi, Arcalis, Kawagoe & Stoger, 2014), a process that the ESCRT-III subunit HvSNF7 appears to follow—first localising to vesicular structures associated with individual protein bodies, and later appearing inside fused ones (Roustan et al., 2020). Alongside this, a cell-layer-specific distribution of the ESCRT-III component HvVPS60 in developing barley grains was reported by Hilscher, Kapusi, Stoger und Ibl (2016). Overall, these findings suggest that the ESCRT machinery, and by extension its upstream TOL-mediated cargo recognition step, is actively involved in the protein sorting events that shape storage organelle biogenesis during grain filling.

Despite these advances, the specific contribution of individual *HvTol* genes to endosomal sorting in barley remains unknown. The TOL family is characterised by a degree of functional redundancy, as demonstrated by the observation that single *tol* mutants in *Arabidopsis* typically exhibit mild phenotypes, whereas higher-order knockouts produce increasingly severe defects

(Korbei et al., 2013; Moulinier-Anzola et al., 2020). Dissecting the role of each family member therefore requires the generation of individual knockout lines that can be phenotypically characterised in isolation and, in the longer term, combined into multi-gene knockouts. In barley, no such lines currently exist. Generating them by stable CRISPR/Cas9-mediated transformation is thus a prerequisite for functional studies of the TOL–ESCRT pathway in cereal crops and constitutes one of the central objectives of the present work.

1.2 CRISPR/Cas9-mediated genome editing

The CRISPR (Clustered Regularly Interspaced Short Palindromic Repeats)/Cas9 system originated as an adaptive immune mechanism in bacteria and archaea, where it provides sequence-specific defence against invading phage and plasmid DNA (Jinek et al., 2012). In its natural form, short fragments of foreign DNA are incorporated into the host CRISPR locus and are later transcribed into CRISPR RNAs (crRNAs). Together with a trans-activating crRNA (tracrRNA), these crRNAs guide the Cas9 endonuclease to complementary target sequences for cleavage. Jinek et al. (2012) demonstrated that these two RNA components can be fused into a single chimeric molecule—the single guide RNA (sgRNA)—without loss of targeting activity, thereby establishing the foundation for programmable genome editing.

The sgRNA comprises a 20-nucleotide spacer sequence at its 5′ end, which determines target specificity through Watson–Crick base pairing, and a conserved scaffold that mediates association with Cas9. Target recognition also requires the presence of a short protospacer adjacent motif (PAM) immediately downstream of the target site. For the widely used *Streptococcus pyogenes* Cas9 (SpCas9), this motif has the sequence 5′-NGG-3′ (Basu et al., 2022; Jinek et al., 2012). Upon binding, the two catalytic domains of Cas9—HNH and RuvC—each cleave one strand of the target DNA, generating a blunt-ended double-strand break (DSB) approximately three nucleotides upstream of the PAM (Jinek et al., 2012).

Cells repair DSBs primarily through two competing pathways. Non-homologous end joining (NHEJ) is the predominant route in plant somatic cells; it is error-prone and frequently introduces small insertions or deletions (indels) at the break site (Basu et al., 2022; Xing et al., 2014). When such indels occur within a protein-coding exon, they can shift the reading frame and produce a premature stop codon, effectively knocking out gene function. Alternatively, homology-directed repair (HDR) can incorporate a supplied donor template to achieve precise sequence modifications, but its efficiency in plant cells remains low, making NHEJ-mediated knockout the standard strategy for loss-of-function studies (Ahmar et al., 2023; Basu et al., 2022).

Since its initial adaptation for eukaryotic genome editing, CRISPR/Cas9 has been applied

extensively in cereal crops. Successful targeted mutagenesis has been reported in rice, wheat, maize, and barley for traits including disease resistance, drought and salt tolerance, grain quality, and yield-related parameters (Ahmar et al., 2023; Basu et al., 2022; Erdoğan et al., 2023). In barley specifically, the system has been used to knock out genes involved in grain development and stress responses, taking advantage of the diploid genome, which simplifies the recovery of homozygous mutant lines compared to polyploid species such as wheat (Ahmar et al., 2023).

A prerequisite for CRISPR/Cas9-mediated editing in any plant species is the delivery of both the Cas9 nuclease and the sgRNA into the target cells, typically via a binary T-DNA vector introduced by *Agrobacterium*-mediated transformation. The vector used in the present study, pHUE411, was designed specifically for monocot applications (Xing et al., 2014). It drives Cas9 expression from the maize ubiquitin 1 (ZmUbi1) promoter, a strong constitutive promoter whose activity in grasses substantially exceeds that of the commonly used CaMV 35S promoter (Christensen, Sharrock & Quail, 1992). The sgRNA, in turn, is transcribed from the rice U3 small nuclear RNA promoter (OsU3), which recruits RNA polymerase III and produces a precisely defined, non-polyadenylated transcript (Xing et al., 2014). Target-specific spacer sequences are inserted into the sgRNA cassette by a single Golden Gate cloning step using the type IIS restriction enzyme *Bsa*I, enabling rapid and modular assembly of constructs directed against different genomic loci (Xing et al., 2014).

1.3 *Agrobacterium*-mediated transformation of barley

Agrobacterium tumefaciens is a Gram-negative soil bacterium that possesses the natural ability to transfer a defined segment of DNA—the T-DNA—from its tumour-inducing (Ti) plasmid into the nuclear genome of plant cells (Gelvin, 2017; Lacroix & Citovsky, 2013). In the wild-type bacterium, the T-DNA carries oncogenes that reprogram host cells to proliferate and produce opines—small molecules that serve as nutrients for the bacterium. For biotechnological applications, these oncogenes are replaced by genes of interest on a small, easily manipulated binary vector, while the virulence (*vir*) genes required for T-DNA processing and transfer are maintained on a separate, disarmed helper plasmid within the same *Agrobacterium* cell (Gelvin, 2012, 2017).

The T-DNA transfer process is initiated when phenolic compounds released from wounded plant tissue are perceived by the bacterial two-component regulatory system VirA/VirG (Stachel, Messens, Montagu & Zambryski, 1985; Stachel & Zambryski, 1986). VirA, a transmembrane histidine kinase, recognises signal molecules such as acetosyringone and autophosphorylates at a conserved histidine residue. The phosphoryl group is then transferred to the response regulator VirG. In its activated form, VirG binds to conserved *vir*-box motifs in the promoters of the

remaining *vir* operons, thereby triggering the expression of the complete T-DNA transfer machinery (Jin, Prusti, Roitsch, Ankenbauer & Nester, 1990; Jin, Roitsch, Ankenbauer, Gordon & Nester, 1990; Winans, Kerstetter & Nester, 1988). Key downstream effectors include the VirD1/VirD2 endonuclease complex, which nicks the T-DNA border sequences and generates a single-stranded transfer intermediate (T-strand), and VirE2, a single-stranded DNA-binding protein that coats and protects the T-strand inside the host cell (Gelvin, 2012; Stachel, Timmerman & Zambryski, 1986).

Agrobacterium was historically regarded as a pathogen of dicotyledonous plants, and monocots were long considered outside its natural host range. A central reason for this limitation is that monocotyledonous species do not release acetosyringone-type phenolics upon wounding, and therefore fail to induce the *vir* regulon efficiently (Hwang, Yu & Lai, 2017; Stachel et al., 1985). This barrier was overcome by supplementing co-cultivation media with synthetic acetosyringone, a strategy that enabled the first reproducible Agrobacterium-mediated transformation of rice in 1994. This has since become standard practice for cereals, including maize, wheat and barley (Azizi-Dargahlou & Pouresmaeil, 2024; Hwang et al., 2017).

Another factor affecting transformation success is the virulence capacity of the *Agrobacterium* strain. Strains carrying the pTiBo542 Ti plasmid, such as AGL1, are termed hypervirulent because they harbour an extended set of *vir* genes—including additional copies of *virB* and *virG* as well as the accessory locus *virH*—that collectively enhance T-DNA transfer frequency several-fold compared to standard-virulence strains (Haryono et al., 2019; Lazo, Stein & Ludwig, 1991). Comparative studies in barley have confirmed that AGL1 yields substantially higher transformation efficiencies than strains such as GV3101 or LBA4404, making it the recommended choice for this species (Murray, Brettell, Matthews, Bishop & Jacobsen, 2004; Tingay et al., 1997).

In barley, *Agrobacterium*-mediated transformation was first demonstrated by Tingay et al. (1997) using the spring cultivar Golden Promise. This cultivar remains the standard genotype for barley transformation, due to its favourable combination of genetic and physiological traits. Quantitative trait locus mapping has identified at least two major transformation amenability (TFA) loci on chromosomes 2H and 3H that together account for a large proportion of the heritable variation in transformability (Hisano et al., 2017). At the cellular level, Golden Promise immature embryos maintain comparatively high endogenous ratios of auxin to cytokinin, which promote callus proliferation and subsequent shoot regeneration (Hisano, Matsuura, Mori, Yamane & Sato, 2016; F. Wang et al., 2023). Under optimized conditions, transformation efficiencies of 9–25% have been reported for this cultivar across different laboratories (Bartlett, Alves, Smedley, Snape & Harwood, 2008; Harwood et al., 2009).

The standard barley transformation pipeline begins with the isolation of immature zygotic

embryos, typically 12–16 days after pollination and measuring 1.5–2.0 mm (Y. Chang, Zitzewitz, Hayes & Chen, 2003; Harwood et al., 2009). Embryo size is a critical parameter: embryos within this size range harbour a high proportion of actively dividing scutellar cells that are competent for both T-DNA uptake and subsequent callus formation. In contrast, oversized embryos tend to germinate prematurely and resist dedifferentiation (Y. Chang et al., 2003). After co-cultivation with *Agrobacterium*, the embryos are transferred to a callus induction medium (CIM) containing the synthetic auxin 2,4-dichlorophenoxyacetic acid (2,4-D) and a selective agent. The most common selective agent is the aminoglycoside antibiotic hygromycin B, which is conferred by the hpt marker gene carried on the T-DNA (Harwood et al., 2009). Surviving calli are moved through a transition phase with reduced auxin and added cytokinin to promote green spot formation, and then to a hormone-free regeneration medium on which shoots elongate (Harwood et al., 2009; F. Wang et al., 2023). Regenerated plantlets are rooted on a separate medium before transfer to soil. The entire process from embryo isolation to soil-grown plants spans approximately three to four months (Harwood et al., 2009).

Taken together, barley represents a cereal crop of considerable economic and scientific importance whose grain development depends, among other factors, on endosomal sorting processes that are only beginning to be understood at the molecular level. The TOL protein family occupies a key position in this pathway as the functional equivalent of ESCRT-0, yet the individual contribution of each *HvTol* gene remains uncharacterized. CRISPR/Cas9-mediated knockout of single family members offers a direct route to dissect their functions, but generating such lines in barley requires a reliable and efficient *Agrobacterium*-mediated stable transformation pipeline—a technically demanding process whose optimization constitutes the central focus of the work described in the following chapters.

2 Aim of this study

The long-term goal of the CELBICS research group is to elucidate the individual functions of the barley TOL protein family members during grain development by generating stable single-gene knockout lines through CRISPR/Cas9-mediated genome editing. A previous attempt to establish this workflow encountered two major obstacles: persistent *Agrobacterium* overgrowth that compromised embryo viability during co-cultivation, and poor regeneration capacity of the resulting calli, which failed to produce surviving plantlets. No plants could be recovered and transferred to soil.

The primary aim of the present work was therefore to overcome these limitations and establish a functional *Agrobacterium*-mediated transformation pipeline for barley cv. Golden Promise that reliably yields viable, soil-grown plants. Over the course of multiple transformation runs, co-cultivation and selection conditions were iteratively adjusted, with particular attention to suppressing bacterial overgrowth and improving callus-to-plant regeneration.

To this end, four CRISPR/Cas9 constructs targeting *HvTol1*, *HvTol2*, *HvTol3*, and *HvTol8* were assembled in the monocot-optimized binary vector pHUE411 via Golden Gate cloning. Construct integrity was verified by transient expression in *Nicotiana tabacum*, and the constructs were introduced into immature barley embryos by *Agrobacterium*-mediated transformation. Regenerated plants were screened by polymerase chain reaction (PCR) for T-DNA integration, with the ultimate objective of identifying transgenic individuals carrying targeted mutations in individual *HvTol* genes thereby demonstrating the complete functionality of the transformation pipeline from construct delivery to stable genomic integration.

3 Materials and Methods

3.1 Materials

3.1.1 Chemicals, additives and solutions

All chemicals, additives, and consumables used in this study were purchased from commercial suppliers unless stated otherwise.

3.1.2 Buffers and media

Table 3.1: Composition of LB medium

Component	Working concentration	Supplier	CAS No.
Peptone	10 g/L	Sigma Aldrich	73049-73-7
Yeast extract	5 g/L	Duchefa Biochemie	8013-01-2
NaCl	10 g/L	Sigma Aldrich	7647-14-5

All reagents were dissolved in Milli-Q filtered water and autoclaved at 121 °C for 20 min. The pH was adjusted to 7.0 using 0.1 M KOH. For solid media, gellan gum or agarose was added prior to autoclaving. The plates and liquid medium were stored at 4 °C.

Table 3.2: Composition of infiltration medium

Component	Working concentration	Supplier	CAS No.
MES	10 mM	Carl ROTH	4432-31-9
$MgSO_4$	10 mM	Sigma Aldrich	10034-99-8
Acetosyringone	150 µM	Sigma Aldrich	2478-38-8

All reagents were dissolved in Milli-Q filtered water and filter sterilized. The medium was stored at 4 °C.

Table 3.3: 100× vitamin stock for callus-inducing medium (CIM)

Component	Working concentration	Supplier	CAS No.
Thiamine HCl	100 mg/L	Sigma Aldrich	67-03-8
Myo-inositol	35 g/L	Sigma Aldrich	87-89-8
Proline	69 g/L	Sigma Aldrich	147-85-3

All reagents were dissolved in Milli-Q filtered water and filter sterilized. The stock solution was stored at 4 °C.

Table 3.4: 100× vitamin stock for transition (TM) and regeneration (RM) media

Component	Working concentration	Supplier	CAS No.
Thiamine HCl	40 mg/L	Sigma Aldrich	67-03-8
Myo-inositol	10 g/L	Duchefa Biochemie	87-89-8

All reagents were dissolved in Milli-Q filtered water and filter sterilized. The stock solution was stored at 4 °C.

Table 3.5: $CuSO_4$ stock solution

Component	Working concentration	Supplier	CAS No.
$CuSO_4 \cdot 5H_2O$	1.25 g/L	Sigma Aldrich	7758-99-8

The reagent was dissolved in Milli-Q filtered water and filter sterilized. The stock solution was stored at -20 °C.

Table 3.6: Dicamba stock solution

Component	Working concentration	Supplier	CAS No.
Dicamba	50 mg/L	Duchefa Biochemie	1918-00-9

The reagent was dissolved in Milli-Q filtered water and filter sterilized. The stock solution was aliquoted and stored at -20 °C.

Table 3.7: 6-benzylaminopurine (BAP) stock solution

Component	Working concentration	Supplier	CAS No.
6-benzylaminopurine	1 mg/mL	Sigma Aldrich	1214-39-7

The reagent was dissolved in Milli-Q filtered water with the addition of NaOH and filter sterilized. The stock solution was stored at -20 °C.

Table 3.8: Biotin stock solution

Component	Working concentration	Supplier	CAS No.
Biotin	0.1 mg/L	Duchefa Biochemie	58-85-5

The reagent was dissolved in Milli-Q filtered water and filter sterilized. The stock solution was stored at 4 °C.

Table 3.9: Composition of MG/L medium

Component	Working concentration	Supplier	CAS No.
Tryptone	5 g/L	Duchefa Biochemie	91079-40-2
Mannitol	5 g/L	Duchefa Biochemie	69-65-8
Yeast extract	2.5 g/L	Duchefa Biochemie	8013-01-2
L-glutamic acid	1 g/L	Sigma Aldrich	56-86-0
KH_2PO_4	250 mg/L	Carl ROTH	7778-77-0
NaCl	100 mg/L	Sigma Aldrich	7647-14-5
$MgSO_4 \cdot 7H_2O$	100 mg/L	Sigma Aldrich	10034-99-8
Biotin stock	10 µL/L	–	–

All reagents were dissolved in Milli-Q filtered water and autoclaved at 121 °C (15 psi) for 20 min. The pH was adjusted to 7.2 using NaOH before autoclaving. For solid medium, gellan gum or agarose was added prior to autoclaving. The plates and liquid medium were stored at 4 °C.

Table 3.10: Composition of callus-inducing medium (CIM)

Component	Working concentration	Supplier	CAS No.
Murashige and Skoog plant salt base (M0221)	4.3 g/L	Duchefa Biochemie	–
Maltose	30 g/L	Duchefa Biochemie	6363-53-7
Casein hydrolysate	1 g/L	Duchefa Biochemie	9000-71-9
CIM vitamin stock	10 mL/L	–	–
Dicamba	2.5 mg/L	–	–
$CuSO_4 \cdot H_2O$	1.25 mg/L	–	–
Gellan gum	2–3% (w/v)	Thermo Scientific	71010-52-1

All components were dissolved in Milli-Q filtered water and autoclaved at 121 °C (15 psi) for 20 min. The pH was adjusted to 5.8 using NaOH before autoclaving. $CuSO_4$, CIM vitamin stock, dicamba, as well as timentin and hygromycin (at working concentrations) were added after autoclaving under sterile conditions in a laminar flow hood. Antibiotics were added only when required. Plates were stored at 4 °C.

Table 3.11: Composition of transition media (TM), modified transition media (TM2) and regeneration medium (RM)

Component	TM (working conc.)	TM2 (working conc.)	RM (working conc.)	Supplier	CAS No.
Murashige and Skoog plant salt base (M0238)	2.7 g/L	2.7 g/L	2.7 g/L	Duchefa Biochemie	–
Maltose	20 g/L	20 g/L	20 g/L	Duchefa Biochemie	6363-53-7
NH_4NO_3	165 mg/L	165 mg/L	165 mg/L	–	–
Glutamine	750 mg/L	750 mg/L	750 mg/L	–	–
TM/RM vitamin stock	10 mL/L	10 mL/L	10 mL/L	–	–
2,4-dichlorophenoxyacetic acid	2.5 mg/L	0.25 mg/L	–	Duchefa Biochemie	94-75-7
$CuSO_4$	1.25 mg/L	1.25 mg/L	–	–	–
6-benzylaminopurine	0.1 mg/L	1.0 mg/L	–	–	–
Gellan gum	2–3% (w/v)	2–3% (w/v)	2–3% (w/v)	Thermo Scientific	71010-52-1

All components were dissolved in Milli-Q filtered water and autoclaved at 121 °C (15 psi) for 20 min. The pH was adjusted to 5.8 using NaOH before autoclaving. $CuSO_4$, TM/RM vitamin stock, 2,4-dichlorophenoxyacetic acid, 6-benzylaminopurine, as well as timentin and hygromycin (at working concentrations) were added after autoclaving under sterile conditions in a laminar flow hood. Antibiotics were added only when required. Plates were stored at 4 °C.

Table 3.12: Antibiotics used in this study

Antibiotic	Working conc. (µg/mL)	Solvent	Supplier	CAS No.
Kanamycin	50	Milli-Q H_2O	Carl ROTH	25389-94-0
Hygromycin	50	PBS	Roche	31282-04-9
Timentin	160	Milli-Q H_2O	Duchefa Biochemie	4697-14-7
Gentamycin	20	Milli-Q H_2O	Carl ROTH	1405-41-0
Tetracycline	5	Milli-Q H_2O	Carl ROTH	64-75-5
Rifampicin	25	DMSO	Carl ROTH	13292-46-1

Stock solutions were aliquoted and stored at -20 °C.

3.1.3 Enzymes, markers and kits

Table 3.13: Kits used in this study

Kit	Use	Supplier	Catalog No.
Phire™ Plant Direct PCR Master Mix	DNA extraction and PCR	Thermo Scientific	F160L
PureYield™ Plasmid Miniprep System	DNA purification	Promega	A1221

Table 3.14: Plasmids, restriction enzymes and buffers used in this study

Name	Supplier	Catalog No.
BsaI-HFv2	New England Biolabs	R3733S
T4 DNA ligase (HF)	Thermo Scientific	EL0014
pHUE411	–	–
HindIII-HF	New England Biolabs	R3104S
rCutSmart buffer	New England Biolabs	–
T4 DNA Ligase Buffer	Thermo Scientific	–

Corresponding buffers were used according to manufacturers description.

3.1.4 Oligonucleotides

Table 3.15: Oligonucleotides used in this study

Name	Sequence (5'-3')
HvTOL1-spacer-BsaI-BsaI-fwd	TGGTCTCGGGCGCCCTTACGCTCATTGAAGCGGTTTGGAGACCA
HvTOL1-spacer-BsaI-BsaI-rev	TGGTCTCCAAACCGCTTCAATGAGCGTAAGGGCGCCCGAGACCA
HvTOL2-spacer-BsaI-BsaI-fwd	TGGTCTCGGGCGAGAGCCAGGTACTGCACCCTGTTTGGAGACCA
HvTOL2-spacer-BsaI-BsaI-rev	TGGTCTCCAAACAGGGTGCAGTACCTGGCTCTCGCCCGAGACCA
HvTOL3-spacer-BsaI-BsaI-fwd	TGGTCTCGGGCGGCGACGAGCGACATGCTGATGTTTGGAGACCA
HvTOL3-spacer-BsaI-BsaI-rev	TGGTCTCCAAACATCAGCATGTCGCTCGTCGCCGCCCGAGACCA
HvTOL8-spacer-BsaI-BsaI-fwd	TGGTCTCGGGCGCGATCGACCAGGATGGACTGGTTTGGAGACCA
HvTOL8-spacer-BsaI-BsaI-rev	TGGTCTCCAAACCAGTCCATCCTGGTCGATCGCGCCCGAGACCA
Cas9fw	GCGCAATGAGATTCCCGAAC
Cas9rv	ACTAACTCTGTTGGCTGGGC
HygR-F	GCCGATCTTAGCCAGACGAG
HygR-R	CATATACGCCCGGAGTCGTG
Hv_hsp90-F	GCAAGAAGGCTGTGGAGAAC
Hv_hsp90-R	CAAGCTTCTTGCCCTCAAAC
M13	TGTAAAACGACGGCCAG

Oligos were purchased from Microsynth AG.

3.1.5 Organisms

Table 3.16: *Hordeum vulgare* lines used in this study

Line	Supplier
Golden Promise	–

Table 3.17: Microbial strains used in this study

Organism	Strain	Use
Escherichia coli	TOP10	Cloning and plasmid propagation
Agrobacterium tumefaciens	GV3101	Plant transformation

3.1.6 Instruments, software and websites

Table 3.18: Instruments used in this study

Instrument	Name	Supplier
Thermocycler	T Professional Thermocycler	Biometra
Thermocycler	T Advanced	Biometra
Thermocycler	Verti 96 Well Thermal Cycler	Applied Biosystems
Centrifuge	Multifuge 4KR Centrifuge	Heraeus
Centrifuge	5417 R	Eppendorf
Gel Analyzer	iBright FL1500	Invitrogen
Nano Drop	Nano Photometer N60	Thermo Scientific
Confocal laser scanning microscope	TCS SP8	Leica

Table 3.19: Software and online tools used in this study

Name	Version / Link	Use
RStudio	2025.09.2+418	Statistical evaluation
ImageJ	1.53k	Image analysis
Excel	Build 16.0.19725.20126	Table calculation
Overleaf	`https://www.overleaf.com/`	Text editing
Inkscape	1.3.2	Picture editing
Powerpoint	Build 16.0.19725.20126	Figure assembly
DeepL	26.2.1	Translation assistance
Claude	`https://claude.ai/`	Code troubleshooting, Text formulation assistance
Anara	`https://anara.com/`	Literature management
JabRef	5.15	Literature management
Benchling	`https://benchling.com/`	*in silicio* cloning

3.2 Methods

3.2.1 Vector Construction, Molecular Cloning, and Nucleic Acid Analysis

To enable targeted genome editing and subsequent functional analysis of individual *HvTol* genes, CRISPR/Cas9-based vectors were developed. Guide RNA (gRNA) sequences were designed to specifically target individual members of the *HvTol* gene family, enabling generation of single knockout lines while avoiding potential confounding effects from simultaneous disruption of

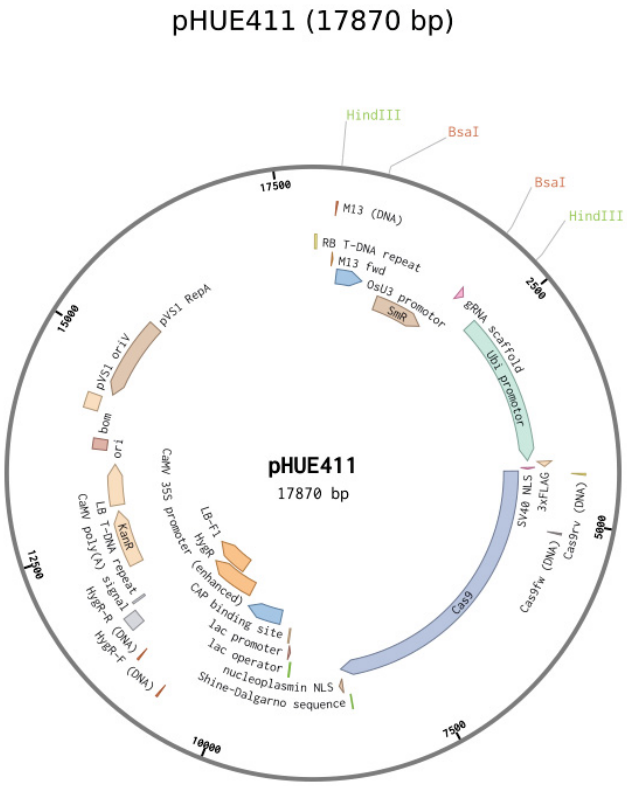

Figure 3.1: pHUE411 plasmid map.
Plasmid map of binary vector pHUE411 created with Benchling.

multiple family members. Development of the cloning strategy as well as primer design (sgRNA) was done by Mag. Dr. Alois Schweighofer (May Perutz Labs) and Madeleine Schnurer (CELBICS).

The binary vector pHUE411 (Xing et al., 2014) served as the backbone for all constructs. pHUE411 was a gift from Qi-Jun Chen (Addgene plasmid # 62203 ; http://n2t.net/addgene:62203; RRID:Addgene_62203). This vector comprises a constitutively expressed Cas9 nuclease and a gRNA expression cassette. Cas9 expression is driven by the maize (*Zea mays*) ubiquitin promoter (*ZmUbi1*), encoding a codon-optimized Cas9 nuclease (zCas9) equipped with multiple nuclear localization signals and a $3\times$FLAG tag (Figure 3.1). The gRNA expression cassette is controlled by the promoter and terminator of the rice (*Oryza sativa*) small nuclear RNA *OsU3*. Target-specific spacer sequences can be introduced into the gRNA scaffold by Golden Gate cloning using *BsaI*. The vector contains a hygromycin resistance marker for plant selection and a kanamycin resistance gene for bacterial selection.

Four single knockout constructs targeting different *HvTol* family members were generated: pHUE411-*HvTol1* (Figure 3.2), pHUE411-*HvTol2* (Figure 7.1), pHUE411-*HvTol3* (Figure 7.2), and pHUE411-*HvTol8* (Figure 7.3).

3.2.1.1 Construction of *HvTol*-targeting vectors

Gene-specific spacer sequences were introduced into the pHUE411 vector backbone via Golden Gate assembly as described in Section 3.2.1.2. For each target gene, complementary oligonucleotides encoding the 20-nucleotide spacer sequence flanked by *BsaI* recognition sites were designed (Table 3.15). Oligonucleotides were annealed and assembled into the linearized pHUE411 vector using the restriction–ligation protocol described in Section 3.2.1.3.

Following Golden Gate assembly, reaction products were transformed into *Escherichia coli*

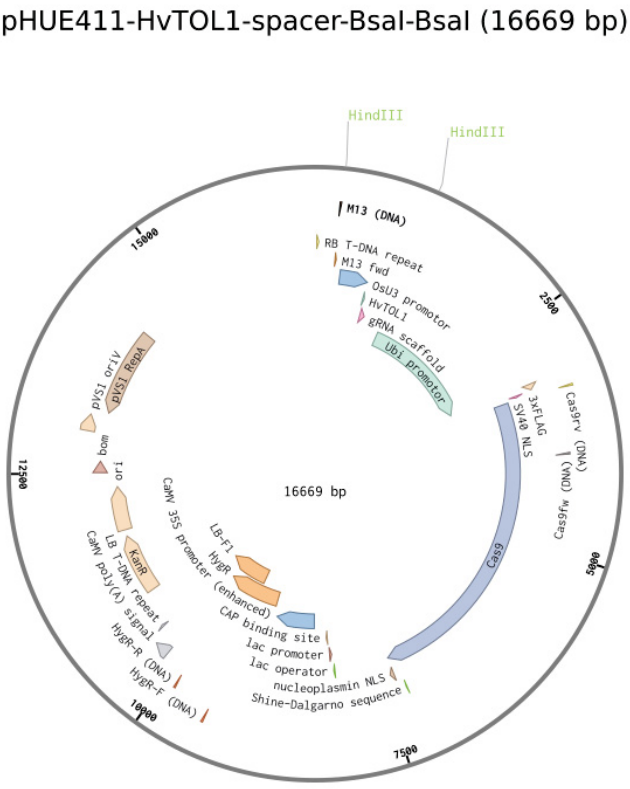

Figure 3.2: pHUE411-*HvTol1* plasmid map.
Plasmid map of pHUE411-*HvTol1* insertion created with Benchling.

(Section 3.2.2.1), and plasmid DNA from positive colonies was isolated (Section 3.2.1.6). Correct assembly was verified by restriction analysis (Section 3.2.1.4) and Sanger sequencing (Section 3.2.1.8). Validated vectors were subsequently transformed into *A. tumefaciens* (Section 3.2.2.3) for downstream plant transformation experiments.

3.2.1.2 Golden Gate assembly—Oligonucleotide assembly

Complementary oligonucleotides (Table 3.15) were annealed to generate double-stranded DNA inserts. These inserts contained a *BsaI* recognition site and all sequence elements required to function as guide RNAs (gRNAs) in combination with the CRISPR/Cas9 system, each targeting a specific *HvTol* gene. For annealing, 3 µL of each primer (forward and reverse; concentrations given in Table 3.15) were mixed in a PCR tube and incubated at 90 °C for 2 min using a thermal cycler. The reaction was then allowed to cool to room temperature to facilitate hybridization of the oligonucleotides. The resulting double-stranded DNA product was diluted 1:1000 in nuclease-free water to obtain a working concentration of approximately 10 fmol/µL. For cloning, 8 µL of this annealed product (corresponding to 80 fmol) was used per reaction.

3.2.1.3 Restriction–ligation reaction

Golden Gate assembly was performed using *BsaI*-HF, T4 DNA ligase, and the binary vector pHUE411. For each reaction, a master mix was prepared according to Table 3.20. Reactions were assembled in PCR tubes and incubated in a thermal cycler using the program shown in Table 3.21. The assembled plasmids were either used directly for transformation or stored at -20 °C until further use.

Table 3.20: Golden Gate restriction–ligation reaction mixture

Component	Working concentration	Volume
T4 DNA ligase buffer (10×)	1×	2 µL
BsaI-HF	20 U	1 µL
T4 DNA ligase	20 U	0.05 µL
pHUE411	40 fmol	X µL
Insert	80 fmol	8 µL
Nuclease-free water	–	to 20 µL
Total volume		20 µL

Table 3.21: Golden Gate restriction–ligation cycling conditions

Step	Temperature	Duration
Digestion	37 °C	20 s
Ligation	37 °C	3 min
Repeat steps 1–2		50×
Final ligation	16 °C	4 min
Enzyme inactivation	50 °C	5 min
Final inactivation	80 °C	5 min
Hold	–	∞

3.2.1.4 Restriction digest

All enzymes, buffers, and the purple (6×) gel loading dye used for restriction digestion and subsequent agarose gel electrophoresis were obtained from New England Biolabs (NEB). Apart from the plasmid DNA, each reaction mixture contained all reactants listed in Table 3.22. Reactions were incubated at 37 °C for 5–15 min. After digestion, 5 µL of loading dye were added to each sample, and the digestion products were separated on a 1% agarose gel at 100 V for 45 min. A DNA ladder was loaded as a molecular size reference. For pre-validation of pHUE411-based CRISPR/Cas9 constructs, plasmid DNA was digested with *HindIII*-HF.

Table 3.22: Restriction digest reaction mixture

Component	50 µL reaction
DNA	1 µg
10× rCutSmart buffer	5 µL
HindIII-HF	1 µL (20 U)
Nuclease-free water	to 50 µL

3.2.1.5 Agarose gel electrophoresis

For the analysis of nucleic acid fragments by size, agarose gel electrophoresis was performed. Agarose (1% (w/v)) was dissolved in 1× TAE buffer by heating in a microwave oven. After brief cooling, the solution was supplemented with a nucleic acid intercalating agent (SYBR Safe) and poured into a gel casting tray. After solidification, the gel was transferred to an electrophoresis chamber and covered with 1× TAE buffer. Samples were mixed with DNA loading buffer and loaded together with a DNA ladder. Electrophoresis was performed at 100 V for 45 min.

Fragments were visualized using an analyzer (Invitrogen, iBright FL1500) with excitation at 515-540 nm.

3.2.1.6 Plasmid purification

Plasmid DNA was purified from *E. coli* cultures using the PureYield™ Plasmid Miniprep System (Promega) following the manufacturer's instructions. For larger culture volumes, the alternative protocol provided by the supplier was applied. Purified plasmids were used for downstream applications such as restriction analysis, sequencing, and bacterial or plant transformation.

3.2.1.7 NanoDrop measurement

The concentration and purity of DNA samples were measured using a NanoDrop spectrophotometer. Absorbance ratios at 260/280 nm were used to assess DNA purity according to the manufacturer's guidelines.

3.2.1.8 Sequencing

Plasmid DNA obtained from miniprep preparations (Section 3.2.1.8) was verified by Sanger sequencing (Microsynth AG) using the M13 primer (Table 3.15). The resulting sequences were aligned to the expected reference sequences using Benchling. For CRISPR/Cas9 construct validation, sequencing was evaluated specifically across the gRNA expression cassette. A plasmid was considered correct when the intended 20-nucleotide target sequence was present and immediately followed by the conserved sgRNA scaffold. Sequencing chromatograms were analyzed for base-calling quality, with particular attention to the spacer–scaffold junction region.

3.2.2 Bacterial Strains and Cultivation

3.2.2.1 Transformation of *Escherichia coli*

Transformations of competent *E. coli* TOP10 cells were performed using the heat-shock method under sterile conditions. Frozen aliquots of chemically competent *E. coli* cells (25 µL per plasmid) were thawed on ice; cells were obtained from laboratory stocks and stored at -80 °C until use. Subsequently, 2 µg of plasmid DNA (20 µL of the entire Golden Gate assembly reaction for each construct; Section 3.2.1.2) were added to each aliquot, mixed gently, and incubated on ice for 20 min. The cells were subjected to heat shock at 42 °C for 45 s, immediately returned to ice, and kept there for an additional 2 min.

Following heat shock, 1 mL of LB medium (Table 3.1) without antibiotics was added to each tube. The mixtures were incubated at 37 °C for 1 h with shaking at 180 rpm to allow cell recovery and expression of antibiotic resistance genes. After recovery, the cultures were centrifuged at 8000 rpm for 1 min. The supernatant was discarded, leaving approximately 100 µL of medium in which the cell pellet was resuspended. The resuspended cells were plated on selective LB agar plates containing kanamycin and streptomycin. Plates were incubated in an inverted position at 37 °C overnight (14–18 h). The following day, five colonies per plate were selected and inoculated into liquid LB medium supplemented with the respective antibiotics and grown overnight at 37 °C with shaking (180 rpm) for subsequent plasmid isolation and restriction analysis.

3.2.2.2 Preparation of *Agrobacterium tumefaciens*

A. tumefaciens strain GV3101 was grown overnight at 30 °C in 100 mL of LB medium (Table 3.1) supplemented with the appropriate antibiotics (20 µg/mL gentamicin, 25 µg/mL rifampicin, and 5 µg/mL tetracycline). Cells were harvested by centrifugation at 4400 rpm for 5 min at 4 °C, washed three times with 50 mL of ice-cold 100% glycerol, and resuspended thoroughly after each wash. The final pellet was resuspended in 1 mL of ice-cold 10% (v/v) glycerol. Aliquots of 40 µL were pipetted into sterile microcentrifuge tubes, flash-frozen in liquid nitrogen, and stored at -80 °C until further use.

3.2.2.3 Electroporation of *Agrobacterium tumefaciens*

For plasmid introduction, 40 µL of electrocompetent *A. tumefaciens* cells (Section 3.2.2.2) were mixed with 50–200 ng of plasmid DNA (Section 3.2.1.6) in a pre-chilled 2 mm electroporation cuvette (manufacturer). Electroporation was performed at 2.5 kV, 25 µF, and 400 Ω, resulting in a time constant of approximately 8–12 ms. Immediately after the pulse, 1 mL of LB medium was added to the cuvette to allow cell recovery, and the suspension was incubated at room temperature with shaking for 2–4 h. Aliquots of 100 µL from each transformation were plated on MG/L agar plates containing gentamicin, rifampicin, tetracycline, and kanamycin and incubated at 28 °C for 2–3 days until colony growth was observed. Colonies were then picked and incubated in liquid MG/L medium, checked by sequencing, and later used for *Agrobacterium*-mediated transformation of *Nicotiana tabacum* (Section 3.2.3.1) and for stable transformation of *Hordeum vulgare* (Section 3.2.5).

3.2.2.4 Glycerol stocks—*Escherichia coli*

Overnight cultures of *E. coli* containing the desired constructs (as confirmed by sequencing; Section 3.2.1.8) were grown in liquid LB medium supplemented with kanamycin and streptomycin at 37 °C with shaking for approximately 16 h. Sterile 87% (v/v) glycerol was pre-chilled on ice prior to use. To prepare glycerol stocks, 820 µL of the overnight culture were mixed with 180 µL of sterile 87% glycerol in a cryogenic tube and gently inverted to resuspend. The mixture was flash-frozen in liquid nitrogen and stored at -80 °C for long-term preservation.

3.2.2.5 Glycerol stocks—*Agrobacterium tumefaciens*

After sequencing, positive colonies of *A. tumefaciens* strain GV3101 carrying the respective binary vectors were used to inoculate 10 mL of MG/L medium supplemented with gentamicin (20 µg/mL), rifampicin (25 µg/mL), tetracycline (5 µg/mL), and kanamycin (50 µg/mL). Cultures were incubated at 28 °C for 40 h with shaking at 180 rpm. After incubation, the bacterial suspension was mixed with an equal volume of sterile 30% (v/v) glycerol solution and gently inverted to ensure homogeneity. Aliquots of 400 µL were transferred into sterile cryogenic tubes and kept at room temperature for 2 h with occasional inversion. The aliquots were then flash-frozen in liquid nitrogen and stored at -80 °C for long-term preservation.

3.2.3 Transient Expression and Confocal Microscopy

All cultured plants were grown and maintained by the gardeners of MOSYS at the University of Vienna.

3.2.3.1 Transient transformation of *Nicotiana tabacum*

For transient expression experiments, *A. tumefaciens* strain GV3101 carrying the desired binary vector was cultured in 10 mL of LB medium (Table 3.1) supplemented with the appropriate antibiotics (gentamicin, rifampicin, and tetracycline). Cultures were incubated for approximately 30 h at 28 °C with shaking at 180 rpm until reaching an optical density (OD_{600}) of 1.0–1.2. Cells were harvested by centrifugation at 4400 rpm for 20 min, and the supernatant was discarded. The bacterial pellets were gently resuspended in infiltration medium (Table 3.2). The OD_{600} of the suspension was adjusted to 0.4 using additional infiltration medium. The cultures were subsequently incubated at room temperature for 3 h under gentle agitation to induce virulence gene expression prior to infiltration.

In parallel, *A. tumefaciens* strains carrying GFP-tagged constructs were prepared in the same manner. These constructs targeted different *HvTol* genes and contained a GFP tag to visualize protein localization. For each *HvTol* gene, one GFP-tagged vector and one corresponding CRISPR construct (Section 3.2.1.2) were generated. *A. tumefaciens* strains carrying the GFP-tagged constructs were obtained from pre-existing glycerol stocks.

3.2.3.2 Infiltration of *Nicotiana tabacum* leaves

For transient expression assays, leaves of four-week-old *Nicotiana tabacum* plants were infiltrated twice. In the first round, *A. tumefaciens* strains carrying GFP-tagged constructs were used. The bacterial suspensions were introduced into the abaxial side of the leaves using a needleless 10 mL syringe, applying gentle pressure to infiltrate the intercellular spaces without damaging the tissue. Infiltrated leaves were labeled and documented, and plants were maintained under standard growth conditions for two to five days post-infiltration. Samples from infiltrated areas were subsequently collected and analyzed by confocal laser scanning microscopy (Section 3.2.3.3) to assess transient expression and subcellular localization of the GFP-tagged fusion proteins.

Following the first analysis, the same leaves were infiltrated a second time. Each leaf was divided along the midrib, with one half infiltrated with an *A. tumefaciens* strain carrying a CRISPR binary vector targeting the corresponding *HvTol* gene and the other half with the respective negative control construct. Two to five days after the second infiltration, leaf samples were again collected and examined using confocal microscopy to evaluate the functionality of the generated vectors (Section 3.2.1.2).

3.2.3.3 Confocal laser scanning microscopy

Fluorescence imaging of infiltrated *Nicotiana tabacum* leaves was performed using a confocal laser scanning microscope (Leica TCS SP8). GFP was excited using an argon laser line at 488 nm wavelength (Output Power: 19.84 %, Shutter on, Intensity: 41.82 %) and emission was detected at 495-550 nm. Images were acquired using 10× magnification (Objective: HC PL FLUOTAR 10x/0.30 DRY). Acquisition settings were kept constant within experiments to allow comparison between samples (Detectors: PMT 1, Gain: 831.6, Offset: -0.02; PMT 2, Gain: 614.6, Offset: -0.1; PMT Trans, Gain: 347.2, Offset: -0.09).

3.2.4 Computational Image Analysis and Statistical Evaluation

Quantitative analysis of fluorescence intensity was performed using ImageJ (Fiji distribution) and RStudio (R Core Team, 2025). Confocal microscopy images obtained from transiently transformed *Nicotiana tabacum* leaves were processed to assess the functional impact of CRISPR constructs targeting individual *HvTol* genes.

3.2.4.1 Image processing and fluorescence quantification

For each experimental condition, six confocal images per treatment were acquired at identical magnification (10×) and with constant acquisition settings. To increase spatial sampling and reduce local intensity bias, each microscopy image was computationally subdivided into four equally sized quadrants using a custom ImageJ macro (Listing 7.1). This procedure yielded a total of 24 regions of interest per condition and *HvTol* gene.

For each quadrant, the mean fluorescence intensity was calculated as the *Mean Grey Value*. Background correction was applied uniformly across all images. As quadrants derived from the same image share systematic sources of variation (e.g., illumination, infiltration efficiency, leaf physiology), they cannot be treated as independent observations. Therefore, the four quadrant values were averaged per image to yield one representative value per biological replicate ($n = 6$ per group). This aggregation step avoids pseudoreplication and ensures that the statistical unit corresponds to the independently treated leaf area. Resulting image-level means were compiled into a spreadsheet for downstream analysis.

3.2.4.2 Data handling and statistical analysis

Statistical analyses were conducted using RStudio (2025.09.2+418) with the `effsize` package (Torchiano, 2020) for effect size estimation. For each *HvTol* gene (*HvTol1*, *HvTol2*, *HvTol3*, and *HvTol8*), image-level mean fluorescence intensities from CRISPR-treated samples were compared to the corresponding negative control samples.

Normality of image-level means was assessed for each group using the Shapiro-Wilk test. For each gene, a one-sided Welch's *t*-test was performed on image-level means, testing the directed hypothesis that CRISPR-mediated targeting of the respective *HvTol* gene results in a reduction of fluorescence intensity compared to the negative control. Welch's *t*-test was chosen over the classical Student's *t*-test as it does not assume equal variances between groups. Statistical significance was assessed at a threshold of $\alpha = 0.05$. As a non-parametric robustness check, one-sided Wilcoxon rank-sum tests were additionally performed.

To characterize the magnitude of observed differences beyond statistical significance, Cohen's *d* with 95 % confidence intervals was calculated as a standardized effect size measure. Furthermore, 95 % confidence intervals for the mean difference between groups and relative percent differences (CRISPR vs. negative control) were reported.

3.2.4.3 Data visualization

Results were visualized using boxplots displaying the distribution of mean fluorescence intensities across all image quadrants for CRISPR-treated and control samples. Image-level means ($n = 6$ per group) were overlaid as individual data points to indicate the biological replicates on which statistical inference was based. Plots were generated in R using the `ggplot2` package (Wickham, 2016) and formatted according to publication standards. Statistical significance was denoted using conventional symbols (ns: $p \geq 0.05$, * $p < 0.05$, ** $p < 0.01$, *** $p < 0.001$). The complete ImageJ macro used for automated image subdivision and fluorescence extraction is provided in Listing 7.1. The full R script used for data processing, statistical analysis, and figure generation is provided in Listing 7.2.

3.2.5 Stable Transformation of *Hordeum vulgare*

Stable transformation of barley (*Hordeum vulgare*) was carried out using *A. tumefaciens* strain GV3101 harboring binary vectors of interest. This method was employed to generate transgenic barley lines for the analysis of gene function and expression. The procedure followed established *Agrobacterium*-mediated transformation principles with modifications optimized for the cultivar used in this study (Harwood et al., 2009; F. Wang et al., 2023).

3.2.5.1 Preparation of *Agrobacterium tumefaciens* cultures

Electrocompetent *A. tumefaciens* GV3101 cells were prepared and transformed with the desired binary vectors as described previously (Section 3.2.2.3). Transformed colonies were maintained as glycerol stocks and used to inoculate 10 mL of MG/L medium supplemented with the appropriate antibiotics (Table 3.9). Cultures were incubated at 28 °C for approximately 40 h with shaking at 180 rpm. Prior to plant transformation, individual colonies were transferred into antibiotic-free MG/L medium and grown overnight at 28 °C with shaking at 200 rpm to generate fresh inocula.

3.2.5.2 Isolation of immature barley embryos

Barley spikes of the cultivar Golden Promise containing immature seeds were collected from conviron-grown plants. The target embryo size was 1.5–2.0 mm in diameter, as recommended in the literature for optimal regeneration and transformation competence (Harwood et al., 2009; Tingay et al., 1997). However, post-hoc image-based measurements revealed that the embryos used in this study exceeded this range, with mean diameters of approximately 3.5 mm in run 1 and 3.0 mm in run 2 (Figure 7.5). After removal of the awns, seeds were surface-sterilized by washing in 70% ethanol for 2 min, followed by a 5% sodium hypochlorite treatment for 4 min, and several rinses with sterile distilled water. Immature embryos were isolated in a laminar flow hood using sterile forceps. The embryonic axis was removed, and the scutellum was placed upward on callus-inducing medium without antibiotics (Table 3.10). Approximately 25 embryos were arranged per plate and incubated overnight at 23–24 °C in the dark.

3.2.5.3 *Agrobacterium* inoculation and co-cultivation

Fresh *Agrobacterium* cultures were used to inoculate isolated barley embryos. A small drop of bacterial suspension was applied to the scutellum surface of each embryo. Plates were briefly tilted to remove excess liquid and allowed to dry for 5–10 min. Embryos were then transferred, scutellum side down, onto fresh CIM plates without antibiotics for co-cultivation. Plates were sealed with Parafilm and incubated for three days at 24 °C in the dark. After co-cultivation, excess bacteria were removed by rinsing the embryos with a sterile timentin solution. Embryos were transferred to CIM plates containing hygromycin and timentin to initiate selection and callus induction. This selection phase was maintained for six weeks.

3.2.5.4 Selection and regeneration

Selection was carried out in three consecutive two-week intervals on fresh CIM plates (Table 3.10) supplemented with hygromycin and timentin. Surviving calli were transferred to transition medium (TM) and its modified version(TM2, Table 3.11), respectively, and incubated for two weeks at 24 °C under low light conditions. During the first week, light intensity was reduced by covering the plates with thin paper sheets. Calli that developed green shoots were transferred to regeneration medium (Table 3.11) lacking growth regulators. Calli that did not develop shoots within two weeks were transferred to fresh TM plates. Plantlets were maintained on RM until a well-defined root system had developed, changing RM plates every two weeks. Fully regenerated plants were transferred to soil and grown under greenhouse conditions for acclimatization.

3.2.5.5 Adaptive handling during tissue culture

During tissue culture, calli exhibited heterogeneous developmental responses that required adaptive handling to maintain viability and regeneration potential. In the first experimental run, calli maintained on transition medium (TM) did not initiate shoot formation within the expected cultivation period. These calli were therefore transferred to a modified transition medium (TM2) to promote regenerative competence, while all other handling conditions were kept identical.

In the second experimental run, calli transferred to regeneration medium (RM) initially developed shoots, which subsequently senesced. To stabilize tissue viability and allow continued development, these calli were retransferred to TM2 prior to further regeneration attempts.

Additional adaptive measures included more frequent transfer of rapidly growing or early-greening calli to fresh media to prevent nutrient depletion or localized stress. In cases of localized contamination, individual embryos or calli were physically separated from neighboring tissue. Where required, larger culture vessels containing CIM, TM/TM2, or RM were used when developing tissues outgrew standard Petri dishes during later regeneration stages.

All medium transitions and handling adaptations were guided by observable developmental outcomes and applied to maintain regeneration potential, rather than to introduce additional experimental variables.

3.2.5.6 Extraction of genomic DNA from *Hordeum vulgare*

To verify the presence of transgenes in plant material at different developmental stages, a direct PCR approach was employed using the Phire™ Plant Direct PCR Master Mix (Thermo Scientific, Cat. No. F-160S). This method allowed for rapid screening of putatively transformed tissues without the need for prior DNA extraction. PCR analyses were performed on young leaves, callus tissue, and regenerated plantlets derived from *A. tumefaciens*-mediated transformation experiments, as well as *A. tumefaciens* cryo-colonies. Small tissue samples (approximately 0.35–0.50 mm in diameter) were excised from each specimen using sterile scalpels to minimize contamination. Each sample was directly used as template material in the PCR reaction without DNA purification. Reactions were assembled in a total volume of 20 µL containing primers and PCR components (Table 3.24). The amplification program was adjusted depending on the annealing temperatures of the primers (Table 3.23). PCR products were visualized by agarose gel electrophoresis (Section 3.2.1.5), taking advantage of the loading dye included in the Master Mix. Positive and negative control reactions were included in each PCR run to confirm amplification specificity and to detect potential contamination.

3.2.5.7 Polymerase chain reaction (PCR)

To determine whether plants and microbial strains were positive for the intended genetic transformation or carried the desired plasmids, PCR analyses were performed. DNA was obtained as described in Section 3.2.5.6. In general, PCRs were carried out using a PCR master mix according to the manufacturer's instructions. DNA fragments were amplified using different primer combinations, with annealing temperatures adjusted to the melting temperatures of the respective primers. To confirm positive transformation, primers binding Cas9 and HygR sequences, respectively, were used as both are encoded on pHUE411, yielding expected amplicon sizes of 694 bp (Cas9) and 426 bp (HygR). As a positive control confirming DNA samples are sufficient for PCR, Hsp90 was chosen (expected amplicon 132 bp). Hsp90 is constitutively expressed in eukaryotes (Silbermann, Vermeer, Schmid & Tych, 2024) and is confirmed as a suitable control in PCR (Janská et al., 2013; Sinha, Saxena, Singh, Krishnamurthy & Varshney, 2015). Samples of transformed *A. tumefaciens* carrying the respective pHUE411 constructs (pHUE411-*HvTol1*, pHUE411-*HvTol2*, pHUE411-*HvTol3*, pHUE411-*HvTol8*, and pHUE411 empty vector) were included as positive controls for primer functionality, and untransformed Golden Promise as a negative control. PCR cycling programs varied depending on the primer pairs and reaction composition. Based on the expected fragment sizes, the resulting amplicons were analyzed by agarose gel electrophoresis (Section 3.2.1.5).

Table 3.23: PCR cycling conditions

Step	Temperature	Duration
Initial denaturation	98 °C	5 min
Denaturation	98 °C	5 s
Annealing	62.7–65 °C	5 s
Extension	72 °C	20 s
Repeat steps 2–4		34×
Final extension	72 °C	1 min
Hold	10 °C	∞

Annealing temperatures used in PCR cycling conditions varied according to the used oligonucleotide. Full sequences are listed in Table 3.15. Cas9fw/rv: 64.7 °C, HygR-F/R: 65.2 °C, Hv_hsp90-F/R: 62.7 °C.

3.2.6 Computational analysis of stable transformation experiments

All observations obtained during *Agrobacterium*-mediated stable transformation of *Hordeum vulgare* were retrospectively analyzed using a fully scripted and reproducible computational

Table 3.24: PCR reaction mixture

Component	20 µL reaction	Final concentration
2× Phire Plant Direct PCR Master Mix	10 µL	1×
Primer A	X µL	0.5 µM
Primer B	X µL	0.5 µM
Plant tissue (direct protocol)	0.5 µL	–
Nuclease-free water	to 20 µL	–

pipeline implemented in R. Raw data tables were imported from spreadsheet files and processed using RStudio, ensuring transparent preprocessing, aggregation, and visualization. Full R script can be seen in Listing 7.3.

3.2.6.1 Primary data collection and scoring of transformation outcomes

All observations obtained during the stable transformation of barley were recorded in a primary observation table at defined time points (`Gesamt_Tag`; days after embryo isolation, DAI). Each entry corresponds to one experimentally handled culture unit (plate or pot) observed at a specific passage and time point. Data acquisition was based on retrospective scoring of documented culture states using photographs acquired during routine handling of the material. No additional measurements were performed beyond visual inspection of the documented images.

At each observation, the following parameters were scored: the presence or absence of *A. tumefaciens* overgrowth, the number of continuing calli or embryos, the occurrence of shoot formation, the presence or absence of roots, and the occurrence of additional clonal regenerants. All scoring criteria were based exclusively on visually discernible features.

Agrobacterium overgrowth was scored as present only when visible bacterial proliferation was observed on the tissue or surrounding medium; no plating, swabbing, or molecular detection was performed. Root formation was scored only when distinct root structures were clearly visible. Shoot formation was scored when green shoots, shoot-like structures, or localized clusters of green cells indicative of shoot initiation were observed. Callus continuation and growth were assessed visually by comparing successive documented states of the same culture unit, scoring growth when an increase in callus mass or developmental progression was apparent.

Scoring was performed at biologically relevant transition points of the tissue culture pipeline, including transfers between culture media (CIM, TM/TM2, RM, and soil), rather than at fixed calendar intervals. Early handling steps at `Gesamt_Tag` 0 reflect standardized protocol operations and were recorded without aggregation. Later observations were documented whenever

cultures progressed to a new developmental stage or required adaptive handling.

Where multiple shoots or plants originated from a single callus, biologically independent regeneration events were distinguished from additional clonal derivatives. Clonal material was explicitly annotated in the raw dataset but did not contribute to early-stage callus or shoot counts. This primary observation table formed the basis for all subsequent data preprocessing, time binning, strand assignment, and quantitative analyses.

3.2.6.2 Data preprocessing and annotation

Only observations associated with defined experimental runs (`Durchgang`, hereafter referred to as runs) were retained for analysis. Records lacking valid temporal information (`Gesamt_Tag`; days after embryo isolation, DAI) were excluded. All quantitative readouts, including *A. tumefaciens* overgrowth, callus development, shoot number, root formation, and plant establishment, were robustly coerced to numeric format to prevent the inclusion of non-numeric annotations.

Culture media were annotated at two hierarchical levels. For computational grouping and visualization, each medium was assigned to a culture stage based on the leading medium identifier, corresponding to callus induction medium (CIM), transition medium (TM), modified transition medium (TM2), regeneration medium (RM), or soil. Detailed medium compositions were retained in the raw dataset and documented separately, but were not encoded directly in graphical representations.

3.2.6.3 Handling of clonal regenerants

During later regeneration stages, multiple shoots or plants occasionally originated from a single callus. To account for this, clonal regenerants were explicitly annotated in the raw dataset using the variable `Zusaetzliche_Klone`. In this annotation scheme, the column `Erfolgreiche_Pflanzen` represents the number of biologically independent plant regeneration events, while `Zusaetzliche_Klone` denotes the number of additional clonal plants derived from these events.

Clonal regenerants that diverged into distinct experimental trajectories (e.g. MAIN versus branch strands) were treated as independent samples from the point of divergence onward. This approach preserves biological interpretability while preventing inflation of early-stage counts by late clonal amplification.

3.2.6.4 Time binning and aggregation strategy

To enable comparison of phenotypic readouts obtained within narrow temporal windows, measurements used for quantitative analyses (Figure 4.2 panels B and C) were aggregated using a controlled time-binning strategy. Binning was performed independently for each experimental run and culture stage. Observations were assigned to the same temporal bin only if their time points differed by no more than two days, ensuring that only biologically comparable measurements were aggregated.

Early handling steps occurring at Gesamt_Tag 0 and 1 reflect standardized protocol operations rather than adaptive experimental interventions and were therefore excluded from the binning procedure. These observations were retained as individual time points without aggregation.

3.2.6.5 Definition of MAIN and branch strands

To avoid biologically misleading averaging across diverging experimental trajectories, a strand-based model was implemented. Within each experimental run, a MAIN strand was defined as the maximal set of culture units following a shared propagation trajectory. Strand assignment was performed once and applied consistently across all downstream analyses. Conceptual Rules and technical decisions are listed more closely in Table 7.2 and 7.3.

For run 1, strand assignment was based on co-occurrence logic. The last time point at which all relevant replicates were observed together within the same temporal bin was identified algorithmically and defined as the end of the joint MAIN trajectory. Beyond this point, cultures diverging in handling or treatment were assigned to branch strands. Negative control cultures were assigned to an independent strand. However, the script includes a logic assigning negative control to different strand from the first temporal bin in which they were no longer observed together with any MAIN culture.

For run 2, strand assignment followed a route-based logic reflecting deviations from the dominant propagation pathway. The MAIN strand was defined as the prevailing culture route within each time window, while replicates persistently deviating from this route were assigned to branch strands. In the case of the *hvtol2* lineage, a temporary split event was resolved by explicit tracking of callus identifiers. Subsets of calli that diverged during this split were treated as independent observational lineages and remained assigned to a branch strand thereafter, even if experimental conditions later converged. Here too, negative control cultures were assigned to an independent strand.

3.2.6.6 Quantification of regeneration and establishment

Shoot development was quantified as the total number of shoots observed per time bin and strand. Root formation was assessed at the plate level, scoring the presence or absence of roots per culture unit. For each time bin and strand, both the number of plates assessed and the number exhibiting root formation were recorded.

For summary performance analyses (Figure 4.4), stage-specific snapshot time points were defined for each run and insert. Plant establishment was quantified as the sum of biologically independent plants and additional clonal regenerants, normalized to the initial number of embryos at `Gesamt_Tag` 0.

3.2.6.7 Visualization

All visualizations were generated using `cowplot` (Wilke, 2025). Background shading indicating culture stages was derived exclusively from the MAIN strand and restricted to time intervals supported by experimental observations. Consistent axis limits, scaling, and color mappings were applied across panels to facilitate comparison between runs. All computational steps were fully scripted and reproducible.

4 Results

The following section presents the experimental results obtained during establishment and evaluation of an *Agrobacterium*-mediated transformation workflow in barley. Our study involved generation and validation of CRISPR/Cas9-based vectors targeting individual *HvTol* genes, transient functional validation of these constructs in *Nicotiana tabacum*, and their subsequent application in a stable transformation pipeline using immature barley embryos. Results are presented in a sequential manner reflecting the experimental progression from vector construction through transient assays to stable plant regeneration.

4.1 Construction and validation of CRISPR/Cas9 vectors targeting *HvTol* genes

Four CRISPR/Cas9 constructs targeting individual *HvTol* genes were successfully generated using Golden Gate assembly. The constructs pHUE411-*HvTol1* (Figure 3.2), pHUE411-*HvTol2* (Figure 7.1), pHUE411-*HvTol3* (Figure 7.2), and pHUE411-*HvTol8* (Figure 7.3) each contain a gene-specific gRNA spacer sequence integrated into the pHUE411 vector backbone (Figure 3.1).

Correct assembly of all constructs was first confirmed by restriction analysis, which yielded the expected fragment patterns in all cases. Subsequently, Sanger sequencing was performed to verify the integrity of the inserted spacer sequences and their correct junction with the gRNA scaffold. Sequencing analysis confirmed that all four constructs contained the intended 20-nt spacer sequences without any sequence alterations (Table 7.1). In each case, the spacer sequence was directly followed by the conserved sgRNA scaffold sequence, confirming correct spacer–scaffold junctions. Decreased base-calling quality toward the end of the sequencing reads, typical for Sanger sequencing, did not affect the critical spacer–scaffold junction region.

Following successful validation, all four CRISPR/Cas9 constructs were introduced into *A. tumefaciens* for subsequent plant transformation experiments.

4.2 Functional Pre-validation in *Nicotiana tabacum*

Transient expression assays in *N. tabacum* were performed to functionally validate the generated CRISPR/Cas9 constructs prior to their use in stable barley transformation experiments. *A. tumefaciens* strain GV3101 carrying the respective binary vectors was used for transient leaf infiltration. To control for variability, a split-leaf experimental design was employed, infiltrating opposite halves of the same leaf with either a CRISPR/Cas9 construct or the respective negative control vector (Section 3.2.3.2). In parallel, GFP-tagged *HvTol* reporter constructs were transiently expressed to verify delivery and expression.

Leaf samples were collected two to five days post-infiltration and analyzed using confocal laser scanning microscopy (Section 3.2.3.3). Fluorescence intensities were quantified as image-level mean grey values ($n = 6$ per group; see Section 3.2.4 for details on image processing and aggregation).

Normality assumptions were met for all groups. Comparative analysis using one-sided Welch's *t*-tests revealed no statistically significant reduction in mean fluorescence intensity for any of

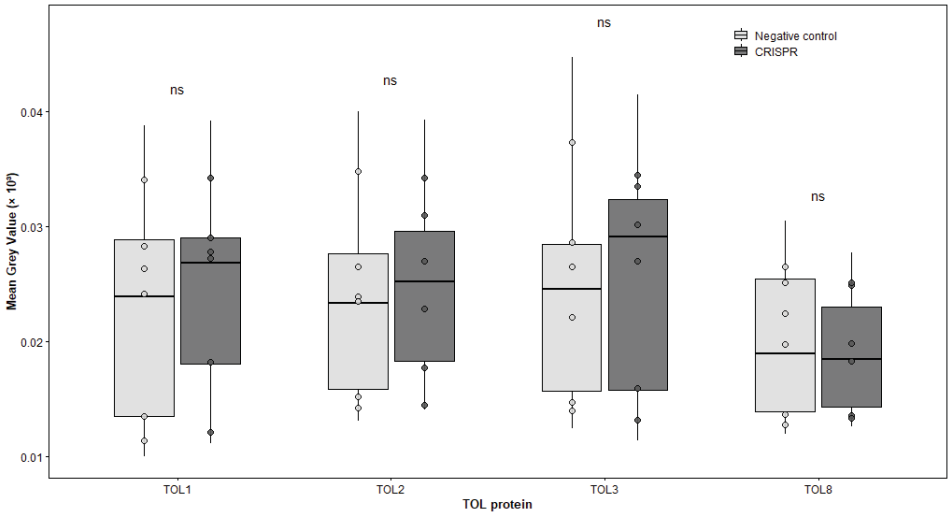

Figure 4.1: Transient CRISPR/Cas9-mediated targeting of *HvTol* genes in *Nicotiana tabacum*. Boxplots show the distribution of mean grey values across image quadrants for CRISPR-treated and negative control samples. Individual points represent biological replicates (image-level means, $n = 6$ per group), obtained by averaging the four quadrants of each fluorescence micrograph to account for spatial correlation within images. The central line indicates the median, boxes the interquartile range, and whiskers extend to 1.5× IQR. Statistical significance was assessed using one-sided Welch's *t*-tests on image-level means, with Wilcoxon rank-sum tests as a non-parametric robustness check. No statistically significant differences were detected for any TOL protein (ns; all $p > 0.05$, $|d| < 0.8$).

the CRISPR/Cas9 constructs relative to their negative controls (Figure 4.1): *HvTol1* ($t = 0.375$, $p = 0.642$, $d = 0.22$), *HvTol2* ($t = 0.343$, $p = 0.631$, $d = 0.20$), *HvTol3* ($t = 0.354$, $p = 0.635$, $d = 0.20$), and *HvTol8* ($t = -0.271$, $p = 0.396$, $d = -0.16$). Non-parametric Wilcoxon rank-sum tests confirmed these results (all $p > 0.05$). Effect sizes were small for all constructs ($|d| \leq 0.22$), and 95 % confidence intervals of the mean differences included zero in every case.

Notably, mean fluorescence in the CRISPR-treated samples was not lower but slightly higher than in the negative controls for *HvTol1* ($+8.0$ %), *HvTol2* ($+6.6$ %), and *HvTol3* ($+7.7$ %). Only *HvTol8* showed a marginal reduction (-4.3 %), which did not reach statistical significance. These results suggest that the CRISPR/Cas9 constructs did not achieve detectable knockout efficiency under the conditions of this transient expression assay.

4.3 Stable Transformation of *Hordeum vulgare*

An *Agrobacterium*-mediated transformation pipeline for barley (*Hordeum vulgare*) was established using immature embryos as explant material. The workflow comprised embryo isolation, bacterial co-cultivation, callus induction on selection medium, transition through regeneration stages, and ultimate transfer to soil (Methods 3.2.5).

4.3.1 *Agrobacterium* elimination and callus induction.

A. tumefaciens overgrowth was observed during early culture stages (0–4 DAI) but declined rapidly following timentin treatment at day 4 after embryo isolation. By 18 DAI, overgrowth was eliminated in both experimental runs (Figure 4.2A; Table 7.4). Callus formation proceeded uniformly across replicates, with retention rates exceeding 75% at 46 DAI for all transgenic lines tested (Figure 4.4).

4.3.2 Shoot regeneration efficiency varies with medium composition.

Run 1 initially employed transition medium (TM) containing cytokinin and auxin derivatives in concentrations previously reported for barley transformation (Harwood et al., 2009). However, no shoot formation was observed throughout the TM culture period (46–60 DAI). Calli were subsequently transferred to modified transition medium (TM2) with altered hormone ratios favoring shoot rather than root development (F. Wang et al., 2023). Following TM2 culture, shoot formation was observed prior to first transfer to regeneration medium (RM): 8 shoots (negative control, 81 DAI), 3 shoots (*hvtol8*, 99 DAI), 1 shoot each (*hvtol2* and *hvtol3*, 99 DAI), and 0 shoots

(*hvtol1*, 109 DAI). All transgenic lines subsequently lost shoot regeneration capacity, while the negative control maintained sustained shoot development through 331 DAI (Figure 4.2B).

Run 2 employed TM2 from the outset. At the time of first RM transfer (74 DAI for all transgenic lines), shoot counts were: 8 shoots (*hvtol1*), 4 shoots (*hvtol2*), and 2 shoots each (*hvtol3*, *hvtol8*, negative control). For comparison, run 1 yielded 0 shoots (*hvtol1*), 1 shoot each (*hvtol2*, *hvtol3*), 3 shoots (*hvtol8*), and 8 shoots (negative control) at the corresponding TM2-to-RM transition (Figure 4.4).

4.3.3 RM transition optimization and root induction.

Initial transfer from TM2 to RM at day 74 after embryo isolation (run 2) resulted in widespread shoot necrosis. Calli were returned to TM2 (88–130 DAI), where new shoot primordia emerged, though original shoots did not recover. For the second RM transfer attempt, hygromycin was omitted from all media formulations to reduce physiological stress, and transfer was delayed (130–154 DAI) to allow increased shoot biomass accumulation. Under these modified conditions, shoots survived RM culture and initiated root formation (Figure 4.2C). By day 154 after embryo isolation, several independent calli bearing roots were observed (*hvtol1*, *hvtol2*, *hvtol3*), compared to one in run 1 (negative control, 171 DAI). Rooted plantlets were transferred to soil at 152–160 DAI, yielding: 1 plant each (*hvtol1*, *hvtol3*), 2 plants initially with an additional 2 plants plus 2 clonal derivatives following extended culture (*hvtol2*, 154 DAI and 160 respectively), and 1 plant plus 1 clonal derivative (negative control) (Figure 4.3; Table 7.4).

4.3.4 Stage-specific transformation efficiency.

Snapshot analysis at defined developmental transitions quantified cumulative losses through the pipeline (Figure 4.4). From initial embryo counts ($n_0 =$ `AnzahlweiterbildenderEmbryos/Kalli` at `Gesamt_Tag` $= 0$), callus retention at the first TM stage (46 DAI) exceeded 75%. Shoot formation efficiency (first RM stage) was 10–30% of n_0 (74–109 DAI), representing the primary developmental bottleneck. Root formation (first soil transfer) occurred in 3–10% of starting embryos (152–171 DAI), and final plant establishment (second soil observation) yielded 3–10% of n_0 (212–225 DAI). The negative control yielded 8 shoots in run 1 and 3 shoots in run 2, while transgenic line performance ranged from 1–3 shoots (run 1) to 3–8 shoots (run 2). Clonal shoot multiplication from single calli was observed in several cases; these clonal derivatives are documented in Table 7.4 but excluded from independent transformation event counts.

4.3.5 Molecular verification.

All regenerants from both runs (run 1: negative control, $n = 1$; run 2: *hvtol1*, $n = 1$; *hvtol2*, $n = 3$; *hvtol3*, $n = 1$; negative control, $n = 2$) as well as four callus samples (callus *hvtol1*, callus *hvtol2.1*, callus *hvtol2.2*, callus *hvtol3*) were subjected to PCR screening for the presence of Cas9, HygR, and the housekeeping gene *HvHsp90* as a genomic DNA quality control (Section 3.2.5.7). No amplification products corresponding to the Cas9 or hygromycin resistance cassette were detected in any barley-derived sample (Figure 4.5). Positive control reactions using transformed *A. tumefaciens* confirmed primer functionality for all primer pairs. Amplification of *HvHsp90* produced strong bands in all leaf-derived plant samples, confirming adequate DNA quality. In contrast, callus-derived samples showed reduced *HvHsp90* signal intensity: callus *hvtol2.1*, callus *hvtol2.2*, and callus *hvtol3* yielded only very faint bands, while callus *hvtol1* produced a weak but visible band (Figure 4.5), suggesting suboptimal DNA quality. These results indicate successful completion of the regeneration pathway but absence of detectable stable transgene integration in any of the screened samples.

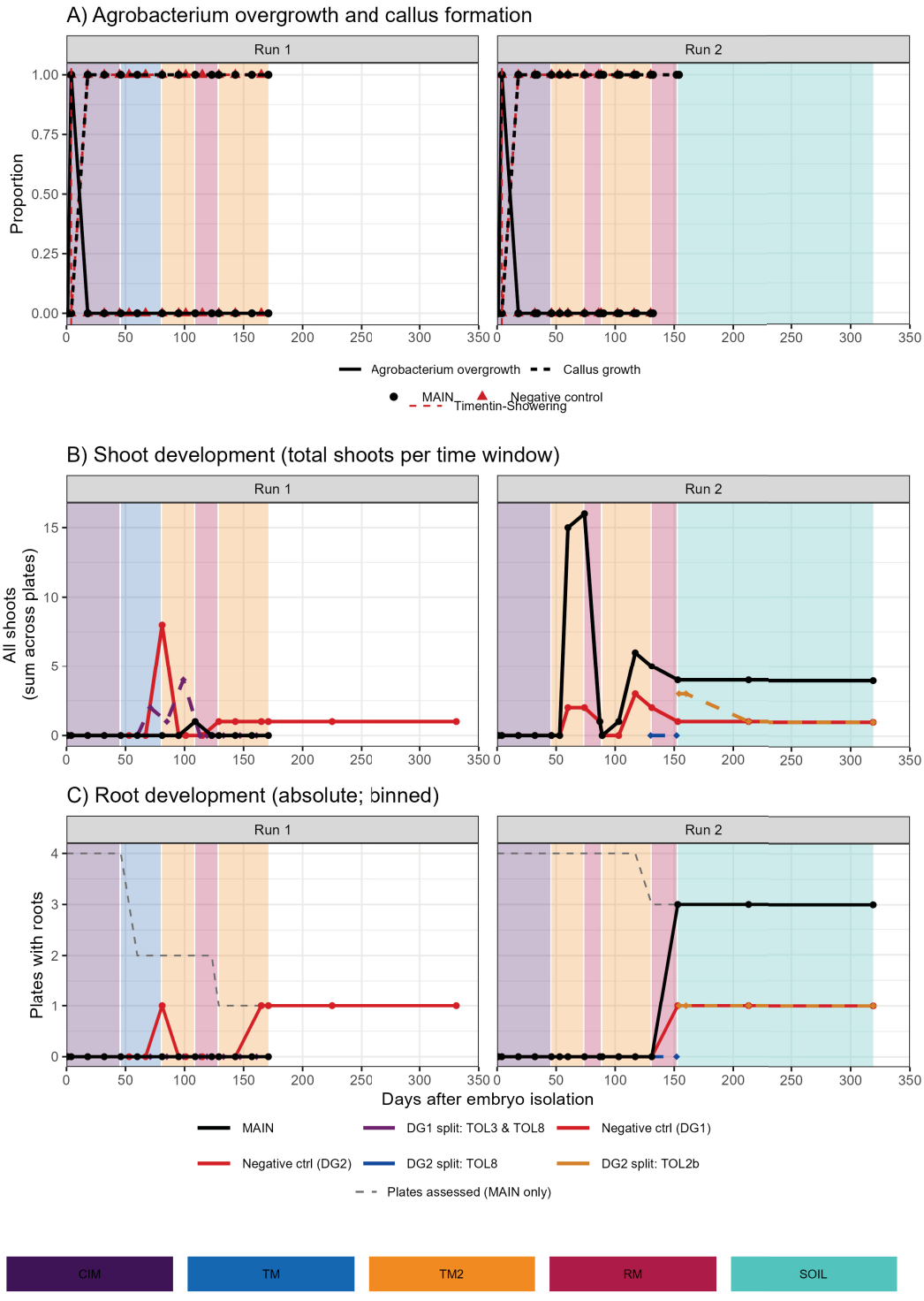

Figure 4.2: Establishment and performance of the stable transformation pipeline in barley. (A) Temporal progression of overgrowth and callus formation. (B) Shoot development. (C) Proportion of root development. Detailed data including protocol deviations are provided in Table 7.2, 7.3, 7.4.

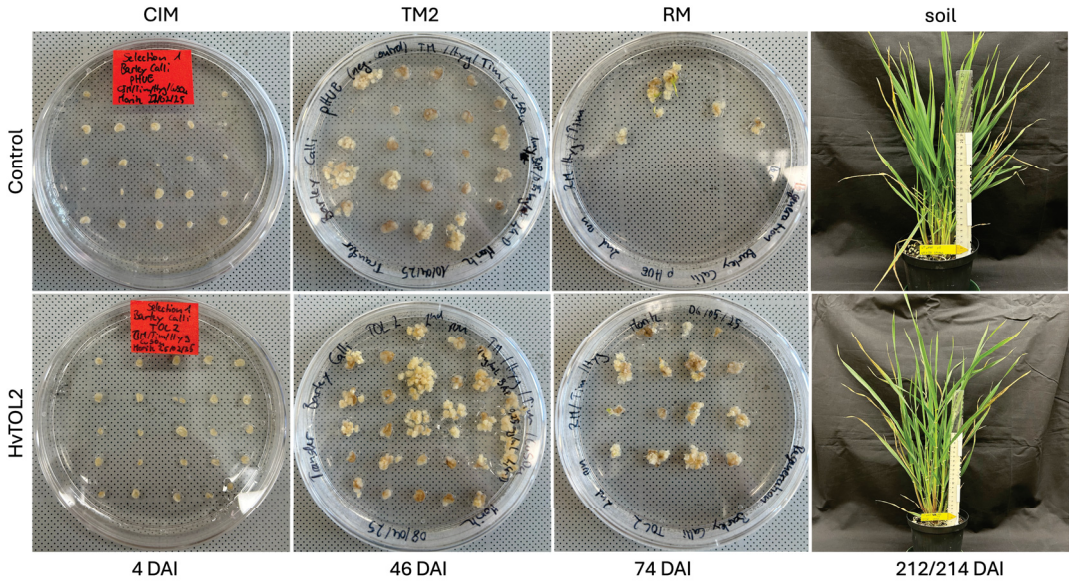

Figure 4.3: Representative images of the barley transformation pipeline stages, from immature embryos (DAI: days after embryo isolation) and callus induction to fully developed plants in soil.

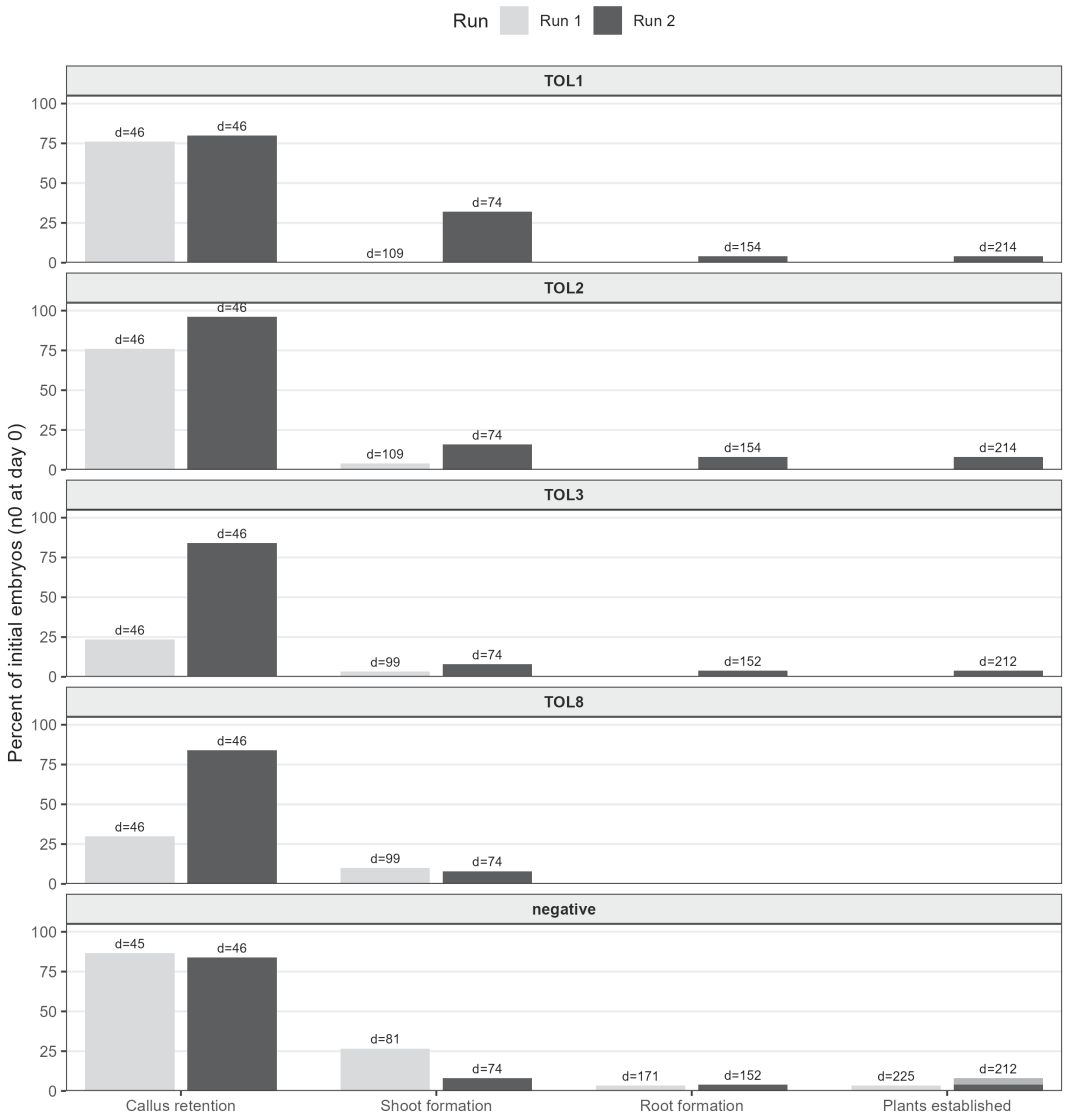

Figure 4.4: Stage-specific performance summary of the barley stable transformation pipeline. For each construct (insert) and experimental run (Run 1 and Run 2), bars show the proportion of starting embryos n_0 (number of embryos at DAI 0), in Table 7.4: "C" at "DAI" $= 0$) that were retained as (i) continuing calli, (ii) shoot-bearing cultures, (iii) root-positive cultures, and (iv) plants established in soil at a specific stage. Stage-specific performance metrics were quantified only after completion of the respective functional phase of the transformation pipeline. Callus retention was assessed after passage through callus-inducing medium (CIM), shoot formation after exposure to transition media (TM/TM2) containing shoot-inducing hormone regimes, and root formation following transfer to hormone-free regeneration medium (RM), where shoot survival depends on autonomous growth competence. Plants established were scored after transfer to soil, representing successful completion of the in vitro regeneration phase. Thus, each snapshot reflects a stabilized biological outcome intrinsic to the pipeline design rather than an arbitrarily selected time point. For *Plants established*, bars are subdivided into biologically independent regeneration events ("Plants") and additional clonal plants ("Extra clones"), such that *Plants established* = (number of plants + number of clonal plants) normalized to the initial embryo count (n_0). The negative control ("negative") is shown as the final insert.

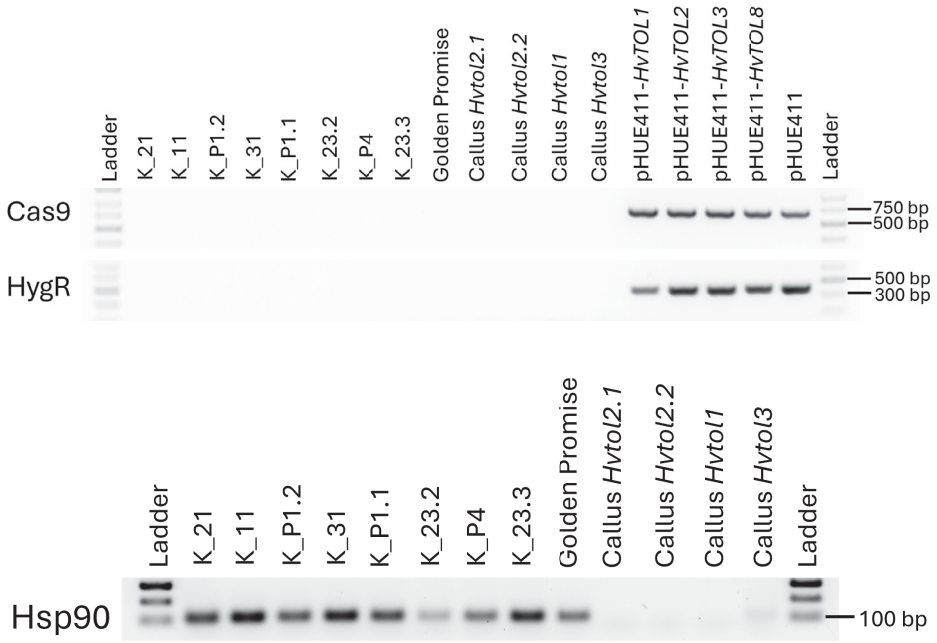

Figure 4.5: PCR screening of putative transgenic barley samples. Gel images show PCR products for Cas9 (expected amplicon 694 bp), HygR (426 bp), and the housekeeping gene *HvHsp90* (132 bp) as genomic DNA quality control. Samples comprise regenerated plant material (K_21, K_11, K_P1.2, K_31, K_P1.1, K_23.2, K_P4, K_23.3) and callus material (callus *hvtol1*, callus *hvtol2.1*, callus *hvtol2.2*, callus *hvtol3*); transformed *A. tumefaciens* carrying the respective pHUE411 constructs served as positive controls and untransformed Golden Promise as negative control. Primer sequences are listed in Table 3.15; PCR conditions are described in Section 3.2.5.7. Marker: O'GeneRuler Express DNA Ladder (Thermo Fisher Scientific). Full uncropped gel images are provided in Figure 7.6.

5 Discussion

This study aimed to create a complete barley transformation pipeline—from vector construction through plant regeneration under selection, to ultimately creating stably transformed plants carrying CRISPR/Cas9 constructs targeting individual *HvTol* genes. The pipeline was developed as well as successfully executed from vector construction through *Agrobacterium*-mediated transformation, tissue culture, and molecular screening of putatively transformed plant tissue; however, no regenerated plant tested positive for stable transgene integration. PCR screening for both the Cas9 transgene and the hygromycin resistance marker was negative across all samples and both experimental runs (Figure 4.5). Importantly, the absence of transgene signal was also observed in negative control tissue indicating that the lack of integration was not construct-specific but rather reflects a general failure of T-DNA transfer or stable integration under the conditions applied.

The possibility that PCR screening yielded false-negative results can be ruled out conclusively—the housekeeping gene *HvHsp90* was amplified successfully from all leaf tissue samples indicating adequate quality and quantity of DNA for PCR-based detection. It should be noted, however, that three of the four callus samples yielded only very faint *HvHsp90* signals, and one sample produced a weak band, suggesting suboptimal DNA quality in these. Nevertheless, the expected amplicons were produced using the Cas9 and HygR primer pairs when testing *A. tumefaciens* containing the respective constructs. This confirms primer functionality and in turn rules out technical failure as an explanation. Therefore, the absence of transgene signal from regenerated plants reflects that this is a true biological outcome rather than a technical artifact of the method used. Nonetheless, a transformation rate of 0% despite hygromycin selection over a period of several weeks warrants further investigation of the reasons that may have contributed to this result.

One such factor affecting *Agrobacterium*-mediated transformation efficiency is their inherently lower amenability of monocotyledonous species to this method compared to dicots (Hwang et al., 2017). *A. tumefaciens* has evolved to preferentially infect dicotyledonous hosts (Azizi-Dargahlou & Pouresmaeil, 2024; Gelvin, 2012; Hwang et al., 2017; Matveeva & Otten, 2019; Nester, 2014). A key aspect of this host preference lies in the role of acetosyringone a phenolic

compound naturally secreted by dicots upon wounding (Azizi-Dargahlou & Pouresmaeil, 2024). It activates the VirA/VirG two-component signaling system, which, in turn induces the expression of the *vir* gene regulon necessary for T-DNA processing, export, and delivery into the plant cell (Azizi-Dargahlou & Pouresmaeil, 2024; C.-H. Chang & Winans, 1992; Gordon & Christie, 2014; Jin, Roitsch et al., 1990; Lee, Jin, Sim & Nester, 1996; Nester, 2014; Stachel et al., 1985, 1986; Winans et al., 1988). Since monocotyledons do not secrete acetosyringone when wounded, supplementation is generally considered essential—at least during co-cultivation—when attempting (efficient) transformation in these species (Azizi-Dargahlou & Pouresmaeil, 2024; Hwang et al., 2017; Orman-Ligeza et al., 2020; Shou et al., 2002). However, reports show that, when transforming the barley cultivar Golden Promise, the addition of exogenous acetosyringone is negligible (Harwood et al., 2009; Wu, McCormac, Elliott & Chen, 1998). Golden Promise has lower concentrations of salicylic acid compared to other less transformable barley cultivars (Hisano et al., 2016). This is favorable since salicylic acid is a known inhibitor of *vir* gene expression (Yuan et al., 2007). Thus, both Harwood et al. (2009) and F. Wang et al. (2023) omitted acetosyringone from their co-cultivation medium and nonetheless achieved satisfactory transformation rates. Likewise, acetosyringone was not supplemented in the current study; however, given that transformation ultimately failed, its inclusion during co-cultivation in future experiments may still be beneficial for successful transformation even though using Golden Promise as described by Shrawat, Becker und Lörz (2007).

To delve deeper into what was just mentioned; beyond the use of acetosyringone, the plant genotype is a key factor determining the success rate when transforming barley. The cultivar Golden Promise, used throughout this study, is the standard for *Agrobacterium*-mediated transformation of barley. It was the first barley cultivar for which a complete transformation protocol was established (Tingay et al., 1997) and remains the most widely used genotype for the generation of transgenic barley (Hisano et al., 2016, 2017; Murray et al., 2004; M.-B. Wang, Abbott, Upadhyaya, Jacobsen & Waterhouse, 2001). It has increased transformability due to the presence of three transformation amenability (TFA) loci located on chromosomes 2H and 3H, along with a favorable hormone profile in developing embryos—notably elevated levels of growth-promoting hormones and comparatively low concentration of salicylic acid and abscisic acid—correlating with regeneration capacities of up to 92% (Hisano et al., 2016). Published transformation efficiencies for Golden Promise range from approximately 9% to over 25% depending on protocols and strains used (Bartlett et al., 2008; Harwood et al., 2009; Murray et al., 2004), far exceeding those reported for other cultivars. Accordingly, it is unlikely that the genotype itself is responsible for the observed transformation failure.

While the choice of cultivar may not be responsible for the observed outcome, the *Agrobac-*

terium strain used for T-DNA delivery is a critical variable. Since the early development of *Agrobacterium*-mediated barley transformation (Tingay et al., 1997), several strains have been evaluated for this cause, including AGL1, AGL0, EHA101, and LBA4404 (Shrawat et al., 2007; Tingay et al., 1997; M.-B. Wang et al., 2001; Wu et al., 1998). A major advance was achieved by Bartlett et al. (2008), who established an optimized high-throughput protocol using strain AGL1 and reported transformation efficiencies of approximately 25% in Golden Promise. AGL1 carries the disarmed Ti plasmid pTiBo542ΔT—characterized as hypervirulent (Lazo et al., 1991)—and has become the predominant strain used in barley immature embryo transformation, with reported efficiencies ranging from 10–38% across comparable protocols (Harwood et al., 2009; Ibrahim, El-Shihy & Fahmy, 2010; Orman-Ligeza et al., 2020). In this study, the *Agrobacterium* GV3101 strain was used instead—primarily due to its ready availability in the laboratory. Furthermore, while *Agrobacterium* cultures were grown for a standardized duration prior to inoculation, systematic optical density measurements were not consistently performed across all experiments, and variation in bacterial density at the time of inoculation cannot be excluded as an additional variable. While GV3101 is used routinely in dicotyledonous transformation systems, limited information exists regarding its use for transformation of barley immature embryos; to our knowledge, GV3101 has primarily been reported for pollen culture-based barley transformation, where it achieved a single-copy integration rate of 69% but an overall efficiency of only 0.6% (Kumlehn, Serazetdinova, Hensel, Becker & Loerz, 2006). No direct comparison between GV3101 and AGL1 for barley immature embryo transformation is currently available in the literature. Anyhow, given the well-documented superiority of hypervirulent strains for monocotyledonous transformation (Azizi-Dargahlou & Pouresmaeil, 2024; Hwang et al., 2017), the use of GV3101 may have contributed to the low transformation efficiency observed in this study, and AGL1—or an *Agrobacterium* strain with similar adaptions—should be used in future experiments.

Another aspect that could have lowered transformation success rates is the size of immature embryos used as explant material. Immature embryos found within a defined developmental window, typically 1.5–2.0 mm in diameter, are widely regarded as critical for successful barley transformation (Bartlett et al., 2008; Harwood et al., 2009; Ibrahim et al., 2010; Tingay et al., 1997). This size range represents an empirical balance between regeneration capacity, ease of handling, and robustness to *Agrobacterium* infection (Shrawat et al., 2007). In a systematic evaluation of embryo size effects on regeneration in barley cv. Morex, Y. Chang et al. (2003) demonstrated that smaller embryos (0.5–1.5 mm) formed significantly more compact embryogenic callus (93.5%) and averaged 4.4–4.8 regenerated shoots per embryo when compared with larger sized embryos exceeding 2.1 mm averaging only 0.6–0.8 shoots per embryo. Although no study has directly related embryo size to transformation efficiency directly, regeneration capacity is a

necessary downstream prerequisite for the recovery of transgenic plants. When linking this, a reduced regeneration potential is therefore expected to limit overall transformation success (Holme, Brinch-Pedersen, Lange & Holm, 2008). In the present study, post-hoc image-based measurements revealed that embryo diameters at the time of isolation were well above the recommended range, with mean diameters of approximately 3.5 mm in run 1 and 3.0 mm in run 2 (Figure 7.5). These measurements fall within or exceed the size class (2.6–3.0 mm) for which Y. Chang et al. (2003) reported the most severe regeneration deficits. The direct impact on T-DNA transfer and stable integration remains uncertain; however, larger sized embryos likely contributed to lower regeneration potential of explant material and may thus represent an additional contributing factor to the absence of confirmed transgenic events.

The analysis described above identified several factors that likely compromised T-DNA delivery and stable integration, and thus resulting in a decreased efficiency of T-DNA transfer—the use of a non-hypervirulent *Agrobacterium* strain, the absence of exogenous acetosyringone during co-cultivation, and oversized embryo explants. However, these factors alone do not explain how non-transformed calli survived prolonged hygromycin selection. If T-DNA transfer did not occur or was inefficient, the calli derived from said cell population would lack a functional hygromycin resistance cassette and therefore should have been eliminated during the selection phase. The persistence of apparently untransformed tissue thus requires an independent explanation. One possible explanation is transient T-DNA expression without stable genomic integration. In this scenario, T-DNA is delivered to the nucleus and transiently expressed, conferring short-term hygromycin tolerance without permanent integration into the host genome. Such transient transformation events are well documented and occur at substantially higher rate than stable integration (Gelvin, 2021); however, this explanation is inadequate when considering both the duration of selective pressure applied in this study and the available evidence on transient expression kinetics. Murray et al. (2004) demonstrated that transient expression of GFP in barley immature embryo-derived callus disappeared within 10–14 days following co-cultivation, while stably transformed callus clusters only became visible three to four weeks post-infection. This temporal dissociation indicates that transient T-DNA expression is relatively short-lived and, as a result, cannot account for callus survival under hygromycin selection for several weeks on CIM and subsequently on TM2. Transient transformation therefore does not provide a satisfactory explanation for the survival of non-transformed tissue subjected to the selection pressure applied here.

A more plausible explanation is a reduction in effective hygromycin concentration due to impaired antibiotic stability. The used hygromycin (Roche, REF 10843555001; 50 mg/mL in PBS) was stored as aliquots at –20°C, consistent with the approach described by Harwood et al. (2009),

however, a critical deviation occurred. Rather than being discarded after single use, aliquots were subjected to repeated freeze-thaw cycles over an extended period. Additionally, the stock had been stored frozen for well over a year prior to use. Unfortunately, the manufacturer's documentation for this specific product provides no information on freeze-thaw stability or freezing in general. Other manufacturers explicitly warn against repeated freeze-thaw cycles (*Hygromycin B 10843555001 Roche*, 2024; *Hygromycin B Gold*, 2024), although it should be noted that the extent to which this corresponds to Roche's formula remains unclear as these manufacturers use a different solvent or supply hygromycin B in powder form. Nonetheless, given the documented sensitivity of hygromycin B to repeated freeze–thaw cycles across multiple formulations, a reduction in effective antibiotic concentration cannot be excluded. Even a partial loss of activity might be enough to compromise selective pressure below a certain threshold, required for a sufficient elimination of non-transformed tissue: Park, Rose, Zapata, Srivatanakul und Smith (1998) demonstrated that suboptimal antibiotic concentrations result in substantial escape rates. Accordingly, the minimum inhibitory concentration is not equivalent to the effective selection dose (Park et al., 1998). This is consistent with the observation by Murray et al. (2004) that very few escapes from hygromycin selection occur when standard experimental conditions are maintained—implying that deviation from standard conditions, such as reduced antibiotic activity, is necessary to account for escape rates of this magnitude. Furthermore, it should be noted that hygromycin was omitted entirely from all media formulations following the first unsuccessful transfer of calli to regeneration medium (RM) in run 2. During this first RM transfer, shoots that had developed on TM2 senesced rapidly, prompting the removal of hygromycin to minimize physiological stress on the developing tissue. While this decision was made to preserve the regeneration potential of putative positive transformants, it also meant that from this point onward, selective pressure against non-transformed tissue was entirely absent allowing any surviving callus regardless of whether they contained T-DNA to complete the regeneration pathway. Taken together, the results of the current study can be explained most simply by the fact that T-DNA transfer either did not occur or did not lead to stable integration into the host genome, and that the remaining callus tissue was able to survive solely due to insufficient selection pressure as a result of impaired hygromycin activity.

To confirm effective gene disruption, CRISPR/Cas9 constructs were pre-validated in transient expression assays in *N. tabacum* prior to their application in barley transformation. The experimental design employed a split-leaf approach—to minimize the inter-leaf variability arising from differences in cell size and transformation efficiency—with a sequential infiltration strategy. Based on sequence analysis of the *GFP-HvTol* fusion construct the sgRNA target site is located upstream of and in frame with the *GFP* coding sequence; consequently, Cas9-mediated cleav-

age followed by error-prone NHEJ repair would be expected to introduce frameshift-inducing indels that prevent the maturation of functional GFP proteins, resulting in a loss of measurable fluorescence. Despite this rationale, no statistically significant differences in fluorescence intensity were detected between CRISPR-treated and control samples for any of the four constructs tested (Figure 4.1).

The most likely explanation for this outcome is the limited activity of monocotyledonous promoters in a dicotyledonous host. The CRISPR/Cas9 cassette on pHUE411 relies on two monocot-derived promoters—the maize ubiquitin promoter ZmUbi1 for Cas9 expression and the rice small nuclear RNA promoter OsU3 for sgRNA transcription (Figure 3.2). The transcriptional machineries between monocots and dicots vary fundamentally in core promoter architecture, GC content requirements, and specificity of transcription factor binding sites (Jores et al., 2021; Kumari, Sherpa & Dey, 2024). Specifically, it has been reported that ZmUbi1 approximately shows a four to five-fold reduced activity in dicotyledonous hosts compared to monocots (Christensen et al., 1992; Kumari et al., 2024). Furthermore, systematic cross-species testing revealed that only a small fraction of monocot regulatory elements retain functional activity in *Nicotiana* species (May et al., 2025). Importantly, when conducting studies to validate their CRISPR constructs in monocot protoplasts (specifically maize protoplasts), Xing et al. (2014)—who developed the pHUE411 vector system—used OsU3 and TaU3 promoters for sgRNA expression, but employed dicot-specific AtU6 promoters when testing in *Arabidopsis*, thus, implicitly confirming that the monocot sgRNA promoters are not intended for use in dicotyledonous systems. While the *GFP-HvTol* reporter construct driven by the rice actin promoter pOsAct1 did produce detectable fluorescence in tobacco, this does not contradict the hypothesis that the used promoters may be incompatible in dicotyledonous systems. The initial detection of GFP fluorescence from the pOsAct1-driven reporter construct indicates that this promoter retains at least partial transcriptional activity in tobacco. However, detectable reporter fluorescence does not imply that expression levels were sufficient for functional CRISPR-mediated genome editing. It requires the concurrent accumulation of Cas9 protein and sgRNA at levels sufficient to form active ribonucleoprotein complexes, locate and cleave the target sequence, followed by mutagenic NHEJ repair—a multi-step process with a considerably larger threshold requirement for expression than simple reporter detection (Xing et al., 2014). In addition, there are considerable limitations due to the transient nature of the assay itself—even if cleavage were to occur, GFP protein synthesized prior to disruption of the coding sequence could continue to exist in the cell until its natural turnover, potentially masking any reduction in *de novo* GFP production within the tested timeframe. Taken together, the non-significant results obtained from the transient expression assay do not provide evidence against the functionality of sgRNA, but rather reflect the

inherent limitations of validating a monocot-optimized CRISPR system in a heterologous dicot host. A more informative pre-validation strategy for future experiments would be to employ a monocot-based transient system, such as barley protoplast transformation (Xu et al., 2023). Ideally using protoplasts derived from a GFP-tagged *HvTol* reporter line, to allow for direct assessment of sgRNA-mediated target disruption within a native host background. However, this approach presupposes the availability of established transgenic reporter lines, which in turn requires a functional stable transformation pipeline—underscoring the circular dependency that motivated the use of the heterologous tobacco system as an interim solution in the first place.

Although stable transgene integration was not achieved, several methodological advances were established in this study that will aid in future transformation experiments. First, the timentin showering step introduced during early co-cultivation effectively suppressed *Agrobacterium* overgrowth throughout both experimental runs. While a formal quantitative comparison was not tested, persistent overgrowth of bacteria was a recurring problem in previous transformation attempts conducted in this laboratory. After implementation, no visible *Agrobacterium* proliferation was observed on any culture plate following the timentin treatment (Figure 4.2A)—it clearly demonstrated its practical use in maintaining sterile culture conditions and removing potential stress for establishing embryos due to prolonged overgrowth. However, it must be noted that the possible influence of timentin on the efficiency of T-DNA transfer was not assessed.

Second, the adoption of the modified transition medium TM2 based on the protocol described by F. Wang et al. (2023). It features an increased BAP concentration alongside with a reduced 2,4-D concentration favoring shoot over callus development and yielded substantially better results than the original TM transition medium used by Harwood et al. (2009)—in run 1, calli maintained on TM failed to initiate shoot formation within the expected cultivation period, whereas shoot development started after transfer to TM2. In run 2, TM2 was employed from the outset, resulting in more vigorous shoot formation across all constructs tested (Figure 4.2B). This observation is consistent with the findings of F. Wang et al. (2023), who demonstrated that using optimized hormone ratios in transition media drastically improves regeneration in barley tissue culture.

Third, this study marks the first successful regeneration of barley plants from tissue culture in this laboratory, establishing the complete pipeline from embryo isolation through callus induction, shoot regeneration, root formation, and transfer to soil. However, the removal of hygromycin from regeneration media should be reconsidered in future experiments—this decision was made to preserve shoot viability of putative positive transformants following initial senes-

cence on RM, having a preceding selection period of several weeks, yet it effectively eliminated selective pressure during the later regeneration stages. Harwood et al. (2009) explicitly maintain hygromycin selection throughout the rooting phase and note that root formation on selective medium represents strong evidence for stable transformation. Maintaining continuous selection throughout all stages up to transplantation into soil should therefore be a prerequisite for all subsequent approaches. More broadly, the transformation pipeline described herein represents its initial establishment in this laboratory, and as such reflects the iterative nature of early-stage protocol development. Decisions were guided primarily by the overarching goal of achieving plant regeneration from tissue culture, with handling adapted in response to observed developmental outcomes. The insights gained from these first experimental runs now provide a concrete basis for implementing a more standardized and stringent protocol in future iterations.

6 Conclusion

This study aimed to establish a complete *Agrobacterium*-mediated transformation pipeline for barley cv. Golden Promise with the intent of generating stable CRISPR/Cas9 knockout lines targeting individual *HvTol* genes. While no stably transformed plants were obtained, this work achieved the first successful regeneration of barley plants from tissue culture in this laboratory and identified several specific factors that likely contributed to the absence of stable transgene integration. These include the use of the non-hypervirulent *Agrobacterium* strain GV3101 rather than the established standard AGL1, the use of oversized immature embryos exceeding the recommended 1.5–2.0 mm range, and compromised hygromycin selection resulting from repeated freeze-thaw cycles and its eventual omission from later culture stages. Furthermore, the transient validation assay in *N. tabacum* proved unsuitable for assessing sgRNA functionality, since the monocot-derived promoters driving the CRISPR/Cas9 cassette likely showed insufficient activity in the heterologous dicot host.

Nonetheless, each of these limitations has well-characterized solutions in existing literature. Future experiments should employ the hypervirulent strain AGL1, follow a strict size selection of immature embryos, use freshly prepared single-use hygromycin aliquots with continuous selection throughout all culture stages, and supplement acetosyringone during co-cultivation. If implemented together with the methodological advances established herein—including effective *Agrobacterium* suppression via timentin treatment and improved shoot regeneration through the TM2 transition medium—these modifications provide a clear path toward successful generation of stably transformed barley *HvTol* knockout lines. Additionally, this work established computational tools allowing documentation and traceability of individual embryos throughout the transformation pipeline, with automated flagging of deviating samples to accommodate handling adapted to emerging developmental circumstances.

7 Supplements

7.1 Supplementary Tables

7.1.1 Verification of constructs by Sanger sequencing.

Table 7.1: Verification of *HvTol* single-target CRISPR/Cas9 constructs by Sanger sequencing.

Construct	`Intended spacer` ($5' \rightarrow 3'$)	`Identified spacer`	Junction	Notes
pHUE411-*HvTol1*	`CCCTTACGCTCATTGAAGCG`	`CCCTTACGCTCATTGAAGCG`	Yes	Sequencing confirmed correct spacer insertion.
pHUE411-*HvTol2*	`AGAGCCAGGTACTGCACCCT`	`AGAGCCAGGTACTGCACCCT`	Yes	Sequencing confirmed correct spacer insertion.
pHUE411-*HvTol3*	`GCGACGAGCGACATGCTGAT`	`GCGACGAGCGACATGCTGAT`	Yes	Sequencing confirmed correct spacer insertion.
pHUE411-*HvTol8*	`CGATCGACCAGGATGGACTG`	`CGATCGACCAGGATGGACTG`	Yes	Sequencing confirmed correct spacer insertion.

Footnote: Spacer sequences were considered validated when the exact 20-nt target spacer was present and directly followed by the conserved sgRNA scaffold sequence in the M13 Sanger read. Decreased base-calling quality toward the end of reads is typical for Sanger sequencing and did not affect the spacer–scaffold junction region.

7.1.2 Supplementary information of stable transformation of barley

Table 7.2: Conceptual rules for strand assignment used in Panels B and C of Figure 4.2. Within each experimental run, MAIN represents the principal propagation trajectory, while branch strands capture experimentally observed divergence.

Run	Strand	Assignment rationale
DG1	DG1_NEG	Negative control once it is no longer propagated together with any MAIN culture within the same time window.
DG1	DG1_TOL3TOL8	Replicates **TOL3** and **TOL8** after divergence from the shared early propagation trajectory.
DG1	MAIN	All cultures following the jointly propagated trajectory before any experimental divergence.
DG2	DG2_TOL8	Replicate **TOL8_2** after sustained deviation from the dominant propagation route.
DG2	DG2_TOL2b	Subset of the **TOL2_2** lineage derived from a temporary callus-level split and tracked as an independent lineage thereafter.
DG2	MAIN	Cultures following the dominant propagation trajectory of run 2.

Note: Strand assignment is applied consistently across Panels B and C.

Technical note: Strand assignment was implemented programmatically using run-specific decision variables (e.g. co-occurrence in shared time windows, persistent route deviation, and callus identifier tracking). Exact decision variables and their evaluation order are documented in Supplementary Table S7.3.

Table 7.3: Technical decision logic for strand assignment (MAIN vs branches). The table summarizes the variables and conditions used to assign observations to strands in the final analysis pipeline.

Run	Strand	Decision variable(s)	Condition	Biological interpretation
DG1	DG1_NEG	**dg1_neg_split_time**	Negative control observed without any MAIN replicate in same Tag_bin	Independent handling of negative control material
DG1	MAIN	**dg1_last_joint_time**	All replicates co-observed within same Tag_bin	Shared early propagation trajectory
DG1	DG1_TOL3TOL8	**dg1_last_joint_time**	**TOL3** or **TOL8** after last joint MAIN time point	Divergence after common early phase
DG2	MAIN	Dominant route key	Observation follows most frequent propagation route	Principal experimental trajectory
DG2	DG2_TOL8	Persistent route deviation	Sustained deviation across consecutive observations	Stable divergence, not transient delay
DG2	DG2_TOL2b	**Substrand** or callus-ID overlap	Observation belongs to diverging callus lineage	Lineage-level split within same initial embryo

Table 7.4: Primary observation table underlying Figures 1 and 2. Each row represents one experimentally observed culture unit (plate or pot) at a defined time point (DAI, days after embryo isolation) for experimental runs (Durchgang, DG) 1 and 2. Culture stages are inferred from the leading token of the medium name (CIM, TM, TM2, RM, SOIL). Additives and special handling steps are listed explicitly. Readouts are encoded in compact form as **O/C/S/R/K**, where O denotes *Agrobacterium* overgrowth (0/1), C the number of continuing calli or embryos (n), S the number of shoots (n), R the presence of roots (0/1), and K the number of additional clonal derivatives beyond the first biologically independent unit (n). Clonal material is thus documented explicitly but does not inflate biological counts.

DG	DAI	Pass.	Replicate	Callus_ID	Medium	Additives	Procedure	O/C/S/R/K
1	0	P1	TOL1_1	–	CIM	–	–	0/25/0/0/0
1	0	P1	TOL2_1	–	CIM	–	–	0/25/0/0/0
1	0	P1	TOL3_1	–	CIM	–	–	0/30/0/0/0
1	0	P1	TOL8_1	–	CIM	–	–	0/30/0/0/0
1	0	P1	negative_1	–	CIM	–	–	0/30/0/0/0
1	1	P2	TOL1_1	–	CIM	–	–	0/25/0/0/0
1	1	P2	TOL2_1	–	CIM	–	–	0/25/0/0/0
1	1	P2	TOL3_1	–	CIM	–	–	0/30/0/0/0
1	1	P2	TOL8_1	–	CIM	–	–	0/30/0/0/0
1	1	P2	negative_1	–	CIM	–	–	0/30/0/0/0
1	4	P3	TOL1_1	–	CIM	Timentin Hygromycin CuSO4	Timentin-Showering	1/25/0/0/0
1	4	P3	TOL2_1	–	CIM	Timentin Hygromycin CuSO4	Timentin-Showering	1/25/0/0/0
1	4	P3	TOL3_1	–	CIM	Timentin Hygromycin CuSO4	Timentin-Showering	1/30/0/0/0
1	4	P3	TOL8_1	–	CIM	Timentin Hygromycin CuSO4	Timentin-Showering	1/30/0/0/0
1	4	P3	negative_1	–	CIM	Timentin Hygromycin CuSO4	Timentin-Showering	1/30/0/0/0
1	18	P3	TOL1_1	–	CIM	Timentin Hygromycin CuSO4	–	0/25/0/0/0
1	18	P3	TOL2_1	–	CIM	Timentin Hygromycin CuSO4	–	0/25/0/0/0
1	18	P3	TOL3_1	–	CIM	Timentin Hygromycin CuSO4	–	0/30/0/0/0
1	18	P3	TOL8_1	–	CIM	Timentin Hygromycin CuSO4	–	0/30/0/0/0
1	18	P3	negative_1	–	CIM	Timentin Hygromycin CuSO4	–	0/30/0/0/0
1	32	P3	TOL1_1	–	CIM	Timentin Hygromycin CuSO4	–	0/25/0/0/0
1	32	P3	TOL2_1	–	CIM	Timentin Hygromycin CuSO4	–	0/26/0/0/0
1	32	P3	TOL3_1	–	CIM	Timentin Hygromycin CuSO4	–	0/19/0/0/0
1	32	P3	TOL8_1	–	CIM	Timentin Hygromycin CuSO4	–	0/16/0/0/0
1	32	P3	negative_1	–	CIM	Timentin Hygromycin CuSO4	–	0/30/0/0/0
1	45	P4.1	negative_1	–	TM	Timentin Hygromycin CuSO4	–	0/26/0/0/0

Continued on next page

Table 7.4: Primary observation table underlying Figures 1 and 2 (continued).

DG	DAI	Pass.	Replicate	Callus_ID	Medium	Additives	Procedure	O/C/S/R/K
1	46	P4.1	TOL1_1	–	TM	Timentin Hygromycin CuSO4	–	0/19/0/0/0
1	46	P4.1	TOL2_1	–	TM	Timentin Hygromycin CuSO4	–	0/19/0/0/0
1	46	P4.1	TOL3_1	–	TM	Timentin Hygromycin CuSO4	–	0/7/0/0/0
1	46	P4.1	TOL8_1	–	TM	Timentin Hygromycin CuSO4	–	0/9/0/0/0
1	53	P4.2	negative_1	–	TM2	Timentin Hygromycin CuSO4	–	0/21/0/0/0
1	60	P4.2	TOL1_1	–	TM	Timentin Hygromycin CuSO4	–	0/19/0/0/0
1	60	P4.2	TOL2_1	–	TM	Timentin Hygromycin CuSO4	–	0/19/0/0/0
1	60	P4.2	TOL3_1	–	TM	Timentin Hygromycin CuSO4	–	0/7/0/0/0
1	60	P4.2	TOL8_1	–	TM	Timentin Hygromycin CuSO4	–	0/9/0/0/0
1	67	P4.2	negative_1	–	TM2	Timentin Hygromycin CuSO4	–	0/21/0/0/0
1	71	P4.2	TOL3_1	–	TM2	Timentin Hygromycin CuSO4	–	0/7/0/0/0
1	71	P4.2	TOL8_1	–	TM2	Timentin Hygromycin CuSO4	–	0/9/2/0/0
1	81	P4.2	TOL1_1	–	TM2	Timentin Hygromycin CuSO4	–	0/19/0/0/0
1	81	P4.2	TOL2_1	–	TM2	Timentin Hygromycin CuSO4	–	0/19/0/0/0
1	81	P5	negative_1	–	RM	Timentin Hygromycin CuSO4	–	0/8/8/1/0
1	85	P4.2	TOL3_1	–	TM2	Timentin Hygromycin CuSO4	–	0/7/0/0/0
1	85	P4.2	TOL8_1	–	TM2	Timentin Hygromycin CuSO4	–	0/9/1/0/0
1	95	P4.2	TOL1_1	–	TM2	Timentin Hygromycin CuSO4	–	0/19/0/0/0
1	95	P4.2	TOL2_1	–	TM2	Timentin Hygromycin CuSO4	–	0/19/0/0/0
1	95	P5	negative_1	–	RM	Timentin Hygromycin	–	0/6/0/0/0
1	99	P5	TOL3_1	–	RM	Timentin Hygromycin CuSO4	–	0/4/1/0/0
1	99	P5	TOL8_1	–	RM	Timentin Hygromycin CuSO4	–	0/7/3/0/0
1	101	P4.2	negative_1	–	TM2	Timentin Hygromycin CuSO4	–	0/6/0/0/0
1	109	P5	TOL1_1	–	RM	Timentin Hygromycin CuSO4	–	0/7/0/0/0

Continued on next page

Table 7.4: Primary observation table underlying Figures 1 and 2 (continued).

DG	DAI	Pass.	Replicate	Callus_ID	Medium	Additives	Procedure	O/C/S/R/K
1	109	P5	TOL2_1	–	RM	Timentin Hygromycin CuSO4	–	0/5/1/0/0
1	113	P5	TOL3_1	–	RM	Timentin Hygromycin	–	0/3/0/0/0
1	113	P5	TOL8_1	–	RM	Timentin Hygromycin	–	0/4/0/0/0
1	115	P4.2	negative_1	–	TM2	–	–	0/6/0/0/0
1	119	P4.2	TOL3_1	–	TM2	Timentin Hygromycin CuSO4	–	0/3/0/0/0
1	119	P4.2	TOL8_1	–	TM2	Timentin Hygromycin CuSO4	–	0/4/0/0/0
1	123	P5	TOL1_1	–	RM	Timentin Hygromycin	–	0/6/0/0/0
1	123	P5	TOL2_1	–	RM	Timentin Hygromycin	–	0/5/0/0/0
1	129	P4.2	TOL1_1	–	TM2	Timentin Hygromycin CuSO4	–	0/3/0/0/0
1	129	P4.2	negative_1	–	TM2	–	–	0/6/1/0/0
1	133	P4.2	TOL3_1	–	TM2	–	–	0/3/0/0/0
1	133	P4.2	TOL8_1	–	TM2	–	–	0/4/0/0/0
1	143	P4.2	TOL1_1	–	TM2	–	–	0/3/0/0/0
1	143	P5	negative_1	K_P4	RM	–	–	0/1/1/0/0
1	147	P4.2	TOL3_1	–	TM2	–	–	0/3/0/0/0
1	147	P4.2	TOL8_1	–	TM2	–	–	0/4/0/0/0
1	157	P4.2	TOL1_1	–	TM2	–	–	0/3/0/0/0
1	161	P4.2	TOL3_1	–	TM2	–	–	0/0/0/0/0
1	161	P4.2	TOL8_1	–	TM2	–	–	0/0/0/0/0
1	165	P6	negative_1	K_P4	RM	–	–	0/1/1/1/0
1	171	P4.2	TOL1_1	–	TM2	–	–	0/0/0/0/0
1	171	P6	negative_1	K_P4	Soil	–	–	–/1/1/1/0
1	225	P6	negative_1	K_P4	Soil	–	–	–/1/1/1/0
1	331	P6	negative_1	K_P4	Soil	–	–	–/1/1/1/0
2	0	P1	TOL1_2	–	CIM	–	–	0/25/0/0/0
2	0	P1	TOL2_2	–	CIM	–	–	0/25/0/0/0
2	0	P1	TOL3_2	–	CIM	–	–	0/25/0/0/0
2	0	P1	TOL8_2	–	CIM	–	–	0/25/0/0/0
2	0	P1	negative_2	–	CIM	–	–	0/25/0/0/0
2	1	P2	TOL1_2	–	CIM	–	–	0/25/0/0/0
2	1	P2	TOL2_2	–	CIM	–	–	0/25/0/0/0
2	1	P2	TOL3_2	–	CIM	–	–	0/25/0/0/0
2	1	P2	TOL8_2	–	CIM	–	–	0/25/0/0/0
2	1	P2	negative_2	–	CIM	–	–	0/25/0/0/0
2	4	P3	TOL1_2	–	CIM	Timentin Hygromycin CuSO4	Timentin-Showering	1/25/0/0/0
2	4	P3	TOL2_2	–	CIM	Timentin Hygromycin CuSO4	Timentin-Showering	1/25/0/0/0
2	4	P3	TOL3_2	–	CIM	Timentin Hygromycin CuSO4	Timentin-Showering	1/25/0/0/0
2	4	P3	TOL8_2	–	CIM	Timentin Hygromycin CuSO4	Timentin-Showering	1/25/0/0/0

Continued on next page

Table 7.4: Primary observation table underlying Figures 1 and 2 (continued).

DG	DAI	Pass.	Replicate	Callus_ID	Medium	Additives	Procedure	O/C/S/R/K
2	4	P3	negative_2	–	CIM	Timentin Hygromycin CuSO4	Timentin-Showering	1/25/0/0/0
2	18	P3	TOL1_2	–	CIM	Timentin Hygromycin CuSO4	–	0/25/0/0/0
2	18	P3	TOL2_2	–	CIM	Timentin Hygromycin CuSO4	–	0/25/0/0/0
2	18	P3	TOL3_2	–	CIM	Timentin Hygromycin CuSO4	–	0/25/0/0/0
2	18	P3	TOL8_2	–	CIM	Timentin Hygromycin CuSO4	–	0/25/0/0/0
2	18	P3	negative_2	–	CIM	Timentin Hygromycin CuSO4	–	0/25/0/0/0
2	32	P3	TOL1_2	–	CIM	Timentin Hygromycin CuSO4	–	0/23/0/0/0
2	32	P3	TOL3_2	–	CIM	Timentin Hygromycin CuSO4	–	0/22/0/0/0
2	32	P3	TOL8_2	–	CIM	Timentin Hygromycin CuSO4	–	0/25/0/0/0
2	32	P3	negative_2	–	CIM	Timentin Hygromycin CuSO4	–	0/24/0/0/0
2	34	P3	TOL2_2	–	CIM	Timentin Hygromycin CuSO4	–	0/25/0/0/0
2	46	P4.1	TOL1_2	–	TM2	Timentin Hygromycin CuSO4	–	0/20/0/0/0
2	46	P4.1	TOL2_2	–	TM2	Timentin Hygromycin CuSO4	–	0/24/0/0/0
2	46	P4.1	TOL3_2	–	TM2	Timentin Hygromycin CuSO4	–	0/21/0/0/0
2	46	P4.1	TOL8_2	–	TM2	Timentin Hygromycin CuSO4	–	0/21/0/0/0
2	46	P4.1	negative_2	–	TM2	Timentin Hygromycin CuSO4	–	0/21/0/0/0
2	53	P4.2	TOL1_2	–	TM2	Timentin Hygromycin CuSO4	–	0/20/0/0/0
2	53	P4.2	TOL2_2	–	TM2	Timentin Hygromycin CuSO4	–	0/24/0/0/0
2	53	P4.2	TOL3_2	–	TM2	Timentin Hygromycin CuSO4	–	0/21/0/0/0
2	53	P4.2	TOL8_2	–	TM2	Timentin Hygromycin CuSO4	–	0/21/0/0/0
2	53	P4.2	negative_2	–	TM2	Timentin Hygromycin CuSO4	–	0/21/0/0/0
2	60	P4.2	TOL1_2	–	TM2	Timentin Hygromycin CuSO4	–	0/20/5/0/0
2	60	P4.2	TOL2_2	–	TM2	Timentin Hygromycin CuSO4	–	0/24/2/0/0
2	60	P4.2	TOL3_2	–	TM2	Timentin Hygromycin CuSO4	–	0/21/3/0/0

Continued on next page

Table 7.4: Primary observation table underlying Figures 1 and 2 (continued).

DG	DAI	Pass.	Replicate	Callus_ID	Medium	Additives	Procedure	O/C/S/R/K
2	60	P4.2	TOL8_2	–	TM2	Timentin Hygromycin CuSO4	–	0/21/5/0/0
2	60	P4.2	negative_2	–	TM2	Timentin Hygromycin CuSO4	–	0/21/2/0/0
2	74	P5	TOL1_2	–	RM	Timentin Hygromycin	–	0/12/8/0/0
2	74	P5	TOL2_2	–	RM	Timentin Hygromycin	–	0/15/4/0/0
2	74	P5	TOL3_2	–	RM	Timentin Hygromycin	–	0/4/2/0/0
2	74	P5	TOL8_2	–	RM	Timentin Hygromycin	–	0/6/2/0/0
2	74	P5	negative_2	–	RM	Timentin Hygromycin	–	0/5/2/0/0
2	86	P5	TOL3_2	–	RM	Timentin Hygromycin	–	0/4/0/0/0
2	86	P5	TOL8_2	–	RM	Timentin Hygromycin	–	0/5/1/0/0
2	86	P5	negative_2	–	RM	Timentin Hygromycin	–	0/4/1/0/0
2	88	P5	TOL1_2	–	RM	Timentin Hygromycin	–	0/7/0/0/0
2	88	P5	TOL2_2	–	RM	Timentin Hygromycin	–	0/8/0/0/0
2	88	P4.2	TOL3_2	–	TM2	Timentin Hygromycin CuSO4	–	0/4/0/0/0
2	88	P4.2	TOL8_2	–	TM2	Timentin Hygromycin CuSO4	–	0/5/0/0/0
2	88	P4.2	negative_2	–	TM2	Timentin Hygromycin CuSO4	–	0/4/0/0/0
2	90	P4.2	TOL1_2	–	TM2	Timentin Hygromycin CuSO4	–	0/7/0/0/0
2	90	P4.2	TOL2_2	–	TM2	Timentin Hygromycin CuSO4	–	0/8/0/0/0
2	102	P4.2	TOL3_2	–	TM2	–	–	0/4/0/0/0
2	102	P4.2	TOL8_2	–	TM2	–	–	0/5/0/0/0
2	102	P4.2	negative_2	–	TM2	–	–	0/4/0/0/0
2	104	P4.2	TOL1_2	–	TM2	–	–	0/7/0/0/0
2	104	P4.2	TOL2_2	–	TM2	–	–	0/8/1/0/0
2	116	P4.2	TOL3_2	–	TM2	–	–	0/4/0/0/0
2	116	P4.2	TOL8_2	–	TM2	–	–	0/5/0/0/0
2	116	P4.2	negative_2	–	TM2	–	–	0/4/3/0/0
2	118	P4.2	TOL1_2	–	TM2	–	–	0/7/2/0/0
2	118	P4.2	TOL2_2	–	TM2	–	–	0/8/4/0/0
2	130	P5	TOL3_2	K_31	RM	–	–	0/1/1/0/0
2	130	P4.2	TOL8_2	–	TM2	–	–	0/5/0/0/0
2	130	P5	negative_2	K_P1.1, K_P1.2, K_P1.3	RM	–	–	0/2/2/0/2
2	132	P5	TOL1_2	K_11	RM	–	–	0/1/1/0/0
2	132	P5	TOL2_2	K_21, K_22, K_23.1, K_23.2, K_23.3, K_23.4	RM	–	–	0/3/3/0/3
2	152	P6	TOL3_2	K_31	Soil	–	–	–/1/1/1/0

Continued on next page

Table 7.4: Primary observation table underlying Figures 1 and 2 (continued).

DG	DAI	Pass.	Replicate	Callus_ID	Medium	Additives	Procedure	O/C/S/R/K
2	152	P4.2	TOL8_2	–	TM2	–	–	0/0/0/0/0
2	152	P6	negative_2	K_P1.1, K_P1.2	Soil	–	–	–/1/1/1/1
2	154	P6	TOL1_2	K_11	Soil	–	–	–/1/1/1/0
2	154	P5	TOL2_2	K_22, K_23.1, K_23.3, K23.4	RM	–	–	0/3/3/1/2
2	154	P6	TOL2_2	K_21, K_23.2	Soil	–	–	–/2/2/1/0
2	160	P6	TOL2_2	K_22, K_23.1, K_23.3, K23.4	Soil	–	–	–/2/3/1/2
2	212	P6	TOL3_2	K_31	Soil	–	–	–/1/1/1/0
2	212	P6	negative_2	K_P1.1, K_P1.2	Soil	–	–	–/1/1/1/1
2	214	P6	TOL1_2	K_11	Soil	–	–	–/1/1/1/0
2	214	P6	TOL2_2	K_21, K_23.2	Soil	–	–	–/2/2/1/0
2	214	P6	TOL2_2	K_23.3	Soil	–	–	–/1/1/1/0
2	318	P6	TOL3_2	K_31	Soil	–	–	–/1/1/1/0
2	318	P6	negative_2	K_P1.1, K_P1.2	Soil	–	–	–/1/1/1/1
2	320	P6	TOL1_2	K_11	Soil	–	–	–/1/1/1/0
2	320	P6	TOL2_2	K_21, K_23.2	Soil	–	–	–/2/2/1/0
2	320	P6	TOL2_2	K_23.3	Soil	–	–	–/1/1/1/0

7.2 Supplementary figures

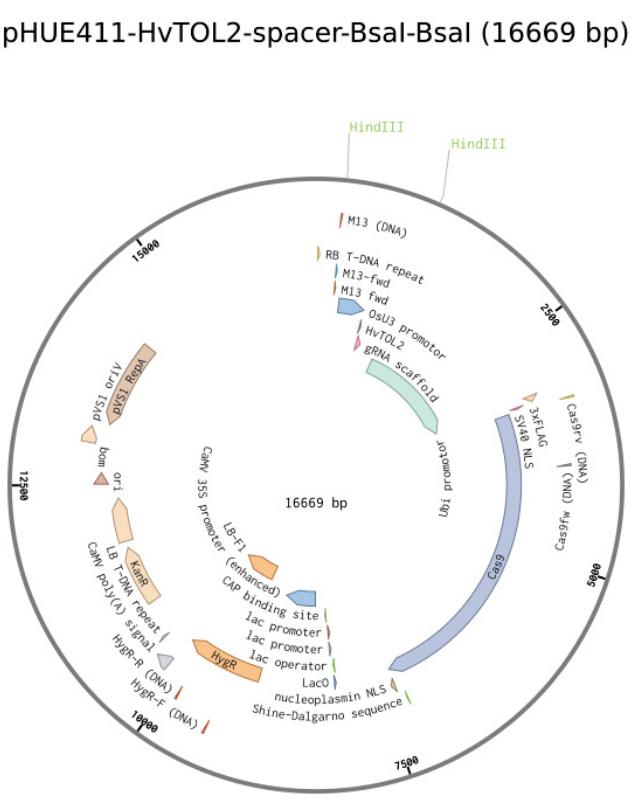

Figure 7.1: pHUE411-*HvTol2* plasmid map.
Plasmid map of pHUE411-*HvTol2* insertion created with Benchling.

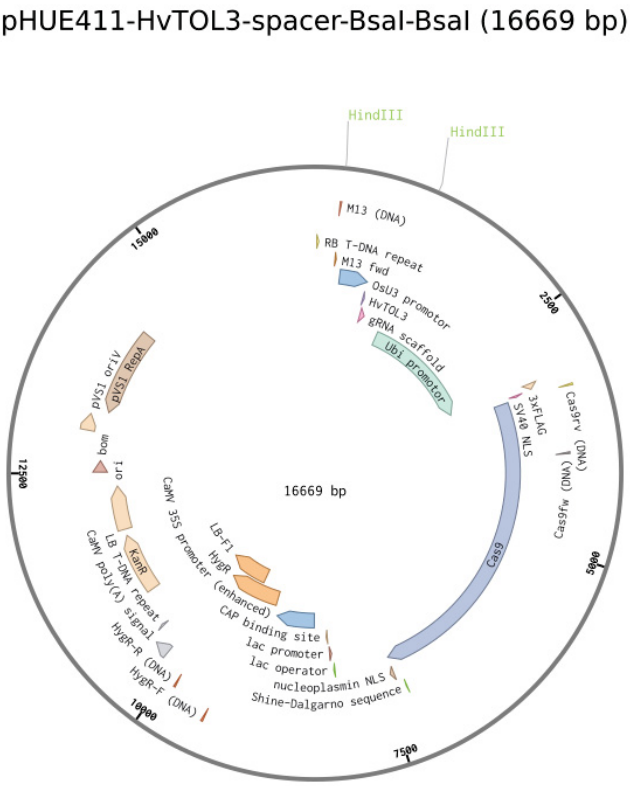

Figure 7.2: pHUE411-*HvTol3* plasmid map.
Plasmid map of pHUE411-*HvTol3* insertion created with Benchling.

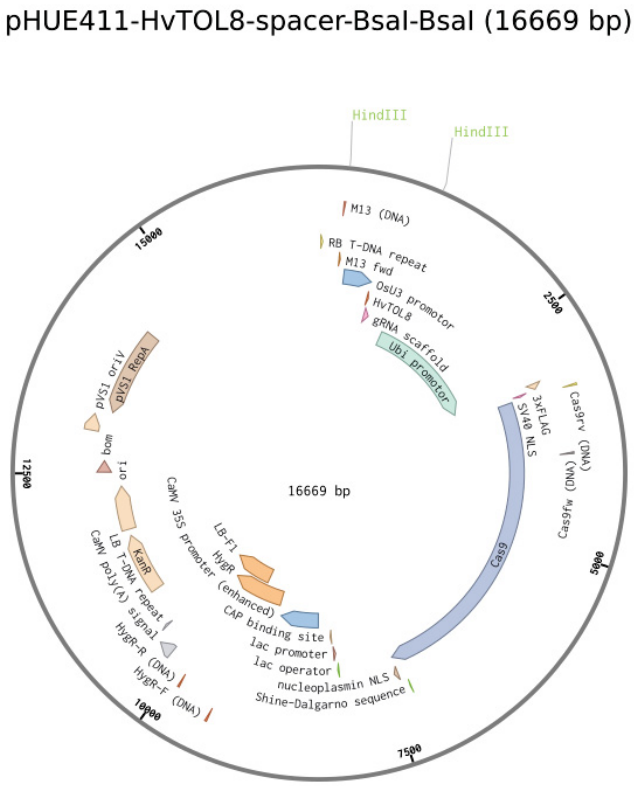

Figure 7.3: pHUE411-*HvTol8* plasmid map.
Plasmid map of pHUE411-*HvTol8* insertion created with Benchling.

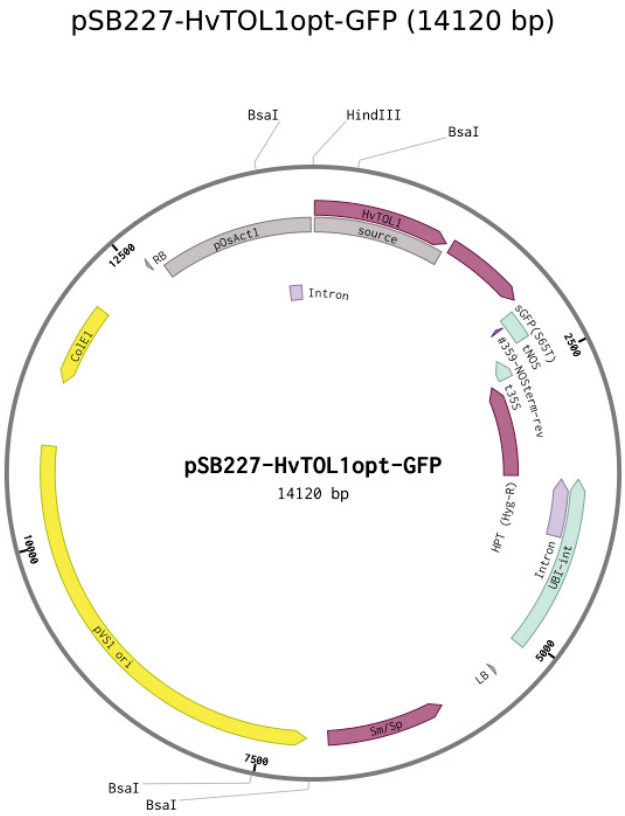

Figure 7.4: pSB227-*HvTol1* plasmid map.
Plasmid map of pSB227-*HvTol1* insertion created with Benchling.

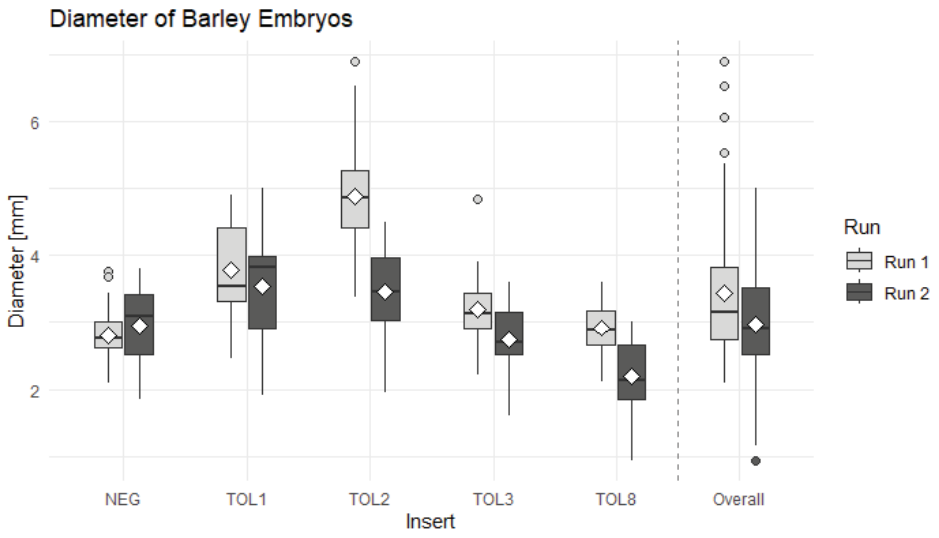

Figure 7.5: Diameter of Barley Embryos. Diameter of embryos during cocultivation at DAI 1. Measurements were calculated in ImageJ from images taken after inoculation.

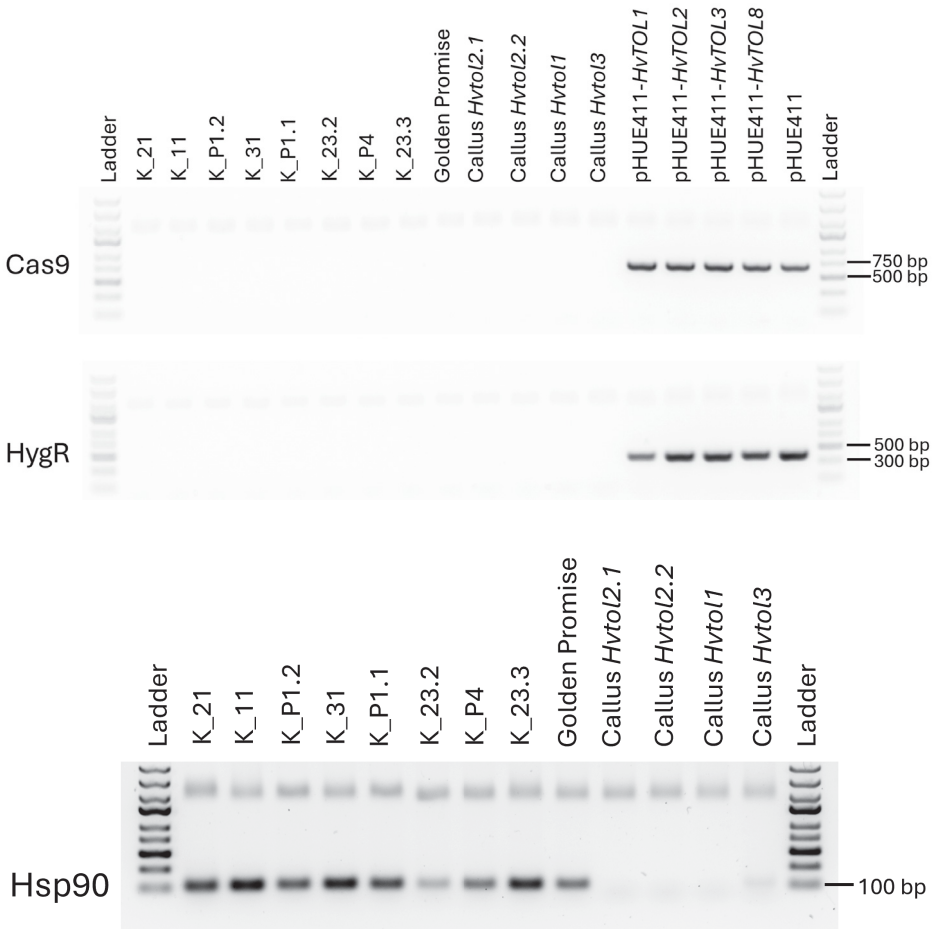

Figure 7.6: Complete uncropped agarose gels of PCR screening of putative transgenic barley samples. Full gel images corresponding to Figure 4.5. Primer pairs, sample identifiers, and PCR conditions are detailed in Table 3.15 and Section 3.2.5.7. Samples comprise regenerated plant material (K_21, K_11, K_P1.2, K_31, K_P1.1, K_23.2, K_P4, K_23.3) and callus material (callus *hvtol1*, callus *hvtol2.1*, callus *hvtol2.2*, callus *hvtol3*); transformed *A. tumefaciens* carrying the respective pHUE411 constructs served as positive controls and untransformed Golden Promise as negative control. Band between 2000 bp and 3000 bp marker refers to residuals of the Phire™ Plant Direct PCR Master Mix. Marker: O'GeneRuler Express DNA Ladder (Thermo Fisher Scientific).

7.3 Supplementary Information: Analysis Code and ImageJ Macros

7.3.0.1 ImageJ macro for automated image subdivision and fluorescence extraction

The following ImageJ macro was used for automated processing of confocal microscopy images obtained from transiently transformed *Nicotiana tabacum* leaves. The macro subdivides each image into four equally sized regions and extracts the mean fluorescence intensity (Mean Grey Value) for each region. This procedure was applied uniformly to all images to ensure consistent and reproducible image analysis.

Listing 7.1: ImageJ macro used for automated subdivision of confocal images and extraction of mean fluorescence intensity (Mean Grey Value).

```
// ImageJ macro for batch processing: splits each image into four quadrants
// The 'path' variable is automatically filled by the batch function with the path
// of the current image. 'outputPath' is also set by the batch function.
// 'arg' contains the file name.

processFolder();

function processFolder() {

// Ensure that an image is open in order to retrieve its dimensions

    if (nImages == 0) return;

    var originalTitle = getTitle();

    getDimensions(width, height, channels, slices, frames);

// Calculate half of the image width and height

    var w2 = width / 2;

    var h2 = height / 2;

// Determine the file name without extension for saving

    var nameWithoutExt = File.getNameWithoutExtension(originalTitle);

// ----------------------------------------------------
// --- IMPORTANT: The 'saveAs' commands save the images
// automatically into the "Output Folder",
// that you select in the Batch processing dialog!
// ----------------------------------------------------
// 1. Top left

    makeRectangle(0, 0, w2, h2);

    run("Duplicate...", "title=Quadrat_1");

    saveAs("Tiff", getDirectory("output") + nameWithoutExt + "_Q1.tif");
```

```
    close();
// 2. Top right
    selectImage(originalTitle);
    makeRectangle(w2, 0, w2, h2);
    run("Duplicate...", "title=Quadrat_2");
    saveAs("Tiff", getDirectory("output") + nameWithoutExt + "_Q2.tif");
    close();
// 3. Bottom left
    selectImage(originalTitle);
    makeRectangle(0, h2, w2, h2);
    run("Duplicate...", "title=Quadrat_3");
    saveAs("Tiff", getDirectory("output") + nameWithoutExt + "_Q3.tif");
    close();
// 4. Bottom right
    selectImage(originalTitle);
    makeRectangle(w2, h2, w2, h2);
    run("Duplicate...", "title=Quadrat_4");
    saveAs("Tiff", getDirectory("output") + nameWithoutExt + "_Q4.tif");
    close();
// Close the original image (optional, but saves memory)
    close();
    print("Bild erfolgreich in 4 Quadrate geteilt: " + originalTitle);
}
```

7.3.0.2 Transient expression: statistical analysis (R)

Listing 7.2: The following R script was used for statistical analysis and visualization of fluorescence intensity data obtained from transient CRISPR/Cas9 assays in *Nicotiana tabacum*. The script performs data import, preprocessing, image-level aggregation, statistical testing (Welch's *t*-test, Wilcoxon rank-sum test, Shapiro-Wilk normality test), effect size estimation (Cohen's *d*), and generation of publication-ready figures (Figure 4.1). All analyses reported in this thesis were conducted using this script. This script uses the packages `readxl` (Wickham & Bryan, 2025), `dplyr` (Wickham et al., 2023), `tidyr` (Wickham et al., 2025), `ggplot2` (Wickham, 2016), and `effsize` (Torchiano, 2020).

```
# ========================
# Transient expression (tobacco)  revised analysis script
# Input:  Tabak_rohdaten.xlsx
# Output: CRISPR_TOL_Boxplot.pdf  +  console statistics
#
# CHANGES vs. v1:
# 1. Pseudoreplication fix: quadrants (Q1Q4) are averaged per image (HD_X)
#    before statistical testing    n = 6 biological replicates per group
# 2. Normality tested (Shapiro-Wilk) on image means
# 3. Welch t-test + Wilcoxon rank-sum as robustness check
# 4. Cohen's d, 95 % CI of the mean difference, and percent difference reported
# 5. Plot labels consistently in English
# ========================

# ---- Packages ----
library(readxl)
library(dplyr)
library(tidyr)
library(ggplot2)
library(effsize)

# ---- File path ----
infile <- "Tabak_rohdaten.xlsx"

# ---- Read data ----
daten <- read_excel(infile)
names(daten) <- gsub("\\s+", "_", names(daten))

# ---- Robust column handling (unchanged) ----
if (!"Mean_Grey_Value" %in% names(daten)) {
  candidates <- c("Mean_Grey_value", "mean_grey_value", "MeanGreyValue", "Mean_GreyValue")
  hit <- candidates[candidates %in% names(daten)]
  if (length(hit) == 1) {
    names(daten)[names(daten) == hit] <- "Mean_Grey_Value"
  } else {
    stop("Required column 'Mean_Grey_Value' not found. Found: ",
```

```
        paste(names(daten), collapse = ", "))
  }
}

req_cols <- c("Name", "Protein", "Transformation", "Mean_Grey_Value")
missing  <- setdiff(req_cols, names(daten))
if (length(missing) > 0) stop("Missing columns: ", paste(missing, collapse = ", "))

# ---- Coerce types / drop NA ----
daten <- daten %>%
  mutate(
    Mean_Grey_Value = suppressWarnings(as.numeric(Mean_Grey_Value)),
    Protein         = as.character(Protein),
    Transformation  = as.character(Transformation),
    Name            = as.character(Name)
  ) %>%
  filter(!is.na(Mean_Grey_Value))

# ---- Extract image ID (remove quadrant suffix) ----
# File names follow: _HD_X_QY.tif   image = everything up to _QY
daten <- daten %>%
  mutate(Image_ID = sub("_Q[1-4]\\.tif$", "", Name))

# ---- Aggregate: mean per image (fixes pseudoreplication) ----
bild_means <- daten %>%
  group_by(Image_ID, Protein, Transformation) %>%
  summarise(Mean_Grey_Value = mean(Mean_Grey_Value, na.rm = TRUE),
            .groups = "drop")

# ---- Scale to match legacy figure ( 1000) ----
bild_means <- bild_means %>%
  mutate(Mean_Grey_Value = Mean_Grey_Value / 1000)

# Also scale the raw quadrant data (for the boxplot, which shows all points)
daten <- daten %>%
  mutate(Mean_Grey_Value = Mean_Grey_Value / 1000)

# ---- Factor levels ----
proteine <- c("TOL1", "TOL2", "TOL3", "TOL8")

bild_means <- bild_means %>%
  mutate(Protein        = factor(Protein, levels = proteine),
         Transformation = factor(Transformation, levels = c("negative", "CRISPR")))

daten <- daten %>%
  mutate(Protein        = factor(Protein, levels = proteine),
         Transformation = factor(Transformation, levels = c("negative", "CRISPR")))

# ============================================================
# ---- Statistical analysis (on IMAGE MEANS, n = 4/group) ----
# ============================================================

results_list <- list()
```

```
for (prot in proteine) {

  cat("\n", strrep("=", 60), "\n")
  cat(" ", prot, "  analysis on image means (n = 6 per group)\n")
  cat(strrep("=", 60), "\n")

  x <- bild_means %>%                          # CRISPR
    filter(Protein == prot, Transformation == "CRISPR") %>%
    pull(Mean_Grey_Value)

  y <- bild_means %>%                           # negative control
    filter(Protein == prot, Transformation == "negative") %>%
    pull(Mean_Grey_Value)

  if (length(x) < 2 || length(y) < 2) {
    cat("   Not enough observations  skipping.\n")
    next
  }

  # --- Descriptives ---
  cat("\n  Negative control : mean =", round(mean(y), 2),
      " SD =", round(sd(y), 2), " n =", length(y), "\n")
  cat("  CRISPR           : mean =", round(mean(x), 2),
      " SD =", round(sd(x), 2), " n =", length(x), "\n")

  pct_diff <- (mean(x) - mean(y)) / mean(y) * 100
  cat("  Percent difference (CRISPR vs. negative): ",
      sprintf("%+.1f %%", pct_diff), "\n")

  # --- Normality (Shapiro-Wilk) ---
  sw_x <- shapiro.test(x)
  sw_y <- shapiro.test(y)
  cat("\n  Shapiro-Wilk (CRISPR)  : W =", round(sw_x$statistic, 4),
      " p =", round(sw_x$p.value, 4), "\n")
  cat("  Shapiro-Wilk (negative): W =", round(sw_y$statistic, 4),
      " p =", round(sw_y$p.value, 4), "\n")

  normality_ok <- sw_x$p.value > 0.05 & sw_y$p.value > 0.05
  cat("   Normality assumption ",
      ifelse(normality_ok, "met (p > 0.05 in both groups)", "violated"), "\n")

  # --- Welch t-test (one-sided: CRISPR < negative) ---
  tt <- t.test(x, y, alternative = "less")
  cat("\n  Welch t-test (one-sided, CRISPR < negative):\n")
  cat("    t =", round(tt$statistic, 3),
      " df =", round(tt$parameter, 1),
      " p =", format.pval(tt$p.value, digits = 4), "\n")

  # 95 % CI of the mean difference (two-sided for reporting)
  tt2 <- t.test(x, y, alternative = "two.sided")
  cat("    95 % CI of mean difference: [",
      round(tt2$conf.int[1], 2), ",", round(tt2$conf.int[2], 2), "]\n")
```

```
  # --- Effect size: Cohen's d ---
  cd <- cohen.d(x, y, hedges.correction = FALSE)
  cat("    Cohen's d =", round(cd$estimate, 3),
      " [", round(cd$conf.int[1], 3), ",", round(cd$conf.int[2], 3), "]\n")

  # --- Wilcoxon rank-sum (robustness check) ---
  wt <- wilcox.test(x, y, alternative = "less", exact = FALSE)
  cat("\n  Wilcoxon rank-sum (one-sided, robustness check):\n")
  cat("    W =", wt$statistic, " p =", format.pval(wt$p.value, digits = 4), "\n")

  # --- Significance label ---
  sig_label <- case_when(
    tt$p.value < 0.001 ~ "***",
    tt$p.value < 0.01  ~ "**",
    tt$p.value < 0.05  ~ "*",
    TRUE               ~ "ns"
  )
  cat("\n   Result: ", sig_label, "\n")

  results_list[[prot]] <- tibble(
    Protein   = prot,
    pval      = tt$p.value,
    signif    = sig_label,
    cohens_d  = cd$estimate,
    pct_diff  = pct_diff,
    ci_lo     = tt2$conf.int[1],
    ci_hi     = tt2$conf.int[2]
  )
}

results_df <- bind_rows(results_list)

# ============================================================
# ---- Plot (boxplot of RAW quadrant data + image-mean points) ----
# ============================================================

# The boxplot shows the spread across all 16 quadrants per protein,
# but overlays the 4 image means as individual points so the reader
# can see both the raw variability and the biological replicates.

# y-positions for significance annotations
ypos <- daten %>%
  group_by(Protein) %>%
  summarise(y = max(Mean_Grey_Value, na.rm = TRUE) * 1.06, .groups = "drop")

pvals <- left_join(results_df %>% select(Protein, signif),
                   ypos, by = "Protein") %>%
  mutate(Protein = factor(Protein, levels = proteine))

p <- ggplot(daten, aes(x = Protein, y = Mean_Grey_Value, fill = Transformation)) +
  # Boxplot of all quadrant values
  geom_boxplot(width        = 0.62,
```

```
              outlier.shape = NA,
              color         = "black",
              alpha         = 0.8) +
  # Overlay image means as points (biological replicates)
  geom_point(data     = bild_means,
             aes(x = Protein, y = Mean_Grey_Value, fill = Transformation),
             position = position_dodge(width = 0.62),
             shape    = 21,
             size     = 2.2,
             color    = "black",
             alpha    = 0.9,
             show.legend = FALSE) +
  # Significance annotations
  geom_text(data        = pvals,
            aes(x = Protein, y = y, label = signif),
            inherit.aes = FALSE,
            size        = 3.6,
            vjust       = 0) +
  # Colours & English labels
  scale_fill_manual(
    values = c("negative" = "grey85", "CRISPR" = "grey35"),
    labels = c("Negative control", "CRISPR")
  ) +
  labs(x = "TOL protein",
       y = "Mean Grey Value (\u00d7 10\u00b3)") +
  theme_classic(base_size = 10) +
  theme(
    legend.position  = c(0.82, 0.92),
    legend.direction = "vertical",
    legend.title     = element_blank(),
    legend.text      = element_text(size = 9),
    legend.key.size  = grid::unit(0.45, "cm"),
    axis.text        = element_text(color = "black", size = 9),
    axis.title       = element_text(face = "bold", size = 10),
    panel.border     = element_rect(color = "black", fill = NA, linewidth = 0.5),
    plot.margin      = margin(5, 5, 5, 5)
  )

print(p)

# ---- Save ----
ggsave(filename = "CRISPR_TOL_Boxplot.pdf",
       plot     = p,
       width    = 16,
       height   = 9,
       units    = "cm",
       dpi      = 600)

# ---- Summary table to console ----
cat("\n\n", strrep("=", 70), "\n")
cat("  SUMMARY TABLE\n")
cat(strrep("=", 70), "\n")
print(results_df %>%
```

```
        mutate(across(where(is.numeric), ~ round(.x, 3))) %>%
        as.data.frame(),
      row.names = FALSE)
cat(strrep("=", 70), "\n")
```

7.3.0.3 Barley stable transformation: analysis pipeline (R)

Listing 7.3: R script used for preprocessing, strand assignment, time binning, and visualization of the barley stable transformation dataset. The script reproduces Figures 4.2 and 4.4 and implements the MAIN/branch logic described in the Methods. This script is using the packages `tidyverse` (Wickham et al., 2019), `readxl` (Wickham & Bryan, 2025), `grid` (R Core Team, 2025) and `cowplot` (Wilke, 2025).

```
############################################################
# Barley Stable Transformation  Figure 1 (A4 full-page, stacked)
# v3-adapted input: reads Barley_Stable_Transformation_v4.xlsx
# Output figure should remain identical to v2 processing.
#
# FIX:
# - Prevent false early binning: Gesamt_Tag 0 and 1 must NOT be merged into one Tag_bin.
############################################################

library(tidyverse)
library(readxl)
library(grid)
library(cowplot)

# =========================
# FILE PATH (edit if needed)
# =========================
infile  <- "C:/Users/Moritz Schmid/OneDrive - Universitt Wien/Desktop/Barley_Stable_Transformation_v4.
    xlsx"
out_png <- "C:/Users/Moritz Schmid/OneDrive - Universitt Wien/Desktop/barley_stable_transformation_RCode_
    v3.png"

# =========================
# Load data
# =========================
df_raw <- read_excel(infile)

# ---- v3 compatibility layer (minimal + safe) ----
# v3 uses 'Insert' instead of 'Behandlung'. Keep downstream code unchanged by renaming.
if ("Insert" %in% names(df_raw) && !("Behandlung" %in% names(df_raw))) {
  df_raw <- df_raw %>% rename(Behandlung = Insert)
}

# ensure clone annotation column exists
if (!("Davon_Klone" %in% names(df_raw))) {
  df_raw <- df_raw %>% mutate(Davon_Klone = 0)
}

# =========================
# Clean + select only required columns
# =========================
df_clean <- df_raw %>%
```

```
  select(any_of(c(
    "Datum",
    "Gesamt_Tag",
    "Passage",
    "Name_Replikat",
    "Kallus_ID",
    "Behandlung",
    "Medium",
    "Durchgang",
    "A_tumefaciens_overgrowth",
    "Kallus_Wachstum",
    "Sprossentwicklung_Anzahl",
    "Wurzelentwicklung_binary",
    "Anzahl_weiterbildender_Embryos/Kalli",
    "Erfolgreiche_Pflanzen",
    "Zusaetzliche_Klone",
    "Davon_Klone",
    "Erfolgreiche_Transformation",
    "Substrand"
  ))) %>%
  filter(!is.na(Durchgang)) %>%
  filter(Durchgang != 0) %>%
  mutate(
    Durchgang = factor(Durchgang),
    Medium = str_squish(as.character(Medium)),
    Name_Replikat = str_squish(as.character(Name_Replikat)),
    Passage = str_to_upper(str_squish(as.character(Passage))),
    Kallus_ID = str_squish(as.character(Kallus_ID)),

    # optional: explicit DG2 sublineage annotation (recommended for TOL2 split)
    Substrand = if ("Substrand" %in% names(df_raw)) str_to_upper(str_squish(as.character(Substrand)))
     else NA_character_,

    # robust numeric coercion (turns non-numeric strings into NA)
    Gesamt_Tag = suppressWarnings(as.numeric(Gesamt_Tag)),
    A_tumefaciens_overgrowth = suppressWarnings(as.numeric(A_tumefaciens_overgrowth)),
    Kallus_Wachstum = suppressWarnings(as.numeric(Kallus_Wachstum)),
    Sprossentwicklung_Anzahl = suppressWarnings(as.numeric(Sprossentwicklung_Anzahl)),
    Wurzelentwicklung_binary = suppressWarnings(as.numeric(Wurzelentwicklung_binary)),
    Erfolgreiche_Transformation = suppressWarnings(as.numeric(Erfolgreiche_Transformation)),
    `Anzahl_weiterbildender_Embryos/Kalli` = suppressWarnings(as.numeric(`Anzahl_weiterbildender_Embryos/
     Kalli`)),
    Erfolgreiche_Pflanzen = suppressWarnings(as.numeric(Erfolgreiche_Pflanzen)),
    Zusaetzliche_Klone = suppressWarnings(as.numeric(Zusaetzliche_Klone)),
    Davon_Klone = suppressWarnings(as.numeric(Davon_Klone))
  ) %>%
  filter(!is.na(Gesamt_Tag))


# =========================
# Kallus_ID parsing helper (for DG2 TOL2 split tracking)
# =========================
parse_kallus_ids <- function(x) {
```

```
  x <- str_squish(as.character(x))
  if (is.na(x) || x == "" || str_to_upper(x) %in% c("K.A.","KA","N/A","NA")) return(character(0))
  parts <- unlist(str_split(x, ","))
  parts <- str_squish(parts)
  parts <- parts[parts != ""]
  # normalize common variant "K23.4" -> "K_23.4"
  parts <- str_replace(parts, "^K(\\d)", "K_\\1")
  parts <- str_replace_all(parts, "\\s+", "")
  unique(parts)
}

df_clean <- df_clean %>%
  mutate(
    kallus_vec = map(Kallus_ID, parse_kallus_ids),
    kallus_sig = map_chr(kallus_vec, ~ paste(sort(.x), collapse = ","))
  )


# =========================
# Helpers: lighten/darken
# =========================
lighten_hex <- function(hex, amount = 0.40) {
  rgb <- grDevices::col2rgb(hex) / 255
  rgb2 <- rgb + (1 - rgb) * amount
  grDevices::rgb(rgb2[1], rgb2[2], rgb2[3])
}
darken_hex <- function(hex, amount = 0.25) {
  rgb <- grDevices::col2rgb(hex) / 255
  rgb2 <- rgb * (1 - amount)
  grDevices::rgb(rgb2[1], rgb2[2], rgb2[3])
}

# =========================
# Stage assignment from first token
# =========================
df_clean <- df_clean %>%
  mutate(
    Medium_stage_raw = str_trim(str_extract(Medium, "^[^,]+")),
    Medium_stage = case_when(
      str_to_upper(Medium_stage_raw) == "CIM"  ~ "CIM",
      str_to_upper(Medium_stage_raw) == "TM"   ~ "TM",
      str_to_upper(Medium_stage_raw) == "TM2"  ~ "TM2",
      str_to_upper(Medium_stage_raw) == "RM"   ~ "RM",
      str_to_upper(Medium_stage_raw) == "SOIL" ~ "SOIL",
      TRUE ~ "OTHER"
    ),
    Medium_stage = factor(Medium_stage, levels = c("CIM","TM","TM2","RM","SOIL","OTHER"))
  )

# =========================
# Stage colors (your desired mapping)
# =========================
stage_base <- c(
```

```
  CIM   = "#4B1D63",
  TM    = "#2F6DB3",
  TM2   = "#F28E2B",
  RM    = "#B0164D",
  SOIL  = "#4ECDC4",
  OTHER = "#6B3A22"
)

# =========================
# FULL Medium palette (all medium variants -> shades within stage)
# =========================
medium_levels <- sort(unique(df_clean$Medium))
medium_palette <- setNames(rep(NA_character_, length(medium_levels)), medium_levels)

for (st in names(stage_base)) {
  meds_st <- medium_levels[medium_levels %in% unique(df_clean$Medium[df_clean$Medium_stage == st])]
  if (length(meds_st) == 0) next

  base <- stage_base[[st]]
  ramp <- grDevices::colorRampPalette(c(
    lighten_hex(base, 0.55),
    base,
    darken_hex(base, 0.10)
  ))

  meds_st_sorted <- sort(meds_st)
  medium_palette[meds_st_sorted] <- ramp(length(meds_st_sorted))
}

if (any(is.na(medium_palette))) {
  missing <- names(medium_palette)[is.na(medium_palette)]
  fb <- grDevices::colorRampPalette(stage_base[c("CIM","TM","TM2","RM","SOIL")])
  medium_palette[missing] <- fb(length(missing))
}

# =========================
# FORCE TIME-BINNING for Panel B + C
# FIX: prevent merging of very early days (0 and 1)
# =========================
max_gap <- 2
early_cutoff <- 2  # days < 2 (i.e., 0 and 1) must NOT be merged across different days

df_binned <- df_clean %>%
  arrange(Durchgang, Medium_stage, Gesamt_Tag, Passage, Name_Replikat) %>%
  group_by(Durchgang, Medium_stage) %>%
  mutate(
    gap = Gesamt_Tag - lag(Gesamt_Tag),

    # new bin if:
    # - first row (is.na(gap))
    # - gap > max_gap
    # - OR we are in early protocol days (< early_cutoff) AND day changes (gap != 0)
    bin_run = cumsum(
```

```
      is.na(gap) |
        gap > max_gap |
        ((lag(Gesamt_Tag, default = first(Gesamt_Tag)) < early_cutoff) &
           (Gesamt_Tag < early_cutoff) &
           (gap != 0))
    )
  ) %>%
  group_by(Durchgang, Medium_stage, bin_run) %>%
  mutate(Tag_bin = round(mean(Gesamt_Tag, na.rm = TRUE))) %>%
  ungroup()

# =========================
# Replicate key + plate_id
# =========================
df_binned <- df_binned %>%
  mutate(
    rep_key = str_squish(Name_Replikat),
    Replicate = str_extract(rep_key, "^(TOL\\d+|negative)"),
    plate_id = interaction(Name_Replikat, Passage, Kallus_ID, drop = TRUE, sep = " | ")
  )



# Add parsed Kallus_ID vectors/signatures to the binned table (used for DG2 TOL2 sub-branching)
df_binned <- df_binned %>%
  mutate(
    kallus_vec = map(Kallus_ID, parse_kallus_ids),
    kallus_sig = map_chr(kallus_vec, ~ paste(sort(.x), collapse = ","))
  )

# =========================
# DG1: determine last_joint_time automatically (on Tag_bin)
# =========================
required_dg1 <- c("TOL1","TOL2","TOL3","TOL8","negative")

dg1_joint_tbl <- df_binned %>%
  filter(Durchgang == "1") %>%
  distinct(Tag_bin, Replicate) %>%
  group_by(Tag_bin) %>%
  summarise(
    reps = list(sort(unique(Replicate))),
    has_all = all(required_dg1 %in% unlist(reps)),
    .groups = "drop"
  )

dg1_last_joint_time <- dg1_joint_tbl %>%
  filter(has_all) %>%
  summarise(last = max(Tag_bin, na.rm = TRUE)) %>%
  pull(last)

if (is.infinite(dg1_last_joint_time) || is.na(dg1_last_joint_time)) {
  dg1_last_joint_time <- max(df_binned$Tag_bin[df_binned$Durchgang == "1"], na.rm = TRUE)
}
```

```
message("DG1 last_joint_time (Tag_bin) = ", dg1_last_joint_time)

# ========================
# DG1: AUTO determine when negative is no longer observed together with MAIN
# ========================
dg1_neg_coobs <- df_binned %>%
  filter(Durchgang == "1") %>%
  mutate(
    is_negative = (Replicate == "negative"),
    is_main_member = (Replicate %in% c("TOL1","TOL2","TOL3","TOL8"))
  ) %>%
  group_by(Tag_bin) %>%
  summarise(
    has_negative = any(is_negative, na.rm = TRUE),
    has_main_member = any(is_main_member, na.rm = TRUE),
    coobs = has_negative & has_main_member,
    .groups = "drop"
  ) %>%
  arrange(Tag_bin)

dg1_neg_split_time <- dg1_neg_coobs %>%
  filter(has_negative, !coobs) %>%
  summarise(first = min(Tag_bin, na.rm = TRUE)) %>%
  pull(first)

if (is.infinite(dg1_neg_split_time) || is.na(dg1_neg_split_time)) {
  dg1_neg_split_time <- Inf
}
message("DG1 negative split_time (Tag_bin) = ", dg1_neg_split_time)

# ========================
# DG2: AUTO split logic (day-based, robust)
# - DG2_TOL8: split when deviation from dominant route persists for >= 2 consecutive observed days
# - DG2_TOL2b: split as an "within-day fork" when TOL2_2 appears in >1 route on the same day
#   (your case: Gesamt_Tag 154 with Passage P5 vs P6 on SOIL)
# ========================

mode_first <- function(x) {
  x <- x[!is.na(x)]
  if (length(x) == 0) return(NA_character_)
  ux <- unique(x)
  ux[which.max(tabulate(match(x, ux)))]
}

# Define a route key (use stage + passage; if you later need additive-sensitive splits,
# you can switch to paste(Medium, Passage, sep="|") safely)
dg2_routes_by_day <- df_clean %>%
  filter(Durchgang == "2") %>%
  mutate(route_key = paste(as.character(Medium_stage), as.character(Passage), sep = "|")) %>%
  group_by(Gesamt_Tag) %>%
  summarise(main_route_ref = mode_first(route_key), .groups = "drop")

# Helper: find first day where divergence persists for >= min_consecutive consecutive OBSERVED days
```

```
find_persistent_split_day <- function(dat_clean, rep_pattern, min_consecutive = 2) {
  d <- dat_clean %>%
    filter(Durchgang == "2", str_detect(str_squish(as.character(Name_Replikat)), rep_pattern)) %>%
    mutate(route_key = paste(as.character(Medium_stage), as.character(Passage), sep = "|")) %>%
    left_join(dg2_routes_by_day, by = "Gesamt_Tag") %>%
    group_by(Gesamt_Tag) %>%
    summarise(diverges = any(route_key != main_route_ref, na.rm = TRUE), .groups = "drop") %>%
    arrange(Gesamt_Tag)

  if (nrow(d) == 0) return(Inf)

  # Run-length encode TRUE blocks on consecutive observed days
  # (requires consecutive in the *vector order*; since we sorted by Gesamt_Tag, it is correct)
  r <- rle(d$diverges)
  ends <- cumsum(r$lengths)
  starts <- ends - r$lengths + 1
  idx <- which(r$values & r$lengths >= min_consecutive)
  if (length(idx) == 0) return(Inf)
  d$Gesamt_Tag[starts[idx[1]]]
}

# DG2_TOL8: persistent deviation (works well for your data)
dg2_tol8_split_day <- find_persistent_split_day(df_clean, "^TOL8_2", min_consecutive = 2)

# DG2_TOL2b: within-day fork (no persistence requirement)
# Split day = first day where TOL2_2 is observed in >1 route on the same day


# DG2_TOL2b: callus-based fork
# Split day = first day where TOL2_2 is observed as >=2 distinct kallus subgroups (kallus_sig)
dg2_tol2b_split_day <- df_clean %>%
  filter(Durchgang == "2", str_detect(str_squish(as.character(Name_Replikat)), "^TOL2_2")) %>%
  filter(lengths(kallus_vec) > 0) %>%
  group_by(Gesamt_Tag) %>%
  summarise(n_groups = n_distinct(kallus_sig), .groups = "drop") %>%
  filter(n_groups > 1) %>%
  summarise(first = min(Gesamt_Tag, na.rm = TRUE)) %>%
  pull(first)

if (is.infinite(dg2_tol2b_split_day) || is.na(dg2_tol2b_split_day)) {
  dg2_tol2b_split_day <- Inf
}

# Identify the "TOL2b" callus-ID set on the split day.
# Primary rule: take the split-day row(s) with Passage == P5 (your intended TOL2b subgroup).
# Fallback: take the subgroup with the largest number of callus IDs on that day.
tol2b_ids <- character(0)

if (is.finite(dg2_tol2b_split_day)) {
  tol2_splitday_rows <- df_clean %>%
    filter(Durchgang == "2",
           str_detect(str_squish(as.character(Name_Replikat)), "^TOL2_2"),
           Gesamt_Tag == dg2_tol2b_split_day) %>%
```

```
    mutate(n_ids = lengths(kallus_vec)) %>%
    filter(n_ids > 0)

  tol2_p5 <- tol2_splitday_rows %>% filter(Passage == "P5")
  if (nrow(tol2_p5) > 0) {
    tol2b_ids <- unique(unlist(tol2_p5$kallus_vec))
  } else if (nrow(tol2_splitday_rows) > 0) {
    tol2b_ids <- unique(unlist((tol2_splitday_rows %>% slice_max(n_ids, n = 1, with_ties = FALSE))$kallus
     _vec))
  }
}

# Flag DG2 TOL2b rows in the BINNED table:
# - If Substrand exists and marks TOL2B, use it.
# - Otherwise, from the split day onward, assign TOL2b if the row's Kallus_IDs overlap with tol2b_ids.
df_binned <- df_binned %>%
  mutate(
    tol2b_flag = case_when(
      Durchgang == "2" & str_detect(rep_key, "^TOL2_2") &
        !is.na(Substrand) & Substrand %in% c("TOL2B","DG2_TOL2B","BRANCH") ~ TRUE,

      Durchgang == "2" & str_detect(rep_key, "^TOL2_2") &
        is.na(Substrand) &
        is.finite(dg2_tol2b_split_day) &
        Tag_bin >= dg2_tol2b_split_day &
        lengths(kallus_vec) > 0 &
        map_lgl(kallus_vec, ~ length(intersect(.x, tol2b_ids)) > 0) ~ TRUE,

      TRUE ~ FALSE
    )
  )

message("DG2 TOL8 split_day (persistent route deviation) = ", dg2_tol8_split_day)
message("DG2 TOL2b split_day (within-day fork) = ", dg2_tol2b_split_day)

message("DG2 TOL2b ids (from split day) = ", paste(tol2b_ids, collapse = "; "))

# =========================
# SINGLE strand variable used for BOTH Panel B and C
# =========================
df_binned <- df_binned %>%
  mutate(
    strand = case_when(
      Durchgang == "1" & Replicate == "negative" ~ "DG1_NEG",

      Durchgang == "1" & Tag_bin <= dg1_last_joint_time ~ "MAIN",
      Durchgang == "1" & Tag_bin >  dg1_last_joint_time & Replicate %in% c("TOL3","TOL8") ~ "DG1_TOL3TOL8
     ",
      Durchgang == "1" ~ "MAIN",

      Durchgang == "2" & Replicate == "negative" ~ "DG2_NEG",

      Durchgang == "2" & str_detect(rep_key, "^TOL8_2") & Tag_bin >= dg2_tol8_split_day ~ "DG2_TOL8",
```

```
      Durchgang == "2" & tol2b_flag ~ "DG2_TOL2b",

      Durchgang == "2" ~ "MAIN",
      TRUE ~ "MAIN"
    ),
    strand = factor(strand, levels = c("MAIN","DG1_TOL3TOL8","DG1_NEG","DG2_NEG","DG2_TOL8","DG2_TOL2b"))
  )

strand_cols <- c(
  DG1_TOL3TOL8 = "#772474",
  DG1_NEG      = "#D62728",
  DG2_NEG      = "#D62728",
  DG2_TOL8     = "#1E4FA8",
  DG2_TOL2b    = "#D58434"
)

# Linetypes: split branches dashed; negatives solid red (DG1 gets an overlay dashed black segment after
    split)
strand_ltypes <- c(
  DG1_TOL3TOL8 = "dashed",
  DG1_NEG      = "solid",
  DG2_NEG      = "solid",
  DG2_TOL8     = "dashed",
  DG2_TOL2b    = "dashed"
)

# =========================
# X-axis alignment
# =========================
x_min <- min(df_clean$Gesamt_Tag, na.rm = TRUE)
x_max <- max(df_clean$Gesamt_Tag, na.rm = TRUE)

tick_step <- 50
x_min_tick <- floor(x_min / tick_step) * tick_step
x_max_tick <- ceiling(x_max / tick_step) * tick_step
x_breaks   <- seq(x_min_tick, x_max_tick, by = tick_step)

x_scale_aligned <- scale_x_continuous(
  limits = c(x_min_tick, x_max_tick),
  breaks = x_breaks,
  expand = c(0, 0)
)

aligned_margins <- theme(
  plot.margin = margin(t = 6, r = 10, b = 6, l = 10),
  panel.spacing = unit(0.8, "lines"),
  panel.grid.minor.x = element_blank()
)

aligned_margins_BC <- theme(
  plot.margin = margin(t = 6, r = 10, b = 6, l = 16),
  panel.spacing = unit(0.8, "lines"),
  panel.grid.minor.x = element_blank()
```

```
)

# =========================
# MAIN-based, continuous stage background (no gaps)
# FIX: ends at last observed MAIN timepoint per Durchgang
# =========================
main_stage_points <- df_binned %>%
  filter(strand == "MAIN") %>%
  distinct(Durchgang, Tag_bin, Medium_stage) %>%
  arrange(Durchgang, Tag_bin)

main_time_range <- main_stage_points %>%
  group_by(Durchgang) %>%
  summarise(
    main_min = min(Tag_bin, na.rm = TRUE),
    main_max = max(Tag_bin, na.rm = TRUE),
    .groups = "drop"
  )

print(main_time_range)

main_stage_runs <- main_stage_points %>%
  group_by(Durchgang) %>%
  arrange(Tag_bin) %>%
  mutate(stage_run = cumsum(Medium_stage != lag(Medium_stage, default = first(Medium_stage)))) %>%
  ungroup()

main_stage_starts <- main_stage_runs %>%
  group_by(Durchgang, stage_run, Medium_stage) %>%
  summarise(start = min(Tag_bin, na.rm = TRUE), .groups = "drop") %>%
  arrange(Durchgang, start)

stage_blocks_main_cont <- main_stage_starts %>%
  group_by(Durchgang) %>%
  arrange(start) %>%
  mutate(end = lead(start) - 1) %>%
  ungroup() %>%
  left_join(main_time_range, by = "Durchgang") %>%
  group_by(Durchgang) %>%
  mutate(
    end = if_else(is.na(end), main_max, end),
    end = pmax(end, start),
    start = pmax(start, main_min),
    end   = pmin(end,   main_max)
  ) %>%
  ungroup() %>%
  select(Durchgang, Medium_stage, start, end)


# =========================
# Panel A (NOT BINNED): MAIN vs negative controls only
# - uses the SAME strand assignment as Panels B + C
# - branch strands are excluded from the calculation and plot
```

```
# ========================
df_A <- df_binned %>%
  mutate(
    Group_A = case_when(
      str_detect(as.character(strand), "NEG") ~ "Negative control",
      strand == "MAIN" ~ "MAIN",
      TRUE ~ NA_character_
    )
  ) %>%
  filter(!is.na(Group_A)) %>%
  mutate(Group_A = factor(Group_A, levels = c("MAIN","Negative control")))

bin_long_A <- df_A %>%
  pivot_longer(
    cols = c(A_tumefaciens_overgrowth, Kallus_Wachstum),
    names_to = "Trait",
    values_to = "Value"
  ) %>%
  mutate(
    Trait = recode(
      Trait,
      A_tumefaciens_overgrowth = "Agrobacterium overgrowth",
      Kallus_Wachstum          = "Callus growth"
    ),
    Trait = factor(Trait, levels = c("Agrobacterium overgrowth", "Callus growth"))
  )

plot_A <- ggplot() +
  geom_rect(
    data = stage_blocks_main_cont,
    aes(xmin = start, xmax = end, ymin = -Inf, ymax = Inf, fill = Medium_stage),
    alpha = 0.28
  ) +
  # ---- NEGATIVE controls (background) ----
  stat_summary(
    data = bin_long_A %>% filter(Group_A == "Negative control"),
    aes(x = Gesamt_Tag, y = Value, group = interaction(Durchgang, Trait), linetype = Trait),
    fun = mean, geom = "line",
    linewidth = 0.70,
    color = "red3"
  ) +
  stat_summary(
    data = bin_long_A %>% filter(Group_A == "Negative control"),
    aes(x = Gesamt_Tag, y = Value, group = interaction(Durchgang, Trait), linetype = Trait),
    fun = mean, geom = "point",
    size = 2.0,
    shape = 17,
    color = "red3"
  ) +
  # ---- MAIN (foreground) ----
  stat_summary(
    data = bin_long_A %>% filter(Group_A == "MAIN"),
    aes(x = Gesamt_Tag, y = Value, group = interaction(Durchgang, Trait), linetype = Trait),
```

```
    fun = mean, geom = "line",
    linewidth = 0.95,
    color = "black"
  ) +
  stat_summary(
    data = bin_long_A %>% filter(Group_A == "MAIN"),
    aes(x = Gesamt_Tag, y = Value, group = interaction(Durchgang, Trait), linetype = Trait),
    fun = mean, geom = "point",
    size = 2.0,
    shape = 16,
    color = "black"
  ) +
  # Timentin showering marker
  geom_vline(
    xintercept = 4,
    linetype = "dashed",
    linewidth = 0.51,
    color = "red3"
  ) +
  facet_wrap(~ Durchgang, labeller = as_labeller(c(‘1‘ = "Run 1", ‘2‘ = "Run 2"))) +
  scale_fill_manual(values = stage_base, guide = "none") +
  x_scale_aligned +
  labs(
    title = "A) Agrobacterium overgrowth and callus formation",
    y = "Proportion",
    x = NULL,
    linetype = NULL
  ) +
  theme_bw(base_size = 11) +
  theme(legend.position = "none") +
  aligned_margins

# Legend under Panel A: traits + groups + Timentin-Showering
plot_A_legend_traits <- ggplot(bin_long_A, aes(x = Gesamt_Tag, y = Value, linetype = Trait)) +
  geom_line(color = "black", linewidth = 0.95) +
  theme_minimal(base_size = 10) +
  theme(
    legend.position = "bottom",
    legend.title = element_blank(),
    plot.margin = margin(0, 10, 0, 10)
  )
trait_legend <- cowplot::get_legend(plot_A_legend_traits)

group_leg_df <- tibble(
  Group_A = factor(c("MAIN","Negative control"), levels = c("MAIN","Negative control")),
  x = c(0, 1),
  y = c(1, 1)
)

plot_A_legend_groups <- ggplot(group_leg_df, aes(x = x, y = y, color = Group_A, shape = Group_A)) +
  geom_point(size = 2.1) +
  scale_color_manual(values = c("MAIN" = "black", "Negative control" = "red3")) +
  scale_shape_manual(values = c("MAIN" = 16, "Negative control" = 17)) +
```

```
  guides(
    color = guide_legend(nrow = 1, byrow = TRUE),
    shape = guide_legend(nrow = 1, byrow = TRUE)
  ) +
  theme_void(base_size = 10) +
  theme(
    legend.position = "bottom",
    legend.title = element_blank(),
    legend.key.width = unit(0.90, "cm"),
    plot.margin = margin(0, 10, 0, 10)
  )
group_legend <- cowplot::get_legend(plot_A_legend_groups)

timentin_leg_df <- tibble(x = c(0, 1), y = 1, Event = "Timentin-Showering")
plot_timentin_legend_source <- ggplot(timentin_leg_df, aes(x = x, y = y, color = Event)) +
  geom_line(linetype = "dashed", linewidth = 0.51) +
  scale_color_manual(values = c("Timentin-Showering" = "red3"),
                     guide = guide_legend(nrow = 2, byrow = TRUE)) +
  theme_void(base_size = 10) +
  theme(
    legend.position = "bottom",
    legend.title = element_blank(),
    legend.key.width = unit(0.90, "cm"),
    plot.margin = margin(0, 10, 0, 10)
  )
timentin_legend <- cowplot::get_legend(plot_timentin_legend_source)

legend_A <- cowplot::plot_grid(
  trait_legend,
  group_legend,
  timentin_legend,
  ncol = 1,
  rel_heights = c(1, 0.95, 0.95)
)

# ========================
# Panel B (BINNED): shoots
# ========================
shoots_binned <- df_binned %>%
  group_by(Durchgang, Tag_bin, strand) %>%
  summarise(
    total_shoots = sum(Sprossentwicklung_Anzahl, na.rm = TRUE),
    .groups = "drop"
  )

shoots_main <- shoots_binned %>% filter(strand == "MAIN")
shoots_branches <- shoots_binned %>% filter(strand != "MAIN")

# DG1: overlay a yellow dashed segment for negative_1 after it splits from MAIN
# (visual cue for schedule divergence without confusing it with MAIN)
dg1_neg_after_shoots <- shoots_binned %>%
  filter(Durchgang == "1", strand == "DG1_NEG", Tag_bin >= dg1_neg_split_time)
```

```
plot_B <- ggplot() +
  geom_rect(
    data = stage_blocks_main_cont,
    aes(xmin = start, xmax = end, ymin = -Inf, ymax = Inf, fill = Medium_stage),
    alpha = 0.28
  ) +
  # ---- NEGATIVES first (background layer) ----
  geom_line(
    data = shoots_binned %>% filter(str_detect(as.character(strand), "NEG")),
    aes(x = Tag_bin, y = total_shoots, group = interaction(Durchgang, strand), color = strand),
    linewidth = 1.06,
    linetype = "solid"
  ) +
  geom_point(
    data = shoots_binned %>% filter(str_detect(as.character(strand), "NEG")),
    aes(x = Tag_bin, y = total_shoots, color = strand),
    size = 1.7,
    shape = 16
  ) +
  # ---- SPLITS (middle layer) ----
  geom_line(
    data = shoots_binned %>% filter(!str_detect(as.character(strand), "NEG"), strand != "MAIN"),
    aes(x = Tag_bin, y = total_shoots, group = interaction(Durchgang, strand), color = strand),
    linewidth = 1.06,
    linetype = "dashed"
  ) +
  geom_point(
    data = shoots_binned %>% filter(!str_detect(as.character(strand), "NEG"), strand != "MAIN"),
    aes(x = Tag_bin, y = total_shoots, color = strand),
    size = 1.7,
    shape = 18
  ) +
    # (negative_1 split overlay disabled  uncomment to show)
#  geom_line(
#    data = dg1_neg_after_shoots,
#    aes(x = Tag_bin, y = total_shoots, group = Durchgang),
#    linewidth = 0.98,
#    linetype = "dashed",
#    color = stage_base[["CIM"]]
#  ) +

  # ---- MAIN last (foreground layer) ----
  geom_line(
    data = shoots_main,
    aes(x = Tag_bin, y = total_shoots, group = Durchgang),
    linewidth = 1.06,
    color = "black"
  ) +
  geom_point(
    data = shoots_main,
    aes(x = Tag_bin, y = total_shoots),
    size = 1.7,
```

```
    color = "black",
    shape = 16
  ) +
  facet_wrap(~ Durchgang, labeller = as_labeller(c(‘1‘ = "Run 1", ‘2‘ = "Run 2"))) +
  scale_color_manual(values = strand_cols, guide = "none") +
  scale_fill_manual(values = stage_base, guide = "none") +
  x_scale_aligned +
  labs(
    title = "B) Shoot development (total shoots per time window)",
    y = "All shoots
(sum across plates)",
    x = NULL
  ) +
  theme_bw(base_size = 11) +
  aligned_margins_BC

# ========================
# Panel C (BINNED): roots + plates assessed
# ========================
roots_by_plate <- df_binned %>%
  group_by(Durchgang, Tag_bin, strand, plate_id) %>%
  summarise(
    has_root = max(Wurzelentwicklung_binary, na.rm = TRUE),
    .groups = "drop"
  )

roots_binned <- roots_by_plate %>%
  group_by(Durchgang, Tag_bin, strand) %>%
  summarise(
    n_plates = n(),
    n_root_plates = sum(has_root > 0, na.rm = TRUE),
    .groups = "drop"
  )

roots_main <- roots_binned %>% filter(strand == "MAIN")
roots_branches <- roots_binned %>% filter(strand != "MAIN")

# DG1: overlay a yellow dashed segment for negative_1 after it splits from MAIN
# (visual cue for schedule divergence without confusing it with MAIN)
dg1_neg_after_roots <- roots_binned %>%
  filter(Durchgang == "1", strand == "DG1_NEG", Tag_bin >= dg1_neg_split_time)


plot_C <- ggplot() +
  geom_rect(
    data = stage_blocks_main_cont,
    aes(xmin = start, xmax = end, ymin = -Inf, ymax = Inf, fill = Medium_stage),
    alpha = 0.28
  ) +
  # plates assessed dashed for MAIN only (always behind)
  geom_line(
    data = roots_main,
    aes(x = Tag_bin, y = n_plates, group = Durchgang),
```

```
    linewidth = 0.51,
    linetype = "dashed",
    color = "grey45"
  ) +
  # ---- NEGATIVES first (background layer) ----
  geom_line(
    data = roots_binned %>% filter(str_detect(as.character(strand), "NEG")),
    aes(x = Tag_bin, y = n_root_plates, group = interaction(Durchgang, strand), color = strand),
    linewidth = 0.94,
    linetype = "solid"
  ) +
  geom_point(
    data = roots_binned %>% filter(str_detect(as.character(strand), "NEG")),
    aes(x = Tag_bin, y = n_root_plates, color = strand),
    size = 1.7,
    shape = 16
  ) +
  # ---- SPLITS (middle layer) ----
  geom_line(
    data = roots_binned %>% filter(!str_detect(as.character(strand), "NEG"), strand != "MAIN"),
    aes(x = Tag_bin, y = n_root_plates, group = interaction(Durchgang, strand), color = strand),
    linewidth = 0.94,
    linetype = "dashed"
  ) +
  geom_point(
    data = roots_binned %>% filter(!str_detect(as.character(strand), "NEG"), strand != "MAIN"),
    aes(x = Tag_bin, y = n_root_plates, color = strand),
    size = 1.7,
    shape = 18
  ) +
    # (negative_1 split overlay disabled  uncomment to show)
#  geom_line(
#    data = dg1_neg_after_roots,
#    aes(x = Tag_bin, y = n_root_plates, group = Durchgang),
#    linewidth = 0.89,
#    linetype = "dashed",
#    color = stage_base[["CIM"]]
#  ) +

  # ---- MAIN last (foreground layer) ----
  geom_line(
    data = roots_main,
    aes(x = Tag_bin, y = n_root_plates, group = Durchgang),
    linewidth = 0.94,
    color = "black"
  ) +
  geom_point(
    data = roots_main,
    aes(x = Tag_bin, y = n_root_plates),
    size = 1.7,
    color = "black",
    shape = 16
  ) +
```

```
  facet_wrap(~ Durchgang, labeller = as_labeller(c(‘1‘ = "Run 1", ‘2‘ = "Run 2"))) +
  scale_color_manual(values = strand_cols, guide = "none") +
  scale_fill_manual(values = stage_base, guide = "none") +
  x_scale_aligned +
  labs(
    title = "C) Root development (absolute; binned)",
    y = "Plates with roots",
    x = "Days after embryo isolation"
  ) +
  theme_bw(base_size = 11) +
  aligned_margins_BC

# ========================
# Legends under Panel C
# ========================
strand_levels_full <- c("MAIN","DG1_TOL3TOL8","DG1_NEG","DG2_NEG","DG2_TOL8","DG2_TOL2b")
strand_leg_df <- tidyr::crossing(
  Strand = factor(strand_levels_full, levels = strand_levels_full),
  x = c(0, 1)
) %>%
  mutate(y = 1)

plot_strand_legend_source <- ggplot(
  strand_leg_df,
  aes(x = x, y = y, color = Strand, group = Strand)
) +
  geom_line(linewidth = 1.1) +
  scale_color_manual(
    values = c(MAIN = "black", strand_cols),
    breaks = strand_levels_full,
    labels = c(
      MAIN = "MAIN",
      DG1_TOL3TOL8 = "DG1 split: TOL3 & TOL8",
      DG1_NEG = "Negative ctrl (DG1)",
      DG2_NEG = "Negative ctrl (DG2)",
      DG2_TOL8 = "DG2 split: TOL8",
      DG2_TOL2b = "DG2 split: TOL2b"
    ),
    guide = guide_legend(nrow = 2, byrow = TRUE)
  ) +
  theme_void(base_size = 10) +
  theme(
    legend.position = "bottom",
    legend.title = element_blank(),
    legend.key.width = unit(0.90, "cm"),
    plot.margin = margin(0, 0, 0, 0)
  )

strand_legend <- cowplot::get_legend(plot_strand_legend_source)

dashed_leg_df <- tibble(x = c(0, 1), y = 1, Type = "Plates assessed (MAIN only)")
plot_dashed_legend_source <- ggplot(dashed_leg_df, aes(x = x, y = y, linetype = Type)) +
  geom_line(color = "grey45", linewidth = 0.6) +
```

```
  scale_linetype_manual(values = c("Plates assessed (MAIN only)" = "dashed"),
                        guide = guide_legend(nrow = 1)) +
  theme_void(base_size = 10) +
  theme(
    legend.position = "bottom",
    legend.title = element_blank(),
    plot.margin = margin(0, 0, 0, 0)
  )

dashed_legend <- cowplot::get_legend(plot_dashed_legend_source)

# ========================
# Panel D (REMOVED from Figure 1)
# Panel D is now exported as a separate Figure 2 (see below)
# ========================

# ========================
# STAGE-ONLY LEGEND PANEL (ultra-compact; labeled color bars)
# ========================
stage_key_df <- tibble(
  Stage = factor(c("CIM","TM","TM2","RM","SOIL"), levels = c("CIM","TM","TM2","RM","SOIL"))
)

plot_medium_legend <- ggplot(stage_key_df, aes(x = Stage)) +
  geom_tile(aes(y = 0.60, fill = Stage), width = 0.92, height = 0.009) +
  geom_text(aes(y = 0.60, label = as.character(Stage)), size = 2.7, vjust = 0.5) +
  scale_fill_manual(values = stage_base, guide = "none") +
  coord_cartesian(ylim = c(0.585, 0.615), clip = "off") +
  theme_void(base_size = 10) +
  theme(plot.margin = margin(0, 2, 0, 2))


# ========================
# ALIGN AC + stack everything (unchanged from stable code)
# ========================
abc_aligned <- cowplot::plot_grid(
  plot_A,
  legend_A,
  plot_B,
  plot_C,
  strand_legend,
  dashed_legend,
  ncol = 1,
  align = "v",
  axis = "lr",
  rel_heights = c(1.05, 0.24, 1, 1.00, 0.16, 0.11)
)

# ========================
# FIGURE 1: Panels AC (unchanged) + legends (A4 PNG)
# ========================
final_figure1 <- cowplot::plot_grid(
  abc_aligned,
```

```
  plot_medium_legend,
  ncol = 1,
  rel_heights = c(3.36, 0.35)
)

cowplot::ggdraw(final_figure1)

# =========================
# Export Figure 1 (A4 PNG)
# =========================
ggsave(
  filename = out_png,
  plot = final_figure1,
  width = 210,
  height = 297,
  units = "mm",
  dpi = 300
)

message("Saved Figure 1 (Panels AC): ", out_png)


# =========================
# FIGURE 2: Panel D (Performance metrics; no time axis)
# =========================

# --- Helper: consistent Run labels ---
run_levels <- c("Run 1","Run 2")
run_labeller <- c(‘1‘="Run 1", ‘2‘="Run 2")

# --- Ensure 'Behandlung' exists and define display label/order (pHUE -> negative, last) ---
panelD_key <- df_clean %>%
  distinct(Behandlung) %>%
  mutate(
    Behandlung_display = if_else(Behandlung == "pHUE", "negative", Behandlung)
  )

# Keep original ordering from data, but move 'negative' to the end
behandlung_levels <- c(setdiff(unique(panelD_key$Behandlung_display), "negative"), "negative")

# ---- Baseline n0 (Insert  Run) ----
# IMPORTANT: n0 is defined as the sum of 'Anzahl_weiterbildender_Embryos/Kalli' at day 0 (per insert  run
    ; pooled across replicates).
baseline_n0 <- df_clean %>%
  filter(Gesamt_Tag == 0) %>%
  group_by(Durchgang, Behandlung) %>%
  summarise(
    n0 = sum(‘Anzahl_weiterbildender_Embryos/Kalli‘, na.rm = TRUE),
    .groups = "drop"
  )

# ---- Helper: first snapshot per stage (returns rows at earliest day for that stage) ----
first_stage_snapshot <- function(stage_name) {
```

```
  df_clean %>%
    filter(Medium_stage == stage_name) %>%
    group_by(Durchgang, Behandlung) %>%
    filter(Gesamt_Tag == min(Gesamt_Tag, na.rm = TRUE)) %>%
    ungroup()
}

# 1) Callus retention (%): first TM (Run 1) or first TM2 (Run 2)
callus_stage <- df_clean %>%
  filter(
    (Durchgang == "1" & Medium_stage == "TM") |
      (Durchgang == "2" & Medium_stage == "TM2")
  ) %>%
  group_by(Durchgang, Behandlung) %>%
  filter(Gesamt_Tag == min(Gesamt_Tag, na.rm = TRUE)) %>%
  summarise(
    callus_num = sum(‘Anzahl_weiterbildender_Embryos/Kalli‘, na.rm = TRUE),
    callus_day = min(Gesamt_Tag, na.rm = TRUE),
    .groups = "drop"
  )

# 2) Shoot formation efficiency (%): first RM
shoots_stage <- first_stage_snapshot("RM") %>%
  group_by(Durchgang, Behandlung) %>%
  summarise(
    shoots_num = sum(Sprossentwicklung_Anzahl, na.rm = TRUE),
    shoots_day = min(Gesamt_Tag, na.rm = TRUE),
    .groups = "drop"
  )

# 3) Root formation proxy (%): first SOIL (transfer to soil)
roots_stage <- df_clean %>%
  filter(Medium_stage == "SOIL") %>%
  group_by(Durchgang, Behandlung) %>%
  filter(Gesamt_Tag == min(Gesamt_Tag, na.rm = TRUE)) %>%
  summarise(
    roots_num = sum(‘Anzahl_weiterbildender_Embryos/Kalli‘, na.rm = TRUE),
    roots_day = min(Gesamt_Tag, na.rm = TRUE),
    .groups = "drop"
  )

# 4) Plants established (%): second SOIL
#    - default: take second SOIL from df_clean (works for all inserts including negative)
#    - special case: Run 2 + TOL2 should use MAIN route (excludes the off-route branch)
# Also: in v4 data, 'Erfolgreiche_Pflanzen' counts independent biological units (clones collapsed);
#       'Zusaetzliche_Klone' contains additional clonal regenerants (n_clones - 1) to be added on top.
soil2_default <- df_clean %>%
  filter(Medium_stage == "SOIL") %>%
  group_by(Durchgang, Behandlung) %>%
  arrange(Gesamt_Tag) %>%
  filter(row_number() == 2) %>%
  summarise(
    plants_bio = sum(Erfolgreiche_Pflanzen, na.rm = TRUE),
```

```
    plants_extra = sum(Zusaetzliche_Klone, na.rm = TRUE),
    plants_day = min(Gesamt_Tag, na.rm = TRUE),
    .groups = "drop"
  )

# MAIN-route soil2 for Run 2 + TOL2 (requires df_binned and 'strand' from the stable code)
soil2_tol2_main <- df_binned %>%
  filter(Durchgang == "2", Behandlung == "TOL2", strand == "MAIN", Medium_stage == "SOIL") %>%
  group_by(Durchgang, Behandlung) %>%
  arrange(Gesamt_Tag) %>%
  filter(row_number() == 2) %>%
  summarise(
    plants_bio = sum(Erfolgreiche_Pflanzen, na.rm = TRUE),
    plants_extra = sum(Zusaetzliche_Klone, na.rm = TRUE),
    plants_day = min(Gesamt_Tag, na.rm = TRUE),
    .groups = "drop"
  )

# Combine: default + overwrite TOL2_2 with MAIN version if available
plants_stage <- soil2_default %>%
  anti_join(soil2_tol2_main %>% select(Durchgang, Behandlung), by = c("Durchgang","Behandlung")) %>%
  bind_rows(soil2_tol2_main)

# ---- Combine all metrics (wide) ----
panelD_wide <- baseline_n0 %>%
  left_join(callus_stage, by = c("Durchgang","Behandlung")) %>%
  left_join(shoots_stage, by = c("Durchgang","Behandlung")) %>%
  left_join(roots_stage,  by = c("Durchgang","Behandlung")) %>%
  left_join(plants_stage, by = c("Durchgang","Behandlung")) %>%
  mutate(
    callus_num   = replace_na(callus_num, 0),
    shoots_num   = replace_na(shoots_num, 0),
    roots_num    = replace_na(roots_num,  0),
    plants_bio   = replace_na(plants_bio, 0),
    plants_extra = replace_na(plants_extra, 0),

    callus_day = replace_na(callus_day, NA_real_),
    shoots_day = replace_na(shoots_day, NA_real_),
    roots_day  = replace_na(roots_day,  NA_real_),
    plants_day = replace_na(plants_day, NA_real_),

    # Percent values
    Callus_retention = if_else(n0 > 0, 100 * callus_num / n0, 0),
    Shoots           = if_else(n0 > 0, 100 * shoots_num / n0, 0),
    Roots_proxy      = if_else(n0 > 0, 100 * roots_num  / n0, 0),

    Plants_bio_pct   = if_else(n0 > 0, 100 * plants_bio / n0, 0),
    Plants_extra_pct = if_else(n0 > 0, 100 * plants_extra / n0, 0),
    Plants_total_pct = Plants_bio_pct + Plants_extra_pct,

    Run = recode(as.character(Durchgang), !!!run_labeller),
    Run = factor(Run, levels = run_levels),
```

```
    Behandlung_display = if_else(Behandlung == "pHUE", "negative", Behandlung),
    Behandlung_display = factor(Behandlung_display, levels = behandlung_levels)
  )

# ---- Long format for plotting (four metrics; Plants is stacked: bio + extra) ----
metric_levels <- c("Callus retention", "Shoot formation", "Root formation", "Plants established")

panelD_long <- panelD_wide %>%
  transmute(
    Run,
    Behandlung_display,
    # callus
    Metric = "Callus retention",
    base_pct = Callus_retention,
    extra_pct = 0,
    snap_day = callus_day
  ) %>%
  bind_rows(
    panelD_wide %>% transmute(
      Run, Behandlung_display,
      Metric = "Shoot formation",
      base_pct = Shoots,
      extra_pct = 0,
      snap_day = shoots_day
    ),
    panelD_wide %>% transmute(
      Run, Behandlung_display,
      Metric = "Root formation",
      base_pct = Roots_proxy,
      extra_pct = 0,
      snap_day = roots_day
    ),
    panelD_wide %>% transmute(
      Run, Behandlung_display,
      Metric = "Plants established",
      base_pct = Plants_bio_pct,
      extra_pct = Plants_extra_pct,
      snap_day = plants_day
    )
  ) %>%
  mutate(
    Metric = factor(Metric, levels = metric_levels)
  )

# ---- Build rectangle data for manual stacked (bio+extra) bars with Run dodge ----
run_cols <- c("Run 1" = "grey85", "Run 2" = "grey35")
run_cols_extra <- c("Run 1" = scales::alpha(run_cols[["Run 1"]], 0.45),
                    "Run 2" = scales::alpha(run_cols[["Run 2"]], 0.45))

# numeric x positions per metric
panelD_long <- panelD_long %>%
  mutate(
    metric_x = as.numeric(Metric),
```

```
    run_offset = if_else(Run == "Run 1", -0.20, 0.20),
    x_center = metric_x + run_offset
  )

bar_w <- 0.35

rect_base <- panelD_long %>%
  transmute(
    Run, Behandlung_display, Metric,
    xmin = x_center - bar_w/2,
    xmax = x_center + bar_w/2,
    ymin = 0,
    ymax = base_pct,
    fill_key = paste0(as.character(Run), "_base")
  )

rect_extra <- panelD_long %>%
  filter(extra_pct > 0, Metric == "Plants established") %>%
  transmute(
    Run, Behandlung_display, Metric,
    xmin = x_center - bar_w/2,
    xmax = x_center + bar_w/2,
    ymin = base_pct,
    ymax = base_pct + extra_pct,
    fill_key = paste0(as.character(Run), "_extra")
  )

rect_df <- bind_rows(rect_base, rect_extra) %>%
  mutate(
    fill_key = factor(fill_key, levels = c("Run 1_base","Run 1_extra","Run 2_base","Run 2_extra"))
  )

fill_vals <- c(
  "Run 1_base" = run_cols[["Run 1"]],
  "Run 1_extra" = run_cols_extra[["Run 1"]],
  "Run 2_base" = run_cols[["Run 2"]],
  "Run 2_extra" = run_cols_extra[["Run 2"]]
)

# ---- Labels: snapshot day for each bar (placed above total height) ----
label_df <- panelD_long %>%
  mutate(
    total_height = base_pct + extra_pct,
    day_label = if_else(is.na(snap_day), "", paste0("d=", as.integer(snap_day)))
  )

# ---- Plot Figure 2 (A4 width, ~3/4 height) ----
plot_D_new <- ggplot() +
  geom_rect(
    data = rect_df,
    aes(xmin = xmin, xmax = xmax, ymin = ymin, ymax = ymax, fill = fill_key),
    color = NA
  ) +
```

```
  geom_text(
    data = label_df,
    aes(x = x_center, y = pmin(total_height + 3, 100), label = day_label),
    size = 2.6,
    vjust = 0
  ) +
  facet_wrap(~ Behandlung_display, ncol = 1) +
  scale_x_continuous(
    breaks = 1:length(metric_levels),
    labels = metric_levels,
    expand = expansion(mult = c(0.02, 0.02))
  ) +
  scale_y_continuous(limits = c(0, 100), expand = expansion(mult = c(0, 0.05))) +
  scale_fill_manual(
    values = fill_vals,
    breaks = c("Run 1_base","Run 2_base"),
    labels = c("Run 1","Run 2"),
    name = "Run"
  ) +
  labs(
    x = NULL,
    y = "Percent of initial embryos (n0 at day 0)"
  ) +
  theme_bw(base_size = 11) +
  theme(
    panel.grid.major.x = element_blank(),
    panel.grid.minor = element_blank(),
    strip.background = element_rect(fill = "grey92"),
    strip.text = element_text(face = "bold"),
    axis.text.x = element_text(angle = 0, hjust = 0.5),
    legend.position = "top"
  )

cowplot::ggdraw(plot_D_new)

# ========================
# Export Figure 2 (Panel D)
# ========================
out_png2 <- sub("\\.png$", "_Figure2_PanelD_v4.png", out_png)

ggsave(
  filename = out_png2,
  plot = plot_D_new,
  width = 210,
  height = 223,
  units = "mm",
  dpi = 300
)

message("Saved Figure 2 (Panel D): ", out_png2)
```

7.3.0.4 Barley embryo size: analysis pipeline (R)

Listing 7.4: R script used to calculate median, mean and standard deviation of the barley embryo size dataset. The script reproduces Figure 7.5. This script is using the packages `readxl` (Wickham & Bryan, 2025) and `ggplot2` (Wickham, 2016).

```
# ============================================================
# Analysis: Diameter of Barley Embryos
# ============================================================

library(readxl)
library(ggplot2)

# --- Load data ---
dat <- read_excel("C:/Users/Moritz Schmid/OneDrive - Universitt Wien/Desktop/Masterarbeit_Abbildungen_
     Code/Diameter_Embryos.xlsx")
dat <- dat[, c("Name", "Insert", "run", "Diameter [mm]")]
colnames(dat) <- c("Name", "Insert", "Run", "Diameter_mm")
dat$Diameter_mm <- as.numeric(dat$Diameter_mm)
dat$Run <- as.factor(dat$Run)
dat <- dat[!is.na(dat$Diameter_mm), ]

# --- Mean per Insert and Run ---
stats <- aggregate(Diameter_mm ~ Insert + Run, data = dat, FUN = function(x) {
  c(Mean = mean(x), N = length(x))
})
stats <- do.call(data.frame, stats)
colnames(stats) <- c("Insert", "Run", "Mean", "N")
cat("\n--- Stats per Insert and Run ---\n")
print(stats)

# --- Overall mean per Run ---
stats_run <- aggregate(Diameter_mm ~ Run, data = dat, FUN = function(x) {
  c(Mean = mean(x), N = length(x))
})
stats_run <- do.call(data.frame, stats_run)
colnames(stats_run) <- c("Run", "Mean", "N")
cat("\n--- Overall stats per Run ---\n")
print(stats_run)

# --- Overall mean ---
cat("\n--- Overall stats ---\n")
cat("Mean:", round(mean(dat$Diameter_mm), 4), "mm\n")
cat("N:   ", nrow(dat), "\n")

# --- Prepare data: add "Overall" as extra Insert category ---
dat_overall <- dat
dat_overall$Insert <- "Overall"
dat_plot <- rbind(dat, dat_overall)
dat_plot$Insert <- factor(dat_plot$Insert,
                          levels = c("NEG", "TOL1", "TOL2", "TOL3", "TOL8", "Overall"))
```

```
# --- Boxplot ---
ggplot(dat_plot, aes(x = Insert, y = Diameter_mm, fill = Run)) +
  geom_boxplot(outlier.shape = 21, outlier.size = 2, width = 0.5) +
  stat_summary(fun = mean, geom = "point", shape = 23, size = 3,
               fill = "white", color = "black",
               position = position_dodge(width = 0.5)) +
  scale_fill_manual(values = c("1" = "grey85", "2" = "grey35"),
                    labels = c("1" = "Run 1", "2" = "Run 2")) +
  geom_vline(xintercept = 5.5, linetype = "dashed", color = "grey50") +
  labs(
    title = "Diameter of Barley Embryos",
    x = "Insert",
    y = "Diameter [mm]",
    fill = "Run"
  ) +
  theme_minimal() +
  theme(legend.position = "right")
```

8 List of Abbreviations

2,4-D	2,4-dichlorophenoxyacetic acid
BAP	6-benzylaminopurine
CaMV 35S	Cauliflower mosaic virus 35S promoter
Cas9	CRISPR-associated protein 9
CIM	Callus-inducing medium
CRISPR	Clustered Regularly Interspaced Short Palindromic Repeats
crRNA	CRISPR RNA
DAI	Days after embryo isolation
DAP	Days after pollination
DMSO	Dimethyl sulfoxide
DNA	Deoxyribonucleic acid
DSB	Double-strand break
ESCRT	Endosomal Sorting Complex Required for Transport
GAT	GGA and Tom1 domain
GFP	Green fluorescent protein
gRNA	Guide RNA
HDR	Homology-directed repair
HygR	Hygromycin resistance gene
ILV	Intraluminal vesicle
IQR	Interquartile range
LB	Lysogeny broth
MES	2-(*N*-morpholino)ethanesulfonic acid
MVB	Multivesicular body
NHEJ	Non-homologous end joining
OD	Optical density
PAM	Protospacer adjacent motif
PBS	Phosphate-buffered saline
PCR	Polymerase chain reaction
RM	Regeneration medium
RNA	Ribonucleic acid
sgRNA	Single guide RNA
SpCas9	*Streptococcus pyogenes* Cas9
T-DNA	Transfer DNA
TFA	Transformation amenability
Ti	Tumour-inducing (plasmid)
TM	Transition medium
TM2	Modified transition medium
TOL	TOM1-like
tracrRNA	Trans-activating CRISPR RNA
UIM	Ubiquitin-interaction motif
VHS	Vps27, Hrs, STAM domain
ZmUbi1	*Zea mays* ubiquitin 1 promoter
OsU3	*Oryza sativa* U3 small nuclear RNA promoter

9 Note on the Use of AI-Supported-Tools

AI-powered tools were employed as follows: Claude (Anthropic; Opus 4.5, Opus 4.6, Sonnet 4.5, Sonnet 4.6) was used between January 2026 and March 2026 for proofreading, code troubleshooting and formulation assistance. DeepL (26.2.1) was used in March 2026 for translation. All AI-generated or AI-suggested content was critically reviewed, revised, and—where necessary—substantiated with appropriated scientific sources. The final intellectual content and written formulation of this paper were produced independently by the author.

Table 9.1:

Intended use*	Name and Version	Input and Output
Translation assistance	DeepL (26.2.1)	–
Code troubleshooting	Claude (Opus 4.5)	–
Formulation assistance, Translation	Claude (Opus 4.6)	–
Code troubleshooting	Claude (Sonnet 4.5)	–
Proofreading	Claude (Sonnet 4.6)	–

*Tools for checking grammar and spelling or for automatically generating bibliographies are excluded from this declaration.

List of Figures

List of Tables

Bibliography

Ahmar, S., Hensel, G. & Gruszka, D. (2023). Crispr/cas9-mediated genome editing techniques and new breeding strategies in cereals – current status, improvements, and perspectives. *Biotechnology Advances*, *69*, 108248. Zugriff auf https://doi.org/10.1016/j.biotechadv.2023.108248 doi: 10.1016/j.biotechadv.2023.108248

Azizi-Dargahlou, S. & Pouresmaeil, M. (2024). Agrobacterium tumefaciens-mediated plant transformation: A review. *Molecular Biotechnology*, *66* (7), 1563-1580. Zugriff auf https://doi.org/10.1007/s12033-023-00788-x doi: 10.1007/s12033-023-00788-x

Bartlett, J. G., Alves, S. C., Smedley, M., Snape, J. W. & Harwood, W. A. (2008). High-throughput agrobacterium-mediated barley transformation. *Plant Methods*, *4* (1), 22. Zugriff auf https://doi.org/10.1186/1746-4811-4-22 doi: 10.1186/1746-4811-4-22

Basu, U., Ahmed, S. R., Bhat, B. A., Anwar, Z., Ali, A., Ijaz, A., … Mushtaq, M. (2022). A crispr way for accelerating cereal crop improvement: Progress and challenges. *Frontiers in Genetics*, *13*, 866976. Zugriff auf https://doi.org/10.3389/fgene.2022.866976 doi: 10.3389/fgene.2022.866976

Bouchard, J., Malalgoda, M., Storsley, J., Malunga, L., Netticadan, T. & Thandapilly, S. (2022). Health benefits of cereal grain- and pulse-derived proteins. *Molecules*, *27* (12), 3746. Zugriff auf https://doi.org/10.3390/molecules27123746 doi: 10.3390/molecules27123746

Chang, C.-H. & Winans, S. C. (1992). Functional roles assigned to the periplasmic, linker, and receiver domains of the agrobacterium tumefaciens vira protein. *Journal of Bacteriology*, *174* (21), 7033–7039. doi: 10.1128/jb.174.21.7033-7039.1992

Chang, Y., Zitzewitz, J. v., Hayes, P. M. & Chen, T. H. H. (2003). High frequency plant regeneration from immature embryos of an elite barley cultivar (hordeum vulgare l. cv. morex). *Plant Cell Reports*, *21* (8), 733-738. Zugriff auf https://doi.org/10.1007/s00299-003-0607-8 doi: 10.1007/s00299-003-0607-8

Christensen, A. H., Sharrock, R. A. & Quail, P. H. (1992). Maize polyubiquitin genes: structure, thermal perturbation of expression and transcript splicing, and promoter activity following transfer to protoplasts by electroporation. *Plant Molecular Biology*, *18* (4), 675–689. doi: 10.1007/BF00020961

Devos, K. M. (2005). Updating the 'crop circle'. *Current Opinion in Plant Biology*, *8* (2), 155-

162. Zugriff auf https://doi.org/10.1016/j.pbi.2005.01.005 doi: 10.1016/j.pbi.2005.01.005

Erdoğan, İ., Cevher-Keskin, B., Bilir, Ö., Hong, Y. & Tör, M. (2023). Recent developments in crispr/cas9 genome-editing technology related to plant disease resistance and abiotic stress tolerance. *Biology*, *12* (7), 1037. Zugriff auf https://doi.org/10.3390/biology12071037 doi: 10.3390/biology12071037

Gao, C., Zhuang, X., Shen, J. & Jiang, L. (2017). Plant escrt complexes: Moving beyond endosomal sorting. *Trends in Plant Science*, *22* (11), 986-998. Zugriff auf https://doi.org/10.1016/j.tplants.2017.08.003 doi: 10.1016/j.tplants.2017.08.003

Gelvin, S. B. (2012). Traversing the cell: Agrobacterium t-dna's journey to the host genome. *Frontiers in Plant Science*, *3*, 52. Zugriff auf https://doi.org/10.3389/fpls.2012.00052 doi: 10.3389/fpls.2012.00052

Gelvin, S. B. (2017). Integration of agrobacterium t-dna into the plant genome. *Annual Review of Genetics*, *51* (1), 195-217. Zugriff auf https://doi.org/10.1146/annurev-genet-120215-035320 doi: 10.1146/annurev-genet-120215-035320

Gelvin, S. B. (2021). Plant dna repair and agrobacterium t-dna integration. *International Journal of Molecular Sciences*, *22* (16), 8458. Zugriff auf https://doi.org/10.3390/ijms22168458 doi: 10.3390/ijms22168458

Gordon, J. E. & Christie, P. J. (2014). The agrobacterium ti plasmids. *Microbiology Spectrum*, *2* (6). Zugriff auf https://doi.org/10.1128/microbiolspec.plas-0010-2013 doi: 10.1128/microbiolspec.PLAS-0010-2013

Harwood, W. A., Bartlett, J. G., Alves, S. C., Perry, M., Smedley, M. A., Leyl, N. & Snape, J. W. (2009). Barley transformation using agrobacterium-mediated techniques. *Transgenic wheat, barley and oats: production and characterization protocols*, 137–147. doi: 10.1007/978-1-59745-379-0_9

Haryono, M., Cho, S.-T., Fang, M.-J., Chen, A.-P., Chou, S.-J., Lai, E.-M. & Kuo, C.-H. (2019). Differentiations in gene content and expression response to virulence induction between two agrobacterium strains. *Frontiers in Microbiology*, *10*, 1554. Zugriff auf https://doi.org/10.3389/fmicb.2019.01554 doi: 10.3389/fmicb.2019.01554

Henne, W. M., Buchkovich, N. J. & Emr, S. D. (2011). The escrt pathway. *Developmental cell*, *21* (1), 77–91. doi: 10.1016/j.devcel.2011.05.015

Hilscher, J., Kapusi, E., Stoger, E. & Ibl, V. (2016). Cell layer-specific distribution of transiently expressed barley escrt-iii component hvvps60 in developing barley endosperm. *Protoplasma*, *253* (1), 137-153. Zugriff auf https://doi.org/10.1007/s00709-015-0798-1 doi: 10.1007/s00709-015-0798-1

Hisano, H., Matsuura, T., Mori, I. C., Yamane, M. & Sato, K. (2016). Endogenous hormone levels affect the regeneration ability of callus derived from different organs in barley. *Plant Physiology and Biochemistry*, *99*, 66-72. Zugriff auf https://doi.org/10.1016/j.plaphy.2015.12.005 doi: 10.1016/j.plaphy.2015.12.005

Hisano, H., Meints, B., Moscou, M. J., Cistue, L., Echávarri, B., Sato, K. & Hayes, P. M. (2017). Selection of transformation-efficient barley genotypes based on tfa (transformation amenability) haplotype and higher resolution mapping of the tfa loci. *Plant Cell Reports*, *36* (4), 611-620. Zugriff auf https://doi.org/10.1007/s00299-017-2107-2 doi: 10.1007/s00299-017-2107-2

Holme, I. B., Brinch-Pedersen, H., Lange, M. & Holm, P. B. (2008). Transformation of different barley (hordeum vulgare l.) cultivars by agrobacterium tumefaciens infection of in vitro cultured ovules. *Plant Cell Reports*, *27* (12), 1833-1840. Zugriff auf https://doi.org/10.1007/s00299-008-0605-y doi: 10.1007/s00299-008-0605-y

Hurley, J. H. (2010). The escrt complexes. *Critical reviews in biochemistry and molecular biology*, *45* (6), 463–487. doi: 10.3109/10409238.2010.415986

Hwang, H.-H., Yu, M. & Lai, E.-M. (2017). Agrobacterium-mediated plant transformation: Biology and applications. *The Arabidopsis Book*, *15*, e0186. Zugriff auf https://doi.org/10.1199/tab.0186 doi: 10.1199/tab.0186

Hygromycin b 10843555001 roche. (2024). Roche Product Datasheet. (Product catalog entry - not a peer-reviewed article)

Hygromycin b gold. (2024). Product Information Sheet. (Commercial product - not a peer-reviewed article)

Ibl, V., Kapusi, E., Arcalis, E., Kawagoe, Y. & Stoger, E. (2014). Fusion, rupture, and degeneration: the fate of in vivo-labelled psvs in developing barley endosperm*. *Journal of Experimental Botany*, *65* (12), 3249-3261. Zugriff auf https://doi.org/10.1093/jxb/eru175 doi: 10.1093/jxb/eru175

Ibrahim, A. S., El-Shihy, O. M. & Fahmy, A. H. (2010). Highly efficient agrobacterium tumefaciens-mediated transformation of elite egyptian barley cultivars. *American-Eurasian Journal of Sustainable Agriculture*, *4* (3), 403–413.

Janská, A., Hodek, J., Svoboda, P., Zámečník, J., Prášil, I. T., Vlasáková, E., … Ovesná, J. (2013). The choice of reference gene set for assessing gene expression in barley (hordeum vulgare l.) under low temperature and drought stress. *Molecular Genetics and Genomics*, *288* (11), 639-649. Zugriff auf https://doi.org/10.1007/s00438-013-0774-4 doi: 10.1007/s00438-013-0774-4

Jin, S., Prusti, R. K., Roitsch, T., Ankenbauer, R. G. & Nester, E. W. (1990). Phosphorylation of

the virg protein of agrobacterium tumefaciens by the autophosphorylated vira protein: Essential role in biological activity of virg. *Journal of Bacteriology*, *172* (9), 4945–4950. doi: 10.1128/jb.172.9.4945-4950.1990

Jin, S., Roitsch, T., Ankenbauer, R. G., Gordon, M. P. & Nester, E. W. (1990). The vira protein of agrobacterium tumefaciens is autophosphorylated and is essential for vir gene regulation. *Journal of Bacteriology*, *172* (2), 525–530. doi: 10.1128/jb.172.2.525-530.1990

Jinek, M., Chylinski, K., Fonfara, I., Hauer, M., Doudna, J. A. & Charpentier, E. (2012). A programmable dual-rna–guided dna endonuclease in adaptive bacterial immunity. *Science*, *337* (6096), 816-821. Zugriff auf `https://doi.org/10.1126/science.1225829` doi: 10.1126/science.1225829

Jores, T., Tonnies, J., Wrightsman, T., Buckler, E. S., Cuperus, J. T., Fields, S. & Queitsch, C. (2021). Synthetic promoter designs enabled by a comprehensive analysis of plant core promoters. *Nature Plants*, *7* (6), 842–855. doi: 10.1038/s41477-021-00932-y

Korbei, B., Moulinier-Anzola, J., De-Araujo, L., Lucyshyn, D., Retzer, K., Khan, M. A. & Luschnig, C. (2013). Arabidopsis tol proteins act as gatekeepers for vacuolar sorting of pin2 plasma membrane protein. *Current Biology*, *23* (24), 2500–2505. doi: 10.1016/j.cub.2013.10.036

Kosová, K., Prášil, I. T., Klíma, M., Nesvadba, Z., Vítámvás, P. & Ovesná, J. (2023). Proteomics of wheat and barley cereals in response to environmental stresses: Current state and future challenges. *Journal of Proteomics*, *282*, 104923. Zugriff auf `https://doi.org/10.1016/j.jprot.2023.104923` doi: 10.1016/j.jprot.2023.104923

Kumari, K., Sherpa, T. & Dey, N. (2024). Analysis of plant pararetrovirus promoter sequence(s) for developing a useful synthetic promoter with enhanced activity in rice, pearl millet, and tobacco plants. *Frontiers in Plant Science*, *15*. Zugriff auf `https://doi.org/10.3389/fpls.2024.1426479` doi: 10.3389/fpls.2024.1426479

Kumlehn, J., Serazetdinova, L., Hensel, G., Becker, D. & Loerz, H. (2006). Genetic transformation of barley (hordeum vulgare l.) via infection of androgenetic pollen cultures with agrobacterium tumefaciens. *Plant Biotechnology Journal*, *4* (2), 251-261. Zugriff auf `https://doi.org/10.1111/j.1467-7652.2005.00178.x` doi: 10.1111/j.1467-7652.2005.00178.x

Lacroix, B. & Citovsky, V. (2013). The roles of bacterial and host plant factors in agrobacterium-mediated genetic transformation. *The International Journal of Developmental Biology*, *57* (6-7-8), 467-481. Zugriff auf `https://doi.org/10.1387/ijdb.130199bl` doi: 10.1387/ijdb.130199bl

Lazo, G. R., Stein, P. A. & Ludwig, R. A. (1991). A dna transformation-competent arabidopsis genomic library in agrobacterium. *Bio/Technology*, *9* (10), 963-967. Zugriff auf `https://doi.org/10.1038/nbt1091-963` doi: 10.1038/nbt1091-963

Lee, Y.-W., Jin, S., Sim, W.-S. & Nester, E. W. (1996). The sensing of plant signal molecules by agrobacterium: genetic evidence for direct recognition of phenolic inducers by the vira protein. *Gene*, *179* (1), 83-88. Zugriff auf https://doi.org/10.1016/s0378-1119(96)00328-9 doi: 10.1016/s0378-1119(96)00328-9

Mascher, M., Gundlach, H., Himmelbach, A., Beier, S., Twardziok, S. O., Wicker, T., … others (2017). A chromosome conformation capture ordered sequence of the barley genome. *Nature*, *544* (7651), 427–433. doi: 10.1038/nature22043

Matveeva, T. V. & Otten, L. (2019). Widespread occurrence of natural genetic transformation of plants by agrobacterium. *Plant Molecular Biology*, *101* (4-5), 415-437. Zugriff auf https://doi.org/10.1007/s11103-019-00913-y doi: 10.1007/s11103-019-00913-y

May, D. B., Pfotenhauer, A. C., Concha, B. L., Li, L., Jones, S. M., Harbison, S. A., … Lenaghan, S. C. (2025). Toward a monocot synbio toolkit: assessing regulatory element performance and eudicot compatibility. *Plant Cell Reports*, *44* (9), 196. Zugriff auf https://doi.org/10.1007/s00299-025-03583-x doi: 10.1007/s00299-025-03583-x

Moulinier-Anzola, J., De-Araujo, L. & Korbei, B. (2014). Expression of *Arabidopsis TOL* genes. *Plant Signaling & Behavior*, *9* (4), e28667. Zugriff auf https://doi.org/10.4161/psb.28667 doi: 10.4161/psb.28667

Moulinier-Anzola, J., Schwihla, M., De-Araújo, L., Artner, C., Jörg, L., Konstantinova, N., … Korbei, B. (2020). Tols function as ubiquitin receptors in the early steps of the escrt pathway in higher plants. *Molecular Plant*, *13* (5), 717-731. Zugriff auf https://doi.org/10.1016/j.molp.2020.02.012 doi: 10.1016/j.molp.2020.02.012

Murray, F., Brettell, R., Matthews, P., Bishop, D. & Jacobsen, J. (2004). Comparison of agrobacterium-mediated transformation of four barley cultivars using the gfp and gus reporter genes. *Plant Cell Reports*, *22* (6), 397-402. Zugriff auf https://doi.org/10.1007/s00299-003-0704-8 doi: 10.1007/s00299-003-0704-8

Nester, E. W. (2014). Agrobacterium: nature's genetic engineer. *Frontiers in Plant Science*, *5*, 730. Zugriff auf https://doi.org/10.3389/fpls.2014.00730 doi: 10.3389/fpls.2014.00730

Orman-Ligeza, B., Harwood, W., Hedley, P. E., Hinchcliffe, A., Macaulay, M. & Uauy, C. (2020). Tra1: A locus responsible for controlling agrobacterium-mediated transformability in barley. *Frontiers in Plant Science*, *11*, 355. Zugriff auf https://doi.org/10.3389/fpls.2020.00355 doi: 10.3389/fpls.2020.00355

Paez Valencia, J., Goodman, K. & Otegui, M. S. (2016). Endocytosis and endosomal trafficking in plants. *Annual review of plant biology*, *67* (1), 309–335. doi: 10.1146/annurev-arplant-043015-112242

Park, S. H., Rose, S. C., Zapata, C., Srivatanakul, M. & Smith, R. H. (1998). Cross-protection and selectable marker genes in plant transformation. *In Vitro Cellular & Developmental Biology - Plant*, *34*, 117–121. doi: 10.1007/BF02823124

Pourkheirandish, M. & Komatsuda, T. (2007). The importance of barley genetics and domestication in a global perspective. *Annals of Botany*, *100* (5), 999-1008. Zugriff auf `https://doi.org/10.1093/aob/mcm139` doi: 10.1093/aob/mcm139

Prasadi, N. P. V. & Joye, I. J. (2020). Dietary fibre from whole grains and their benefits on metabolic health. *Nutrients*, *12* (10), 3045. Zugriff auf `https://doi.org/10.3390/nu12103045` doi: 10.3390/nu12103045

R Core Team. (2025). R: A language and environment for statistical computing [Software-Handbuch]. Vienna, Austria. Zugriff auf `https://www.R-project.org/`

Roustan, V., Hilscher, J., Weidinger, M., Reipert, S., Shabrangy, A., Gebert, C., … others (2020). Protein sorting into protein bodies during barley endosperm development is putatively regulated by cytoskeleton members, mvbs and the hvsnf7s. *Scientific Reports*, *10* (1), 1864. doi: 10.1038/s41598-020-58769-2

Shahinnia, F., Carrillo, N. & Hajirezaei, M.-R. (2021). Engineering climate-change-resilient crops: New tools and approaches. *International Journal of Molecular Sciences*, *22* (15), 7877. Zugriff auf `https://doi.org/10.3390/ijms22157877` doi: 10.3390/ijms22157877

Shou, H., Chikwamba, R. K., Zhang, Z., Xiang, C., Fonger, T. M., Pegg, S. E. K., … Frame, B. R. (2002). Agrobacterium tumefaciens-mediated transformation of maize embryos using a standard binary vector system. *Plant Physiology*, *129* (1), 13-22. Zugriff auf `https://doi.org/10.1104/pp.000653` doi: 10.1104/pp.000653

Shrawat, A. K., Becker, D. & Lörz, H. (2007). Agrobacterium tumefaciens-mediated genetic transformation of barley (hordeum vulgare l.). *Plant Science*, *172* (2), 281-290. Zugriff auf `https://doi.org/10.1016/j.plantsci.2006.09.005` doi: 10.1016/j.plantsci.2006.09.005

Silbermann, L.-M., Vermeer, B., Schmid, S. & Tych, K. (2024). The known unknowns of the hsp90 chaperone. *eLife*, *13*, e102666. Zugriff auf `https://doi.org/10.7554/eLife.102666` doi: 10.7554/eLife.102666

Sinha, P., Saxena, R. K., Singh, V. K., Krishnamurthy, L. & Varshney, R. K. (2015). Selection and validation of housekeeping genes as reference for gene expression studies in pigeonpea (cajanus cajan) under heat and salt stress conditions. *Frontiers in Plant Science*, *6*, 1071. Zugriff auf `https://doi.org/10.3389/fpls.2015.01071` doi: 10.3389/fpls.2015.01071

Sreenivasulu, N., Borisjuk, L., Junker, B. H., Mock, H.-P., Rolletschek, H., Seiffert, U., … Wobus, U.

(2010). Barley grain development: Toward an integrative view. *International Review of Cell and Molecular Biology*, *281*, 49-89. Zugriff auf https://doi.org/10.1016/S1937-6448(10)81002-0 doi: 10.1016/S1937-6448(10)81002-0

Stachel, S. E., Messens, E., Montagu, M. V. & Zambryski, P. (1985). Identification of the signal molecules produced by wounded plant cells that activate t-dna transfer in agrobacterium tumefaciens. *Nature*, *318* (6047), 624-629. Zugriff auf https://doi.org/10.1038/318624a0 doi: 10.1038/318624a0

Stachel, S. E., Timmerman, B. & Zambryski, P. (1986). Generation of single-stranded t-dna molecules during the initial stages of t-dna transfer from agrobacterium tumefaciens to plant cells. *Nature*, *322* (6081), 706-712. Zugriff auf https://doi.org/10.1038/322706a0 doi: 10.1038/322706a0

Stachel, S. E. & Zambryski, P. C. (1986). vira and virg control the plant-induced activation of the t-dna transfer process of a. tumefaciens. *Cell*, *46*, 325–333. doi: 10.1016/0092-8674(86)90653-7

Teng, Z., Chen, Y., Meng, S., Duan, M., Zhang, J. & Ye, N. (2023). Environmental stimuli: A major challenge during grain filling in cereals. *International Journal of Molecular Sciences*, *24* (3), 2255. Zugriff auf https://doi.org/10.3390/ijms24032255 doi: 10.3390/ijms24032255

Tingay, S., McElroy, D., Kalla, R., Fieg, S., Wang, M., Thornton, S. & Brettell, R. (1997). Agrobacterium tumefaciens-mediated barley transformation. *The Plant Journal*, *11* (6), 1369-1376. Zugriff auf https://doi.org/10.1046/j.1365-313x.1997.11061369.x doi: 10.1046/j.1365-313X.1997.11061369.x

Torchiano, M. (2020). effsize: Efficient effect size computation [Software-Handbuch]. Zugriff auf https://CRAN.R-project.org/package=effsize (R package version 0.8.1) doi: 10.5281/zenodo.1480624

Vietri, M., Radulovic, M. & Stenmark, H. (2020). The many functions of escrts. *Nature Reviews Molecular Cell Biology*, *21* (1), 25-42. Zugriff auf https://doi.org/10.1038/s41580-019-0177-4 doi: 10.1038/s41580-019-0177-4

Wang, F., He, B., Hong, Y., Fu, L., Shen, Q. & Zhang, G. (2023). Time-course of genotype and hormone-related effects on callus proliferation in barley genetic transformation. *Crop Design*, *2* (2), 100043. Zugriff auf https://www.sciencedirect.com/science/article/pii/S2772899423000216 doi: 10.1016/j.cropd.2023.100043

Wang, M.-B., Abbott, D. C., Upadhyaya, N. M., Jacobsen, J. V. & Waterhouse, P. M. (2001). Agrobacterium tumefaciens-mediated transformation of an elite australian barley cultivar with virus resistance and reporter genes. *Australian Journal of Plant Physiology*, *28* (2), 149-156. Zugriff auf https://doi.org/10.1071/pp00103 doi: 10.1071/PP00103

Wickham, H. (2016). *ggplot2: Elegant graphics for data analysis*. Springer-Verlag New York. Zugriff auf `https://ggplot2.tidyverse.org`

Wickham, H., Averick, M., Bryan, J., Chang, W., McGowan, L. D., François, R., … Yutani, H. (2019). Welcome to the tidyverse. *Journal of Open Source Software*, *4* (43), 1686. doi: 10.21105/joss.01686

Wickham, H. & Bryan, J. (2025). readxl: Read excel files [Software-Handbuch]. Zugriff auf `https://CRAN.R-project.org/package=readxl` (R package version 1.4.5) doi: 10.32614/CRAN.package.readxl

Wickham, H., François, R., Henry, L., Müller, K. & Vaughan, D. (2023). dplyr: A grammar of data manipulation [Software-Handbuch]. Zugriff auf `https://CRAN.R-project.org/package=dplyr` (R package version 1.1.4) doi: 10.32614/CRAN.package.dplyr

Wickham, H., Vaughan, D. & Girlich, M. (2025). tidyr: Tidy messy data [Software-Handbuch]. Zugriff auf `https://CRAN.R-project.org/package=tidyr` (R package version 1.3.2) doi: 10.32614/CRAN.package.tidyr

Wilke, C. O. (2025). cowplot: Streamlined plot theme and plot annotations for 'ggplot2' [Software-Handbuch]. Zugriff auf `https://CRAN.R-project.org/package=cowplot` (R package version 1.2.0) doi: 10.32614/CRAN.package.cowplot

Winans, S. C., Kerstetter, R. A. & Nester, E. W. (1988). Transcriptional regulation of the vira and virg genes of agrobacterium tumefaciens. *Journal of Bacteriology*, *170* (9), 4047–4054. doi: 10.1128/jb.170.9.4047-4054.1988

Wu, H., McCormac, A. C., Elliott, M. C. & Chen, D.-F. (1998). Agrobacterium-mediated stable transformation of cell suspension cultures of barley (hordeum vulgare). *Plant Cell, Tissue and Organ Culture*, *54*, 161–171. doi: 10.1023/A:1006165223577

Xing, H.-L., Dong, L., Wang, Z.-P., Zhang, H.-Y., Han, C.-Y., Liu, B., … Chen, Q.-J. (2014, 29. 11). A crispr/cas9 toolkit for multiplex genome editing in plants. *BMC Plant Biology*, *14* (1), 327. doi: 10.1186/s12870-014-0327-y

Xu, H., Chang, Q., Huang, L., Wei, P., Song, Y., Guo, Z., … Fan, J. (2023). An agrobacterium-mediated transient expression method for functional assay of genes promoting disease in monocots. *International Journal of Molecular Sciences*, *24* (8), 7636. Zugriff auf `https://doi.org/10.3390/ijms24087636` doi: 10.3390/ijms24087636

Yuan, Z.-C., Edlind, M. P., Liu, P., Saenkham, P., Banta, L. M., Wise, A. A., … Nester, E. W. (2007). The plant signal salicylic acid shuts down expression of the vir regulon and activates quormone-quenching genes in agrobacterium. *Proceedings of the National Academy of Sciences*, *104* (28), 11790-11795. Zugriff auf `https://doi.org/10.1073/pnas.0704866104` doi: 10.1073/pnas.0704866104

Zeng, Y., Pu, X., Du, J., Yang, X., Li, X., Mandal, M. S. N., … Yang, J. (2020). Molecular mechanism of functional ingredients in barley to combat human chronic diseases. *Oxidative Medicine and Cellular Longevity*, *2020*, 1-26. Zugriff auf https://doi.org/10.1155/2020/3836172 doi: 10.1155/2020/3836172

Zhang, J., Deng, H., Bai, J., Zhou, X., Zhao, Y., Zhu, Y., … Sun, Q. (2023). Health-promoting properties of barley: A review of nutrient and nutraceutical composition, functionality, bioprocessing, and health benefits. *Critical Reviews in Food Science and Nutrition*, *63* (9), 1155-1169. Zugriff auf https://doi.org/10.1080/10408398.2021.1972926 doi: 10.1080/10408398.2021.1972926